1-1-2011

Preliminary Report: Evaluating the Potential of Archaeogeophysical Surveying on Viking Age and Medieval Sites in Greenland, 2 – 16 August, 2010

Douglas J. Bolender
University of Massachusetts Boston

John M. Steinberg
University of Massachusetts Boston, john.steinberg@umb.edu

Brian N. Damiata
University of Massachusetts Boston

John W. Schoenfelder
University of Massachusetts Boston, john.schoenfelder@umb.edu

Kathryn Caitlin
University of Massachusetts Boston

Preliminary Report: Evaluating the Potential of Archaeogeophysical Surveying on Viking Age and Medieval Sites in Greenland, 2 – 16 August, 2010

By:

Douglas J. Bolender, John M. Steinberg, Brian N. Damiata, John W. Schoenfelder, and Kathryn Caitlin

Cultural Resource Management Study No. 51

Table of Contents

Figures

Tables

Fiske Center for Archaeological Research

The Andrew Fiske Memorial Center for Archaeological Research at the University of Massachusetts Boston was established in 1999 through the generosity of the late Alice Fiske and her family as a living memorial to her late husband Andrew. The Fiske Center was formally known as the Center for Cultural and Environmental History.

As an international leader in interdisciplinary research, the Fiske Center promotes a vision of archaeology as a multi-faceted, theoretically rigorous field that integrates a variety of analytical perspectives into its studies of the cultural and biological dimensions of colonization, urbanization, and industrialization over the past thousand years in the Americas and the Atlantic World. Intellectually the Center's staff is committed to building a highly integrated archaeology that embraces the multiplicity of methodological and theoretical approaches the field offers. As part of a student centered urban public university, the Center maintains a program of local archaeology with a special emphasis on research that meets the needs of cities, towns, and Tribal Nations in New England and the greater Northeast. The Fiske Center also seeks to understand the local as part of a larger Atlantic World.

Acknowledgements

We thank the National Science Foundation (NSF) for its generous support of this project (ARC-1038339). We also thank Jette Arneborg, Christian Koch Madsen, and Konrad Śmiarowski for their support and encouragement.

John Steinberg obtained the GPS (Global Positioning System) points. Doug Bolender specified the location and position of the survey grids. John Schoenfelder mapped the surface features and set out the corners of the survey grid. Brian Damiata, Kathryn Catlin, Doug Bolender, and John Steinberg carried out the archaeogeophysical surveys. John Steinberg and Brian Damiata are responsible for the quality control of the surveys and for interpretation of the data.

None of the suggestions or recommendations in this report should be construed as geological interpretations (although Brian Damiata is a licensed geophysicist in the State of California). Rather, these are archaeological interpretations of shallow geophysical data, in reference to previous excavations whenever possible. The interpretations presented herein should be ground truthed with targeted archaeological excavations. The interpretations and assessments are the responsibility of John Steinberg.

Project Summary

This research was conducted as part of a high-risk archaeogeophysical study funded by the National Science Foundation (ARC, 1038339) to test the effectiveness of using shallow geophysical methods on Viking Age and Medieval sites in Greenland. Specifically, whether electromagnetics (EM), electrical resistivity, magnetometry, and ground penetrating radar (GPR) can be used to assess the nature, the extent, the depth, and the preservational status of Norse sites in Greenland. Our preliminary investigation suggests that archaeogeophysics will be hard pressed to identify buried Viking Age turf walls that do not have stone foundations. We have found that both magnetometry and the in-phase component of electromagnetics are well suited to identify buried Viking Age stone foundations and other important cultural features and that GPR is effective for identifying Viking Age Christian graves.

Objectives

The primary goal of this research is to begin to overcome biases in the Greenlandic Norse archaeological record. Assessing the establishment dates and organization of Norse sites in Greenland is difficult because substantial cultural deposits can be hidden under deep windblown sand deposits as well as later occupations. Shallow geophysical methods were used to help recover information on the nature, extent and depth of subsurface cultural deposits. Assessing these site characteristics is a first step in overcoming the bias towards the later, the larger, and the more visible sites in the archaeological record.

Norse Greenland presents a relatively visible medieval landscape with many ruins preserved on the surface. Survey archaeologists have taken advantage of these conditions to do comprehensive surveys of Norse settlements producing inventories of farm buildings and settlements (Guldager, et al. 2002; Keller 1990). Coring surveys and excavation at known sites have demonstrated that some sites are buried under significant aeolian deposits and that areas within many other sites can be deep and contain ruins that are not visible on the surface. In many cases Viking Age deposits cannot be accessed by archaeological excavation, as this would damage later occupational phases. In these cases, application of archeogeophysics may be the only way to assess this unique cultural history. The identification, characterization, and dating of these subsurface architectural remains are critical to systematic survey programs and to the production of regional settlement patterns and chronologies that can help explain the ecological and political dynamics of Norse colonization, land use, and the eventual demise of Norse Greenland.

Over the past 10 years the Skagafjörður Archaeological Settlement Survey (SASS) has developed an intensive subsurface survey protocol to systematically recover, date, and characterize Viking Age landscapes in Iceland. While we believe the SASS subsurface protocol can be effective in Greenland there are many questions that must be resolved before any wide-scale application of the methods can be developed. The project set out to address two basic questions: (1) what is the actual subsurface record at Norse sites, and (2) which methods work best and how are they most effectively employed? In this initial investigation, we tested and adapted this protocol to conditions in Greenland. We hope that the preliminary test of these methods will significantly expand the range of sites and periods accessible to researchers working in Greenland and allow for new questions regarding the long-term political and environmental histories of the region.

The successful integration of archaeogeophysics with archaeological survey and excavation will result in a more holistic approach to the preservation of Norse archaeological sites in Greenland. These sites suffer from increased modern impacts resulting from mineral exploitation, sheep farming, and tourism. Additionally, there is now total summer sub-surface thaw and conditions that were once ideal for preserving organic remains are now deteriorating, especially in well-drained areas. In the coming years the Greenland National Museum will begin a program of scheduling and protecting some of these sites.

We believe that the application of archaeogeophysics could be a great asset in determining which sites are in danger and worthy of preservation.

Results

Our results indicate that archeogeophysics can be a valuable addition to archaeological survey, excavation, and heritage management efforts in Greenland. The study employed the standard suite of archaeogeophysical methods: electromagnetics, electrical resistivity, magnetometry, and GPR. Three Norse sites on the Igaliku fjord were surveyed to varying intensities: Ø64 in Innoqquassaq, Ø66 in Igaliku Kujalleq, and Ø172 in Tatsipataakilleq. We examined a range of archaeological contexts: medieval farm mounds, a churchyard, a heavily eroded ruin, and homefield areas with no visible architecture. In general, the archaeogeophysics provided complementary datasets while some methods proved particularly effective. In particular, we find that magnetometry and electromagnetics (specifically the in-phase component) can be used for site prospection. That is, these two methods could identify buried Viking Age architecture with stone foundations that do not present a surface sign. Furthermore, these two methods can also delineate partially visible ruins. GPR (using GPR-Slice processing) shows significant promise in identifying individual buried features, including graves. Unfortunately, GPR is difficult to use in areas of visible ruins with significant surface topography and scattered stones. Both GPR and electrical resistivity produced complementary two-dimensional (2D) datasets allowing subsurface features to be mapped at specific depths. We conclude that by combining several methods, much of the buried Norse Greenlandic archaeology can be efficiently and accurately investigated with archaeogeophysics.

In Greenland, as in Iceland, turf was a primary building material in Norse sites. In Iceland, turf generally manifests as electrically resistive anomalies against a relatively conductive background. The sites we examined in Greenland all had highly resistive soils. In this resistive background, turf appears to marginally elevate soil conductivity. As a result, magnetometry, as opposed to the apparent ground conductivity component of electromagnetics, appears to be the most effective general method for site prospection and mapping buried architecture, especially for structures with stone foundations. Magnetometry, used in conjunction with the in-phase component of electromagnetics can distinguish different structural elements such as walls, floors, and hearths. Electrical resistivity can detect buried turf walls, in addition to stone foundations, but further research and ground-truthing excavations are necessary to fully evaluate the potential of archaeogeophysics to map and distinguish different elements of buried structures.

Archaeogeophysical surveying also proved an effective means of investigating site geology and, in some cases, anthropogenic changes to site geology. Electromagnetics was used to identify a buried irrigation canal at Ø66 and both resistivity and GPR successfully mapped buried surfaces and features such as glacial till, moraines, and bedrock.

Recommendations

Greenland presents a whole host of logistical and environmental challenges to the application of archaeogeophysics. At the same time, we see profound benefits to archaeology and heritage management from a program that incorporates archaeogeophysical surveying. The most important benefit is the ability to identify buried or unobtrusive important cultural features. Most of the instruments that we experimented with demonstrated some efficacy depending on the problem and conditions.

For site and feature prospection, magnetometry provided the sharpest images of buried site features and structures of any of the methods that were deployed. Magnetometry, especially when using a gradiometer, can be difficult to set up and operate because it is so sensitive. The interpretation of magnetometery data can also be difficult because each physical target can produce spatial distinct positive and negative geophysical anomalies. We also found that magnetometry was not useful for detecting

graves. That being said, magnetometry did produce easily interpretable images of complex Viking Age structures and features.

The in-phase component of the EM-31 and EM-38 was useful for identifying irrigation ditches, stone walls, floors, and middens. The in-phase data appears to identify many of the same anomalies as seen in the magnetometry but with less clarity. Nonetheless, in-phase data may serve to help discriminate between magnetic anomalies. In general, the shallow depth of investigation of the EM-38 is sufficient for most applications in Greenland.

GPR is an outstanding tool for identifying individual graves. However, because so many of the Viking Age sites in Greenland have uneven ground surfaces (and the sites are relatively close to the surface) GPR is not an effective site prospection tool. However, when the surface is even, soil conditions appear to be excellent for collecting high-quality GPR datasets and can be used to provide pseudo 3D images of buried features. GPR also seems to be well suited for defining site boundaries.

Resistivity can clearly delimit site boundaries and yield specific depth information of features. Its use does not appear to be well suited to identifying graves, although this was not thoroughly tested. If surfaces are too uneven for GPR, then resistivity can yield important information. At the sites investigated, resistivity appears to be the best method for identifying and mapping turf walls.

The least effective of any of the methods we experimented with was apparent ground conductivity (Q or quadrature-phase component) using the EM-31 and EM-38. Apparent ground conductivity may provide valuable additional information on geology and landscape features such as relative depth to bedrock, the nature of buried soils and the existence of fields. Additionally, apparent ground conductivity could be used to identify possible irrigation canals and ditches. For the present study, however, the apparent ground conductivity data was not very diagnostic given the extremely resistive conditions of background soils and targets.

In sum, we suggest a multi-method approach. We recommend that sites be examined first with either in-phase surveying using an EM-38 or magnetic gradient surveying using a cesium-vapor gradiometer. This will produce the best pseudo two-dimensional (2D) images in plan view. Follow-up work to obtain pseudo three-dimensional (3D) images should be done with GPR surveying using a 500 MHz antenna if conditions permit. If the surface is too uneven, then we recommend using resistivity.

The Potential for Archaeogeophysical Surveying in Greenland

Norse Greenland, settled in the late 10th century, represents the furthest permanent frontier of the Viking Age European world. It also represents one of the most extreme environmental settings for Norse agro-pastoralism. Ultimately the Norse settlements failed as the Greenlanders succumbed to various pressures. While the particular combination of factors is debated – deteriorating climate, competition with expanding Inuit populations, its marginal position in the emerging Northern European economy – it is clear that the end of the Norse settlement was accompanied by hardship and adaptation to the difficult environment (Arneborg, et al. 1999; Barlow, et al. 1997; Buckland, et al. 1995; Dugmore, et al. 2007; McGovern 1980, 1981, 1991, 1994, 2000). The contrasting fates of the Norse and Inuit in Greenland provides one of history's best examples of cultural adaptation to climate change (cf. Diamond 2005).

During the late 10th century, when Greenland was initially settled, the North Atlantic experienced a sustained period of unusually warm climatic conditions, the Medieval Climatic Optimum (ca. AD 950-1250) (Lamb 1982; Mann, et al. 2009; Ogilvie, et al. 2000; Trouet, et al. 2009). Greenland, instead of being the failed margin of the European world, was the expanding frontier (Arneborg 2000, 2001; Keller 1990). According to the traditional saga histories, it was rapidly colonized, primarily from Iceland (Þorgilsson 1930). A century before, Iceland had been the open frontier, inspiring a generation of Viking farmers to pack up their Scandinavian homes, take to the seas, and claim new lands (Dugmore, et al. 2005; McGovern, et al. 2007; Smith 1995). By the end of the 10th century Iceland was fully settled and there was limited productive land available for new farms. In many ways, the settlement of Greenland was a continuation of the Norse colonization of the North Atlantic.

To archaeologists, Norse Greenland presents a relatively visible medieval landscape with many ruins preserved on the surface. Survey archaeologists have taken advantage of these conditions to do comprehensive surveys of Norse settlements producing inventories of farm buildings (Keller 1989; McGovern 1992; Vésteinsson, et al. 2002). Much of what we know about Norse Greenland, especially from survey, pertains to the late medieval world that is best preserved on the surface (Vésteinsson, et al. 2002). Studies of soil development, archaeological coring surveys and excavations have demonstrated that some sites are buried under significant aeolian deposits and that areas within many other sites can be deep and contain ruins that are not visible on the surface (Jacobsen 1987; Jacobsen and Jakobsen 1986; Śmiarowski 2008b, 2009). The Greenland record may therefore be biased against buried – and likely earlier – sites. The landscape of settlement – the first farms, the dynamics of colonization, early land-use patterns and interactions between frontier and later farms – is obscure, hidden under aeolian sands and later occupations. It is the settlement of Greenland that links it to the North Atlantic expansion of the Viking Age as part of the process and underlying dynamics that sent Norse farmers into Northern Scotland, the Faeroes, Iceland, Greenland, and ultimately to North America. To understand the end of Norse Greenland we must also understand its origins.

This project was designed to test in Greenland a subsurface survey protocol that was developed by the Skagafjörður Archaeological Settlement Survey to systematically assess and access the Viking Age settlement of Iceland. The protocol involves extensive coring and the application of various archaeogeophysical methods including electromagnetics, electrical resistivity, and ground-penetrating radar (GPR). This protocol is now well-developed for Iceland's geological and geographic conditions where substantial subsurface remains from the Viking Age, including entire farm complexes, may not be visible from the surface but was entirely untested in geologically older Greenland. Magnetometry was added to the survey protocol for Greenland.

Research was conducted in conjunction with the Vatnahverfi Project, an on-going survey project that began in 2005 and is directed by Jette Arneborg, Danish National Museum. The Vatnahverfi region in the center of the Eastern Settlement was relatively densely populated in the Middle Ages, and it holds farms

of different size and status that are broadly representative of the Norse Greenland society. The experimental research was conducted at three farms previously surveyed by the Vatnahverfi Project: the large high status farm Ø66 in Igaliku Kujalleq, which was the religious and economic center of the region, the nearby farm Ø64, which has one of the older churches in the northern part of Vatnahverfi, and Ø172 in Tatsipataakilleq.

This proposal was submitted under the EAGER program because exploratory archaeogeophysics is almost always a high-risk undertaking. We were not sure which methods and techniques are most appropriate, if any, to Greenland Norse Archaeology. The work confronted a series of unknowns, specifically environmental and preservational conditions. Our timeframe was short, the questions we asked were particular to Norse Eastern Settlement sites, and our scope limited to the protocol we had established in Iceland. While the preliminary research conducted during the summer of 2010 has not answered all of our questions, we believe this test of archaeogeophysical methods in Greenland has demonstrated their potential in site prospection, mapping, the identification of specific features such as graves, and the investigation of local geological conditions including anthropogenic changes to soil deposits. It is clear that archaeogeophysics holds the promise of making Greenland's buried history accessible and has the potential to make a profound contribution to archaeological survey, excavation, and heritage management in Greenland. From this point we must refine these methods and begin to integrate this kind of subsurface protocol into existing survey, excavation, and preservational efforts.

Spatial Controls: dGPS and total station

The effectiveness and utility of archaeogeophysical surveying is highly dependent on the degree of spatial control over the collection, integration, and presentation of the datasets. Accurate grids allow for the precise collection of data and correlation with surface features, pre-existing excavation data, and coring. They are also essential for the integration of results for the various geophysical methods that may yield complementary information. Slight differences between the actual location of a geophysical reading and the coordinate assigned during survey can weaken or mask anomalies. The effects of inaccurate surveying can be magnified when the data are post-processed and filtered.

Grid Establishment

At each survey site we collected GPS base points using a Trimble GeoXH with a Zepher antenna. Base points were established based on hundreds of measurements, in which a GPS position was recorded at 5-second intervals. When possible, multiple data campaigns were conducted to include different satellite configurations. Readings were then averaged to produce control points that were subsequently used for total station set up. Normally GPS points are post-corrected but due to the lack of either real time dGPS correction or internet access in the field we used uncorrected GPS points for grid establishment. These initial GPS based points were then used as resectioning points for the Topcon GPT9005A robotic total station. GPS base points were then remeasured to establish a locally consistent set of reference points for subsequent total station set ups and now serve as semi-permanent benchmarks on the UTM zone 23 North coordinate system using the WGS84 reference spheroid (see page 26). These points are within 20 cm of the actual east coordinate, within 10 cm of the north coordinate, and within 50 cm of the actual elevation.

Original base points were determined using multiple measurements collected over hours. In general we preferred collection periods with the lowest error readings as opposed to averaging multiple collection sets of varying quality. Optimizing project efficiency often required that a team be sent to collect GPS data ahead of the rest of the team as no work could begin until the grid was established. To this end John Steinberg and John Schoenfelder often arrived at sites the night before everyone else. These 'midnight runs' always required boat transportation and we are grateful to the generous captains who often sacrificed precious sleep time to make this possible.

Geophysical survey grids were established initially by total station (Figure 1). Survey flags were placed at 10-meter intervals across target areas. Then a fiberglass measuring tape was drawn along the ends of the intended survey area (either the north-south or east-west baselines for survey transects) and each meter was flagged with flags of alternating colors. During the survey, tapes were laid at 1- meter intervals to mark the location of transects. These transect tapes were used to ensure a straight line for data collection and to mark fiducials. Most surveys included sub-meter transect spacing (usually at 0.50 m, 0.33 m, 0.25 m, or 0.20 intervals); these transects were based on the nearest tape.

Figure 1. Survey grid establishment: (a) GPT9005A robotic total station, and (b) Trimble GeoXH GPS with a Zepher antenna.

Topographic Mapping

Accurate topographic information is essential to the proper interpretation of geophysical datasets, especially methods such as GPR and resistivity that yield 2D data. Also, for one-dimensional (1D) methods, such as magnetometry and electromagnetics, it is important to ensure that results are not affected by surface topography, which can change the relative distance of the instrument's sensor to the ground surface.

Topographic data were collected using the total station. The density of collected data varied based on surface conditions, the types of geophysical methods to be used, and to some degree the inherent time constraints of a short project. In general areas covered by GPR were collected at a 1-meter or less sampling interval and XYZ data were collected for each electrode location along transects for resistivity.

Low altitude aerial photography

Kite-based, low-altitude aerial photography (KAP) is a low-cost and relatively quick way to map sites. The resulting photographs can be georeferenced and used to establish a visual overview of site and

surface conditions including the location of visible ruins, vegetation and other surface features to aid in the interpretation of geophysical anomalies.

A Canon Powershot A570 IS compact digital camera was used, running the CHDK (Canon Hack Development Kit) custom software suite from the camera's SD card. A CHDK intervalometer script automatically triggered the shutter during flight; this was usually set to take photographs every 6 to 10 seconds. To maximize shutter speed without unduly sacrificing quality, it proved effective to place the camera in aperture-priority mode with the aperture at or near its maximum setting.

Following design advice from Dr. Bruce Owen (Sonoma State University), layers of closed-cell polyethylene foam were used to suspend the camera inside a Ziploc brand plastic box, which was hung from the kite line via a "Picavet" string suspension (Figure 2). This design proved effective in protecting the camera during "hard landings" and in keeping the camera pointed downward at near-vertical angles during flight.

Three kites were used during the 2010 Greenland survey, and all provided sufficiently stable flight to generate useable images. In high-wind conditions, an Air Affairs Sutton Flow Form 8 was preferred. The most-used kite was an Air Affairs Sutton Flow Form 16, which is appropriate for 8-25 mph winds. Because its design features breakable spars, the G-Kites Fled was preferred only in gust-free lower-wind conditions in which the Flow Form kites were unable to lift the camera. While completely still conditions precluded the use of all kites, it is possible to lift the Fled (and camera) for short periods in extremely light wind conditions by walking rapidly upwind; however, the time-consuming logistics of this method make it appropriate only for exceptional situations.

Our standard photograph collecting procedure was for the kite operator to walk a loose grid pattern, walking a set number of strides, stopping long enough for the camera to take 2-3 shots, and repeating. When available, a second person stood either directly under the camera or to the side in order to keep the operator appraised of the area being photographed. Two flights were made over Ø64 resulting in complete coverage of the church, medieval farm mound, and immediately surrounding areas. At Ø66 a single flight was made concentrating on the extensive medieval ruins. Unfortunately, the near complete lack of wind during the survey at Ø172 prevented launching the kite despite multiple efforts.

Kite-based aerial photography datasets include:

1) Unprocessed images. Full collection of digital photos from each kite flight (3072 x 2304 pixels; ca. 3-5 MB each). Photos vary in subject, focus, and camera tilt relative to ground surface.
2) Lens corrected images. Full collection of digital photos from each kite flight processed to correct lens distortion (3072 x 2304 pixels; ca. 3-5 MB each). Photos vary in subject, focus, and camera tilt relative to ground surface.
3) Georeferenced images. High-quality, lens corrected kite photos were georeferenced for projection in GIS software. Images were georeferenced based on measured locations on the ground (usually geophysical survey grid flags) using a second order polynomial transformation to correct for angular distortion. The root mean square error on georeferenced images is generally under 0.010 meters. Georeferenced images are currently in ESRI formats with georeferencing data held in a separate .aux file from the raster image. Individual georeferenced images usually cover only a small portion of each site.
4) Composite georeferenced images. ESRI raster catalogs have been assembled from individual georeferenced kite photos to provide fuller coverage of sites.

Figure 2. Kite-based aerial photography: (a) KAP box and Picavet string suspension, and (b) kite in flight at Ø66.

Archaeogeophysical Methods

Archaeogeophysics, in general, is the application of non-destructive geophysical methods and principles to archaeological settings. More specifically, archaeogeophysics is the interpretation of buried archaeological sites and features based on the results of shallow geophysical investigations. Archaeological features, important subsurface geology, and sometimes artifacts and ecofacts can be located and partially analyzed using geophysical signatures. Broad-coverage geophysical surveys can be immensely helpful in site prospection, site reconnaissance and, for investigating broad settlement patterns.

Archaeogeophysics is not an exact science. Small differences in the environment (e.g., soil moisture, surface cover, changes in ambient temperature) can affect geophysical measurements, and therefore change the nature and shape of the interpreted geophysical anomalies. A geophysical anomaly is a general term that is applied to an area that exhibits a significant change in measurement value, and therefore a change in the physical property that is being measured. A geophysical anomaly can be identified by its contrast with the surrounding environment. Defining an anomaly, however, is subjective. In addition, the causes of an anomaly can be either natural (such as a glacial erratic) or artificial (such as a wall). Determining the cause of an anomaly can be difficult.

In archaeogeophysics, the choice of method, equipment, and technique can have as much or more effect on the reliability of the identification of archaeological features as the contrasts between the features and the surrounding matrix. For example, inappropriate transect direction, transect spacing, or instrument

height could make strong and important anomalies undetectable even under proper conditions. Because the work is non-destructive, surveys can, and usually are, preformed multiple times using different geophysical methods that provide complementary data.

In general, interpretations based on archaeogeophysical data are more accurate when ground truthed through archaeological excavations. Even small excavations of targeted geophysical anomalies can greatly enhance the archaeological interpretation by allowing correlation of anomalies with specific archaeological features. Similarly, the placement of excavations becomes considerably more efficient when based on archaeogeophysical results. The reflexive use of archaeology and geophysics can establish a geophysical signature of an archaeological feature. That is, when archaeological investigations are in a feedback loop with geophysical results we can more confidently interpret a given geophysical anomaly in terms of a buried archaeological feature.

It is possible that a given archaeological feature will not produce a measureable geophysical contrast to be identified with the methods and post-processing applied herein. It is common for important archaeological deposits to be identified in areas without significant anomalies. We generally use multiple geophysical methods that yield complementary information to try to mitigate this problem. In some cases anomalies that show up with one method may not show up in another. Sometimes contrasting how an anomaly manifests itself in various geophysical methods can make for more accurate archaeogeophysical interpretations. However, anomalies that manifest themselves in multiple methods are usually substantial. For the present study, we employed the four geophysical methods most commonly used in archaeological settings: electromagnetics electrical resistivity, magnetometry, and GPR.

Electromagnetics

Electromagnetics holds great potential for Greenland because the method does not require direct contact with the ground, and therefore can be used to survey over very rough terrain. The very low conductivity of the soils in Greenland, however, in general suggests that the measurement of apparent ground conductivity may not be effective in Greenland. The electromagnetic method works best in detecting conductive targets within a resistive medium. Conversely, measuring the in-phase component, which is a function of the magnetic susceptibility, has potential in Greenland.

Principles of Method

With electromagnetic surveying, a primary time-varying magnetic field is generated at or near the ground surface by transmitting an alternating current through a loop of wire. In response to this primary magnetic field, induced or eddy currents will flow in any electrically conductive material that may be present within the field of measurement (i.e., the earth). In turn, these induced currents will create secondary magnetic fields. The secondary fields are generally not in-phase with the transmitted sinusoidal signal and therefore can be measured separately from the original signal. Thus, the received signal consists of two parts or phases: one signal that is in-phase with the transmitter (called the in-phase component) and another that is 90 degrees out of phase (called the quadrature [quad] or out-of-phase component). The ratio of secondary to primary magnetic fields, as measured by a receiver, is proportional to a weighted average of ground conductivity and is thus termed apparent ground conductivity.

Apparent ground conductivity is measured in milliSiemens per meter (mS/m). MilliSiemens per meter is the inverse of ohm-meters which is a measure of the resistivity of the soil (McNeill 1980). Electrical resistivity is a complementary method that can yield 2D profiles of the subsurface resistivity structure pseudo profiles of the soil across the site (see below). Measurements of apparent ground conductivity are responsive to bulk changes in lithology, groundwater and ground contamination.

The in-phase component of the received signal contains the primary magnetic field as well as any secondary fields that are in-phase with that signal. The magnitude of the in-phase component is measured

in parts per thousand (ppt). Because of the arbitrary way the in-phase is calibrated, in-phase readings from one survey to another need to be tied to a common base station and baseline adjusted to be comparable. In EM surveys, negative in-phase readings are possible. The change in in-phase readings is, in most cases, comparable between surveys. Conversely, the quad component is more consistent from survey to survey. Metal produces strong secondary fields, so the in-phase component is a useful indicator of buried metal objects. Along the same lines, the in-phase component is approximately proportional to a measure of magnetic susceptibility, and will detect many of the same features that are detectable with magnetometry. The in-phase component is ideal for identifying soils that have been heated or trampled.

Based on spatial variations of apparent ground conductivity, regions with differing electrical properties may be discerned. Clays and saline soils, especially those associated with middens, tend to be conductive. Sandy soils, rocks, dried turf, especially stone and turf walls, tend to have low conductivity (i.e., resistive). By mapping these contrasts through a series of closely spaced transects, buried subsurface features can be identified (e.g., Rodrigues, et al. 2009). Since EM data (like all geophysical data) are typically collected along closely spaced transects, tighter spacing between transects will yield better resolution of features, but will take more time to collect.

Instrumentation and Field Procedures

For the Greenland study, we used two electromagnetic instruments: the Geonics EM-31 MK2 and the EM-38 RT (Figure 3). The EM31 operates at a frequency of 9.8 kHz and has an intercoil spacing of 3.66 m which provides a depth of penetration up to 6 m. The EM-38 operates at a frequency of 14.6 kHz and has an intercoil spacing of 1 m which provides for a relatively shallow depth of investigation (ca. 10-100 cm) when operated in the vertical dipole mode. We used an EM-38 RT that was manufactured in 2001 but was temperature compensated by Geonics Ltd. in December of 2009. This modification reduces (but does not eliminate) the sensitivity of the unit to changes in ambient temperature caused by changes in sun, shade, or ground heat. Unfortunately, for the particular model of EM-38 that was used (RT), only one component (e.g., in-phase or apparent ground conductivity) can be logged at a time. In most cases, both instruments were used on all the locations that were tested.

All of the EM data were recorded using the Juniper Allegro CX data logger. The data were collected using a station spacing that varied from 10 cm to 25 cm along transects separated by 0.20 to 1 m. The amount of data that was collected per day depended on the transect spacing. Using a spacing of 0.25 cm, an area of approximately 25- x 25-m could be covered in a typical 10-hour field day. At 1-m spacing, an area ranging from 100- x 250-m could be covered.

Figure 3. Electromagnetic surveying with (a) the Geonics EM-31 and (b) the Geonics EM-38.

Preliminary Results

At Ø64 the apparent ground conductivity results from the EM-31 suggest that this type of surveying is the least effective component of our work. Although marginally elevated apparent ground conductivity is observed over the farm mound, the difference over the whole survey is minimal (3 mS/m). The in-phase component over the church and neighboring farm mound does suggest structure and specific elements of stonewalls and foundations can be identified. The long boom combined with relatively large transect spacing gives rise to substantial striping in both phases, especially over the sloping ground along the coastal edge in which instrument height above the ground surface varied due to the bi-directional surveying. The apparent ground conductivity data from the EM-38 survey at Ø66 did not provide any better data than the EM-31. However, the in-phase component over both the farm mound and the church detected substantial structure and specific elements of stonewalls and foundations. Neither the EM-31 nor EM-38 surveys seem to be suited to the identification of graves.

At Ø172, over the farm mound much of the range in apparent ground conductivity values in the EM-31 east-west survey is due to the two low areas that are metal dumps (the larger one is associated with a buried wheelbarrow discarded in the old excavation). Without these two areas, the variation in values would have a much smaller range. The higher values are probably due to greater thickness of soils and fewer rocks. Some structure is visible in the data. The EM-31 in- phase data over the farm mound exhibits substantial variation but is difficult to interpret. The small strip of EM-38 data also suggests structure was detected in both the apparent ground conductivity and in the in-phase data, with the latter suggesting greater variability and more defined structure. General comparison of the EM-31 and EM-38 datasets to the resistivity profiles along the same transects indicate that the two machines are sensitive to conductivity at different depths, as expected (see Figure 4 and Figure 5).

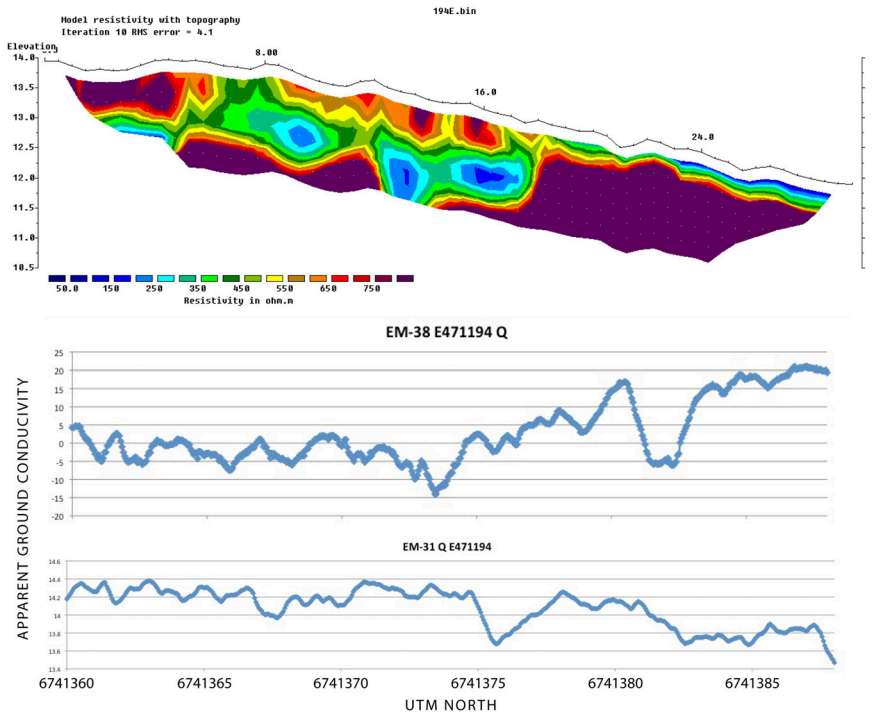

Figure 4. Comparison of resistivity (upper) and apparent ground conductivity data (middle – EM-31, lower – EM-38) along UT E471194 at Ø172.

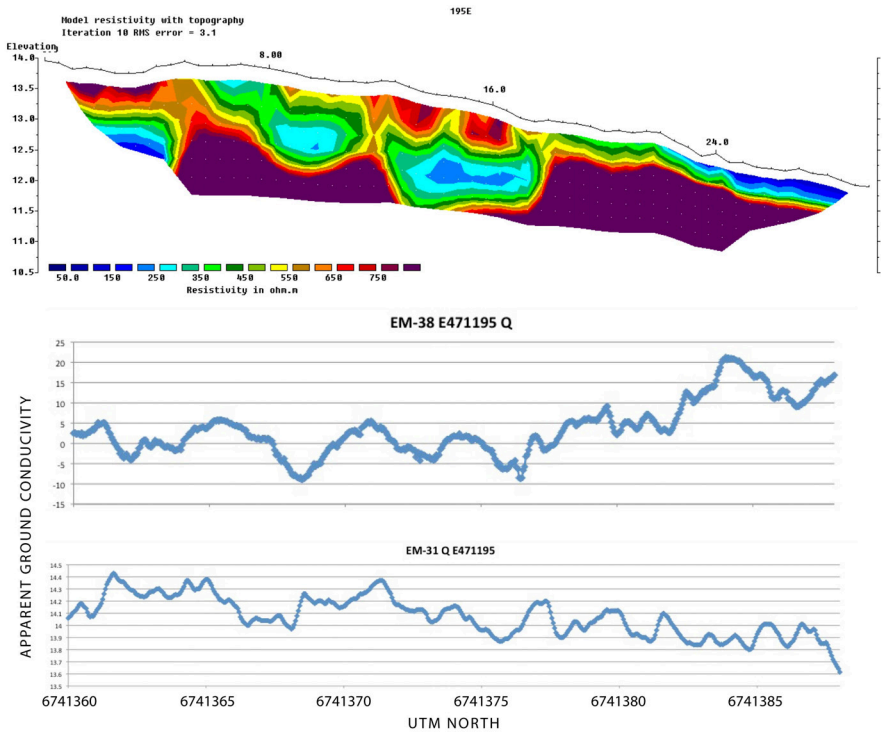

Figure 5. Comparison of resistivity (upper) and apparent ground conductivity data (middle – EM-31, lower – EM-38) along the E471195 at Ø172.

At Ø66 the largest EM-31 survey was conducted in hopes of identifying targets buried under the aeolian sand. The apparent ground conductivity results suggest different thicknesses of sand and possibly areas of more intensively used grass fields. The in-phase results show a distinct linear anomaly that corresponds to a possible irrigation ditch that is visible in some air-photos. The anomaly also shows up in the apparent ground conductivity results but not as distinct. An ordinary least squares regression model was run comparing the apparent ground conductivity and in-phase values for the entire survey dataset (Figure 6). In general, lower in-phase values are associated with increase fill. No anomalies suggestive of buildings or other structures were identified.

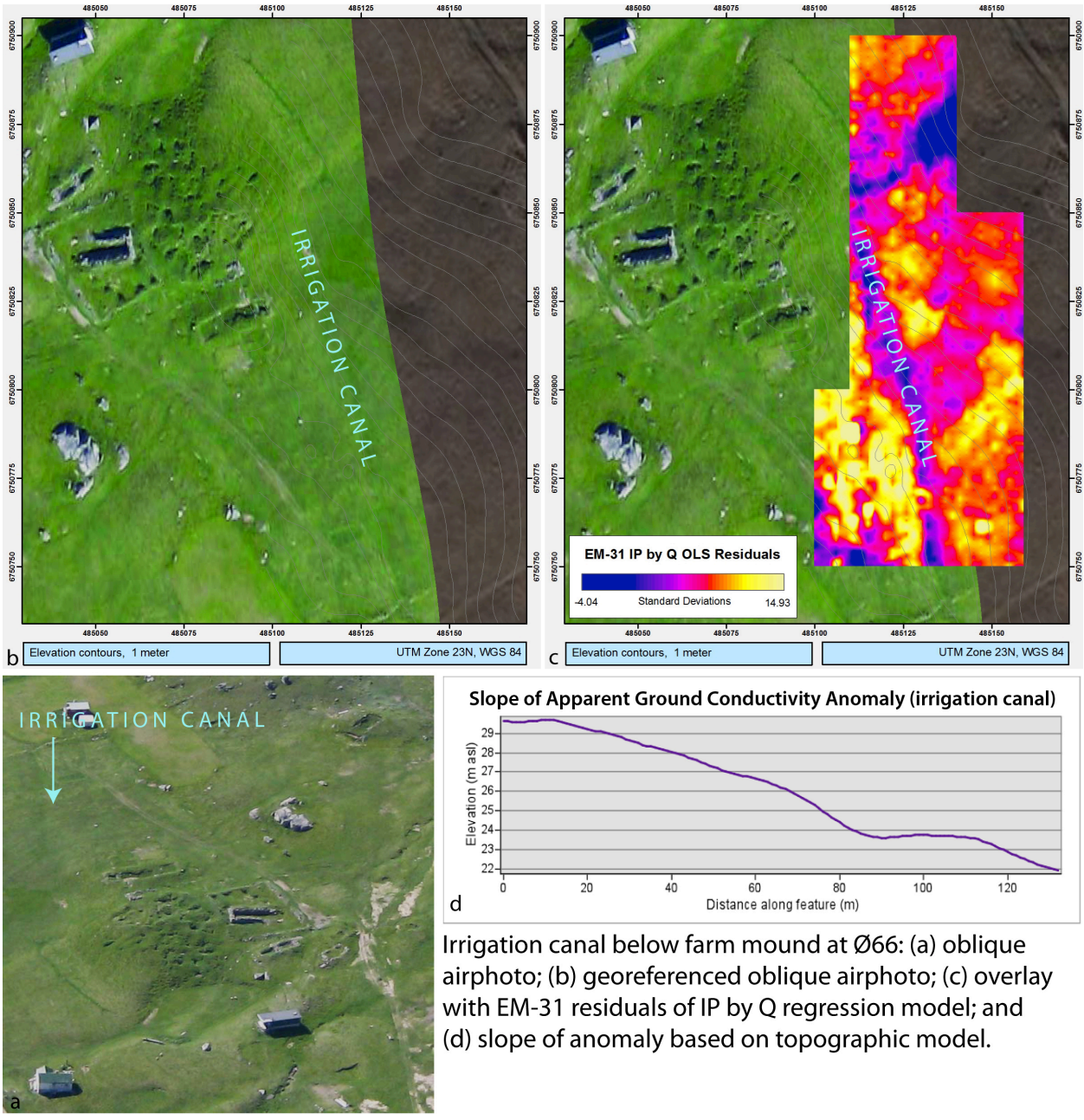

Irrigation canal below farm mound at Ø66: (a) oblique airphoto; (b) georeferenced oblique airphoto; (c) overlay with EM-31 residuals of IP by Q regression model; and (d) slope of anomaly based on topographic model.

Figure 6. Ø66 irrigation canal in air photo and results of EM-31 survey.

In our previous work in Iceland, apparent ground conductivity surveying, along with coring, has been our primary methodology for site prospection. It is relatively quick and large areas of uneven terrain can be covered. In Iceland, buried and collapsed turf walls appear as relatively resistive anomalies as compared to the surrounding conductive soils. Unlike Iceland, the areas surveyed in Greenland have highly resistive soils. Based on the investigations, EM surveying to measure apparent ground conductivity is not useful for site prospection or delineation of archaeological features when the targets are too resistive to produce conductive anomalies.

It is important to stress that the test sites for the present study are not representative of all geophysical conditions in Greenland and that apparent ground conductivity surveying may yield excellent results in other geological regions or site conditions, especially those with higher concentrations of salt or organics in the soil (i.e., even more than at sites Ø172 and Ø66). Nonetheless, the characteristic signature of buried turf walls and turf collapse that were successfully identified in Iceland–resistive anomalies in a conductive soil matrix–may be reversed in Greenland where buried turf walls appear relatively as more conductive in comparison to the surrounding soil matrix. Similarly, stone foundations, which are usually distinctively resistive compared to surrounding conductive soils, may be barely visible in the resistive Greenlandic soils. Fortunately the magnetic properties of stone are quite distinct when compared to the Greenlandic soils and show up as distinct anomalies in the EM in-phase component and in magnetic surveys. Although apparent ground conductivity surveying may not be useful for site prospection in Greenland it may reveal qualities of the soil that are useful: such areas of relatively high organic content, water retention, depth to bedrock, and potentially buried landscape features such as irrigation canals and ditches. In general, the in-phase results are complementary to the magnetic results

Electrical Resistivity

The electrical resistivity method is ideal for detecting resistive targets in a conductive medium. Using a 24-channel electrode system yields a 2D vertical profile of the resistivity structure of the subsurface (Gaffney and Gater 2003).

Principles of Method

With the resistivity method, direct current is injected into the ground through a pair of metal electrodes and the earth's response, in the form of potential difference (or voltage), is measured through a second pair of electrodes. Various configurations for arranging the electrodes can be used (Hargrave, et al. 2002). For the Greenland project, the Wenner array was selected in order to find graves (Hunter and Cox 2005:71). This array employs four electrodes (one pair of outer current electrodes and an inner pair of potential electrodes) and is designed to map horizontal changes in resistivity. A fixed constant spacing, termed "a-spacing", is maintained between adjacent electrodes (Figure 7). After the first measurement, the electrodes are shifted over by one a-spacing for the next measurement and so on.

For the Wenner array, the depth of investigation is a function of the a-spacing. By increasing this spacing, a greater volume of material is sensed to a greater depth. The effective depth of investigation is approximately equal to 1/2 that of the a-spacing. For example, if a 2-m spacing between electrodes is used, then the upper 1 m of the subsurface is effectively sensed. The actual measurement reflects some weighted average of resistivity of all the material that is sensed, so it is termed an apparent resistivity. By convention, the value is plotted at the midpoint between the four electrodes. Plotting all such measurements along a transect yields a profile of apparent resistivity versus horizontal distance.

If measurements are made for more than one a-spacing, then the data can be plotted in a 2-D pseudosection that gives simultaneous display of both horizontal and vertical variations in apparent resistivity. The *z* coordinate is termed pseudodepth and based on theoretical considerations is usually set equal to 0.519 times the a-spacing used for the given measurement. Note that use of the term pseudosection emphasizes that the plot is not to be viewed in a strict sense of assigning the data to these

definite points in the vertical cross section. The pattern of apparent resistivities associated with a given subsurface structure is often complex, and rarely corresponds to the distribution of true resistivities that can only be obtained, in most cases, through modeling. For present study, the data were inversely modeled using RES2DINV, and incorporating a topographic correction where appropriate. The modeled profiles that are presented herein are in terms of true 2D resistivity structure of the subsurface (for example see Figure 4 and Figure 5).

Instrumentation and Field Procedures

An Iris Instruments' Syscal Kid 24-channel system was used for surveying. This is a state-of-the-art system that consists of a transmitter/receiver (TX/RX) unit that takes input from two cables, each of which has 12 take-outs that are connected to metal electrodes emplaced into the ground. The system permits a setup of 24 electrodes for a given spread, with the TX/RX unit situated between the two cables. Thus, measurements can be made for up to seven different a-spacings per spread, noting that the greater the a-spacing, the deeper the sensing.

For measurement, the TX/RX unit automatically cycles through the various a-spacings starting with the shortest. After measurements have been taken for spacings involving the first 12 electrodes (approximately 25 minutes duration), the first cable is physically disconnected from the unit and then "rolled over" to the front of the spread (i.e., moved to the end of the second cable) in preparation for continuing the profile. During the process, measurements are still being made using various combinations of the remaining electrodes (i.e. 13 through 24). Upon completion of measurements for about 2/3 of the remaining combinations (approximately 21 minutes duration), the TX/RX unit is disconnected from the beginning of the second cable and moved to the far end, which is also the beginning of the rolled-over cable. The cables are then re-connected to the unit whereupon measurements are resumed. Moving the unit is necessary to ensure complete coverage for the longer a-spacings. This rollover procedure can be repeated for as many times as desired to produce long pseudosections. We used a minimum a-spacing of 0.5 m for all resistivity data collected in Greenland. With this value the following possible a-spacings can be obtained for a given spread of 24 electrodes: 0.5, 1.0, 1.5, 2.0, 2.5, 3.0 and 3.5 m. Thus, the effective depth of investigation ranged from the ground surface to approximately 1.8 m.

Figure 7. Electrical resistivity surveying with Syscal Kid meter.

Preliminary Results

Resistivity data were collected at two sites: Ø64 over the churchyard and Ø172 over the farm mound. In general, the modeled resistivity profiles revealed highly resistive anomalies within the generally resistive

environment found at the test sites. These resistive anomalies appear to include natural gravel and rock layers, stone architecture, and possibly turf. At Ø64 a long east-west profile running along the UTM N6753640 grid line corresponds closely to other measures of geology. Results of GPR (discussed below) and resistivity indicate a reflective and a resistive layer, respectively, in the west at approximately 10 centimeters below the ground surface (BGS). The western wall of the churchyard is evident in the resistivity profiles as is the cluster of stones at the central church. A resistive anomaly roughly corresponding to the eastern side of the buried churchyard wall and beginning at approximately 50 centimeters BGS also is matched in the corresponding GPR profiles by a reflective surface, possibly a geological feature as the churchyard wall is generally higher in both the GPR and resistivity profiles. North-south profiles along UTM E486086, E486090 , and E486094 grid lines show resistive anomalies corresponding to the eastern side of the buried churchyard wall. These also correspond closely in horizontal and vertical dimensions to strong reflections in the GPR. For example, a resistive anomaly at approximately UTM E486090 N6753646 that extends from approximately 30-110 centimeters BGS appears as a highly reflective surface at its upper interface (Figure 8). At this location, the resistive anomaly extends beyond the reflectors that are identified in the GPR profile, especially to the north, and supports the idea that resistive anomalies are associated with wall fall – perhaps an increased concentration of rocks, void spaces, or turf debris.

At Ø172, two parallel resistivity transects were collected across the farm mound running south-north along the UTM E 471194 and E 471195 grid lines. The two modeled profiles show similar structure over the main part of the mound and is highly suggestive of buried architecture (Figure 4 and Figure 5).

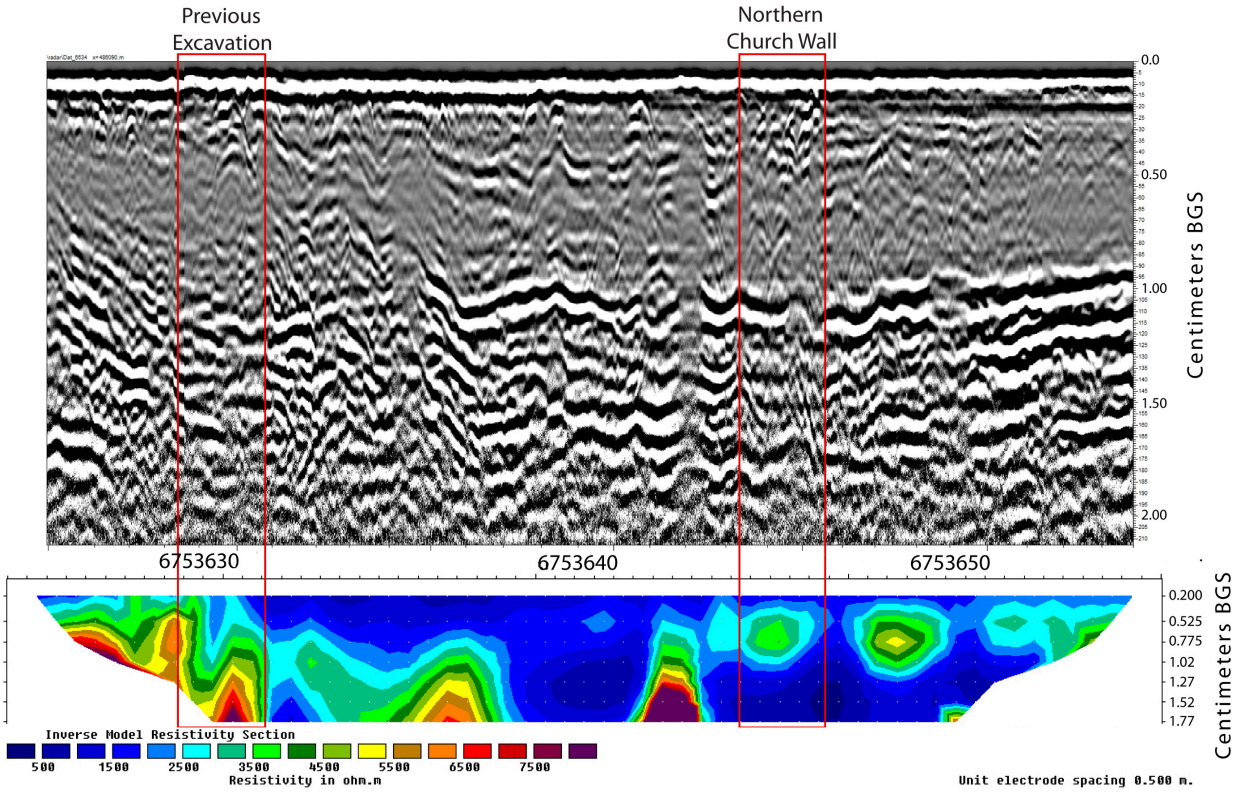

Figure 8. Comparison of GPR (top) and resistivity profiles (bottom) at Ø64 along the UTM E486090 grid line. In the resistivity profile, the red area is more resistive than blue.

Magnetometry

Magnetometry is a primary archaeogeophysical tool because of its capability to detect a wide range of features (Becker 2009; Linford, et al. 2007). Magnetometry measures variations in the Earth's magnetic field. There are two main sources of local variations or anomalies that magnetometry can identify: natural remnant magnetization and induced magnetism. The strength of a magnetic field, sometimes called the magnetic flux density, is measured in nanoteslas (nT). The background of the Earth's magnetic field changes constantly due to diurnal, seasonal, yearly, and solar cycles. The field can vary from 25000 to 65000 nT (Griffin 1987). Anomalies act like magnets with a positive and negative pole and as a result typically have a dipolar signature. In the northern hemisphere, at the latitudes of Iceland and Greenland, the positive aspect of a magnetic anomaly will be positioned over the actual feature causing the geophysical anomaly.

Principles of Method

Natural remnant magnetization (sometimes, called thermoremnant magnetism) is much stronger than induced magnetism. Natural remnant magnetism is created during either the formation of igneous rocks or the reheating and subsequent cooling of rocks or soil past the Curie point. When these rocks are still in place, the remnant magnetization aligns to and enhances the Earth's magnetic field. If these rocks are subsequently moved, the associated anomaly can be identified because the dipolar signature will not align with the declination of the current magnetic field.

Induced magnetism is due to a whole of host of complex natural and anthropogenic processes that increase the magnetic susceptibility (Schmidt 2007). The anthromorphic changes in induced magnetism is an order of magnitude smaller than the natural remnant magnetization (Gaffney and Gater 2003). Nonetheless, ditches, filled holes, formerly heated rocks, clay concentrations, and even trampled soil can act as small weak magnets that can alter the Earth's magnetic field (Kvamme 2006). The strength of the magnetic disturbance decreases rapidly with distance from the source and is usually very small relative to the background field. Note that the in-phase component of EM surveying approximately corresponds to variations in magnetic susceptibility and thus there may be some correspondence with the presence of induced magnetic anomalies and in-phase anomalies. (Tabbagh 1984; Tabbagh, et al. 1988).

In Iceland, we have found that magnetometry is not particularly effective for identifying buried Viking Age turf structures. This is attributed to the remnant magnetization of volcanic basalts that comprise the bedrock which can overpower the subtle variations associated with cultural deposits, including even pyrotechnic deposits like hearths (Steinberg and Byock 2000). However others have had some success with magnetometry in Iceland (Horsley and Dockrill 2002; Horsley, et al. 2003). Clearly, Greenland's older geology is more suitable for magnetometry than Iceland's. Based on our preliminary work, magnetometry has the potential to become a critical tool for archaeogeophysical surveying in Greenland.

Instrumentation and Field Procedures

In Greenland, we used a Geometrics G-858 cesium-vapor gradiometer, which has an upper and a lower sensor. The sensors were oriented at 45° to maximize signal response to prevailing magnetic conditions. A recording interval of 10 readings per second was used and fiducials were recorded every 5 meters based on reference to survey tapes and flags. The operator maintanined an even pace and lines were walked unidirectionally from south to north. A repurposed PVC survey flag post was used to help ensure a consistent distance between the lower sensor and the ground (Figure 9). While the total fields from both sensors were analyzed, the differential or "gradient" (i.e., difference in values between the lower sensor minus the upper sensor, and divided by the distance between sensors) yielded much more information on buried structure than using the total field data alone. The upper sensor did yield information on broad geological trends. Note that no corrections were made for diurnal variations.

Figure 9. Magnetic surveying with the Geometrics G-858 cesium-vapor gradiometer.

Preliminary Results

In general, the expected utility of magnetic surveying in Greenland was borne out in the results. Unlike Iceland, Greenland is not the product of recent volcanic activity, which has resulted in the highly magnetized bedrock that can overwhelm the magnetic signatures associated with more subtle archaeological features. Also, Norse Greenlandic architecture used stones as a primary building material, and these provide an excellent target for magnetometry. In fact, magnetometry proved to be the most effective method for site prospection and mapping, especially in delineating architecture with stone foundations. Geological and archaeological conditions, however, do present a couple of specific issues with the general application of magnetic surveying in Greenland. Magnetometry survey was primarily used at Ø64 with a small section at Ø172. The controller unit shorted out during the survey at Ø172 and therefore could not be used at all at Ø66.

At Ø64 we surveyed several locations, with emphasis on the church and nearby farm mound. The results of these surveys show excellent structure in both areas (e.g., Figure 29). Many of the small anomalies with relatively large negative magnetic gradient values (dark areas without corrsponding highs) in the churchyard are associated with sharp dips in the topography, likely the locations of previous test excavations. The churchyard wall shows outstanding structure, as does the possible central chapel. The farm mound also presents very good structure, although it is hard to interpret. The reading do suggest a complex occupational sequence.

Many Norse sites are situated in areas with either shallow soil accumulation or eroded surfaces. In these areas there may be little "subsurface" component to sites and geophysical surveying may reveal little that is not already apparent on the surface. These conditions were most evident at the "longhouse" of large stones approximately 17 meters in length and 7 meters at its greatest width (UTM E486150, N6753940; see Figure 10) at Ø66. Nearby are two small circular stone rings, approximately 4.5 and 6 meters in diameter, demarcating semi-subterranean structures. The stone foundations are visible on the surface and there is little evidence of other archaeological features. We surveyed the area over the "longhouse" with the magnetometer. Individual stones are clearly delineating in the magnetic results and in general the outline of the building is similar to that visible on the surface (Figure 30). This is somewhat surprising as the entire area is a rocky ledge; nonetheless the rocks outlining walls are clear against the general background of stone scatter and bedrock. While magnetometry appears to be capable of mapping stone

structures in areas of limited soil accumulation or where erosion has occurred, it may add little value in these areas beyond traditional surface survey and mapping.

At Ø172 our limited survey over the farm mound also shows definite structure, although it is also difficult to interpret especially with such a small surveyed area (Figure 39). The buried wheelbarrow, located in a backfilled midden excavation, presents a significant dipole. Nonetheless, there is a substantial range of gradient changes over short distances (greater than at Ø64) that suggest that this method will yield very good results when more broadly applied.

Many known Norse sites in Greenland have standing and ruined stone architecture. These stones affect geophysical surveys, especially magnetic surveying which is highly responsive to the magnetic properties of rocks and the proximity of surface rocks to the sensors. Surface rocks are visible in the magnetic surveys as strong anomalies. Magnetic surveying also detects the presence of buried rocks but due to the 1D nature of the data it is difficult to separate the various responses. In complex multiphase sites, such as farm mounds, it is important to separate surface rocks and visible architecture from subsurface anomalies that may show early phases of site architecture and other archaeological features. We have experimented with mapping surface rocks and then using their locations to filter the data to minimize their response but this process is complicated and requires more research as well as complimentary excavations to test both the relationship between surface and subsurface rocks belonging to the same architectural phase and the interpretation of underlying site structures.

Figure 10. Canyon House at Ø64

Ground Penetrating Radar

Ground Penetrating Radar (GPR) has become The Fiske Center's principal archaeogeophysical method for high-resolution mapping of buried architecture and cultural deposits (Goodman, et al. 2008; Goodman, et al. 2007). A GPR antenna/receiver unit pulses electromagnetic energy into the ground. Interfaces that exhibit significant contrasts in electromagnetic properties (specifically, the dielectric constant) can reflect some of the energy back to the receiver. In general, the longer it takes for the energy to return, the deeper the reflector. The more energy a feature reflects, the "stronger" the reflector. Buried flat rocks, lying parallel to the ground, are some of the strongest reflectors. Saline environments, and conductive media in general, absorb energy and do not reflect much energy back. We can combine individual GPR transects and produce multiple subsurface "slices" of underlying reflectors at varying

depths (e.g., Figure 41). Finally, by combining GPR and electromagnetic results, preservation can be assessed.

GPR can be a very effective method for detecting graves when general conditions are suitable for use of the method (King, et al. 1993). Stronger reflectors that arise from the coffin (if present), the body, and the shaft itself will generally suggest burials. Breaks in the soil stratigraphy and the corresponding grave shaft fill can also be identified (Jones 2008). In addition, either the sides or the bottom of the pit can sometimes be detected if the pit has cut through and disturbed preexisting soil layers (Conyers 2006a:154). Void spaces (e.g., air pockets) from relatively intact coffins and possibly the skull and chest cavity (Hammon, et al. 2000) are potential targets but bones are usually too small to be detected at any depth (Doolittle and Bellantoni 2010). Therefore several possible interfaces can create reflections in GPR data: the vertical grave shaft against the undisturbed soil around it; the interment itself against the backfill of the grave shaft; and any void spaces against the grave shaft and its backfill (e.g., Conyers 2006b; Dionne, et al. 2010).

Principles of Method

GPR uses microwave and radiowave propagation and scattering to image, locate, and quantify changes in subsurface electromagnetic properties (Appel, et al. 1997; Conyers 2005; Goodman and Conyers 1997; Olhoeft 2000). The raw data output from GPR surveying is usually displayed in the form of a radargram which plots the strength and two-way travel time (which can be converted to depth if a velocity is assumed) of the reflections along a transect over which the radar antenna is pulled (Scollar, et al. 1990). The radargram is akin to a profile, but it is notoriously difficult to interpret. Difficulties in interpretation are exacerbated close to the ground surface where reverberations and strong ground-surface waves distort the radargrams. To facilitate interpretations, a series of radargrams from closely spaced transects can be can be combined and "sliced" across the site at a given depth to create an image in plan view. Note that GPR surveying through wet soils with high clay content and conductive media in general can render whole radargrams of archaeological sites uninterpretable (Leckenbusch 2002).

The depth and resolution of GPR depends in part on the frequency of the antenna used, the density of transect spacing, and the vertical scan rate. Lower frequency antennae have higher energy and greater depth of penetration but lower resolution of features. Conversely, higher frequency antennae tend to have higher resolution but lower penetrating power and are more easily dispersed (Conyers 2005). In Iceland we have largely abandoned the use of 250 MHz antenna for anything other than geological mapping and have instead relied heavily on higher frequency 500 and 800 MHz antennae.

Instrumentation and Field Procedures

GPR surveying was performed using a Malå X3M integrated radar control unit with a XV10 Monitor (Figure 11). Both 500 and 800 MHz antennae were tested. The GPR results yielded some of the highest quality of data that we have ever collected in the North Atlantic and indicate the potential value of this method. I n Iceland we generally have to remove the overlying sod to achieve similar data quality. Being able to collect this high quality of data directly on top of grass in Greenland is particularly important given the difficulty of accessing mechanical means for turf removal, such as backhoes, on most survey sites and the exceptionally long recovery time for the local environment.

In general, the quality of GPR data decreases when surveying over dramatically uneven or rocky surfaces such as degraded farm mounds. We were able to record, however, strong reflections from interfaces over 3 m BGS which we attribute to the very high resistivity of the soil (thousands of ohm-m). Transect spacings of 20, 25 and 33 cm were used. The radargrams were sliced using GPR-Slice software and after some experimentation, we settled on using 14-cm thick slices (25 samples within 5 ns) every 10 cm. This provides significant overlap and continuity between slices, yet gives good resolution.

Figure 11. GPR surveying with the Malå unit equipped with the 500 MHz antenna.

Preliminary Results

The soils at the three tested sites were well suited for GPR and data quality was very good. The low grass cover on most sites and soil conditions helped to mitigate one of the most serious potential limitations on the application of GPR to sites in Greenland: removing topsoil in preparation for surveying. In Iceland, the best GPR results were obtained when the surface turf was removed; a technique that provided better coupling between the antenna and ground and resulted in more energy being put into the subsurface. In Iceland we only deturfed sites that were the focus of excavation. Removal of turf is unsuitable to large survey areas and impracticable in Greenland where mechanical means to deturf are not readily available at most sites. Most importantly, the far more fragile Greenlandic ecosystem would be severely damaged by widespread deturfing.

Of the available geophysical methods that we have used in Iceland, GPR has proven particularly effective at identifying buried churchyards. Their most diagnostic feature is a circular enclosure wall but the church structures and graves also are detectable in the data. For this reason the churchyard at Ø64 was intensively surveyed with both the 500 and 800 MHz antennae. The stone enclosure wall which is partly visible on the surface to the north, west, and south is also visible in the GPR results, as is the likely continuation of the wall below the surface to the east (Figure 12) and is consistent with anomalies present in the surveys using other methods: the in-phase component of EM, magnetometry, and resistivity. The central areas of the churchyard were not surveyed with GPR due to the high concentration of surface rocks.

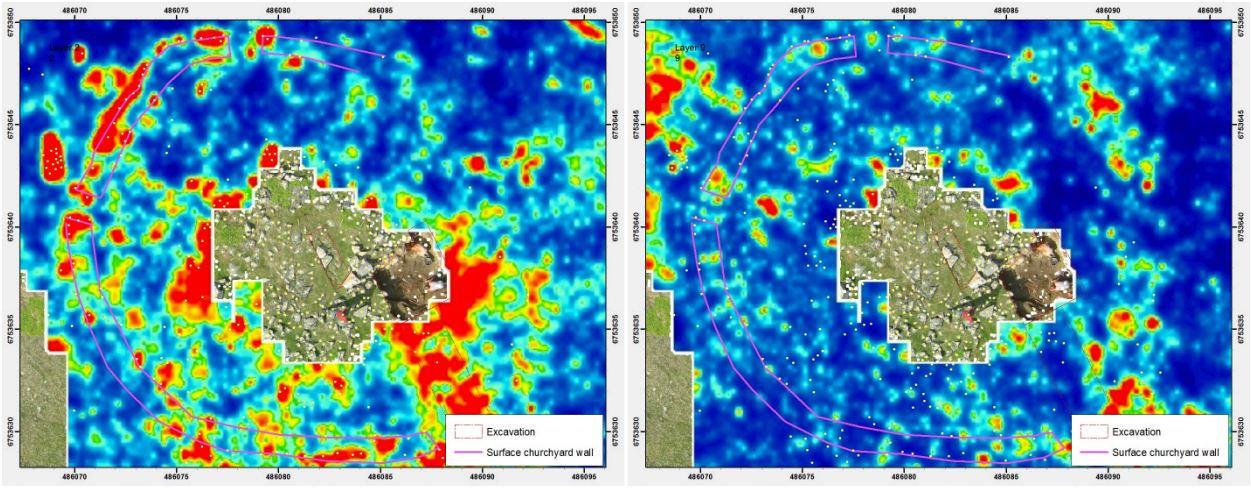

(a) 500 MHz GPR, layer 2, 4-10 cm below ground surface.

(b) 500 MHz GPR, layer 9, 28-35 cm below ground surface.

Figure 12. Results of GPR survey with 500 MHz antenna at Ø64 Churchyard showing circular enclosure wall at different depths: (a) 4-10 centimeters BGS corresponding to visible surface features, and (b) 28-35 centimeters BGS corresponding to buried wall in the eastern part of the churchyard.

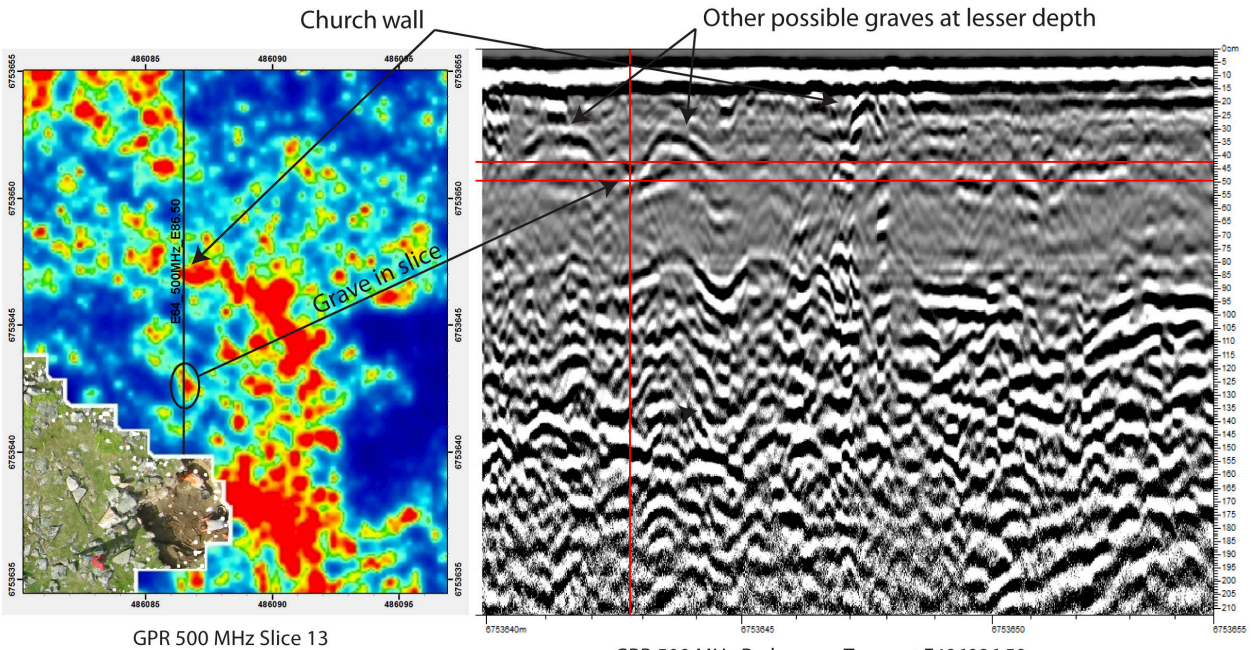

GPR 500 MHz Slice 13
42-49 cm below ground surface

GPR 500 MHz Radargram Transect E486086.50

Figure 13. Results of GPR survey with 500 MHz antenna at Ø64 Churchyard, showing possible grave in the time slice and radargram.

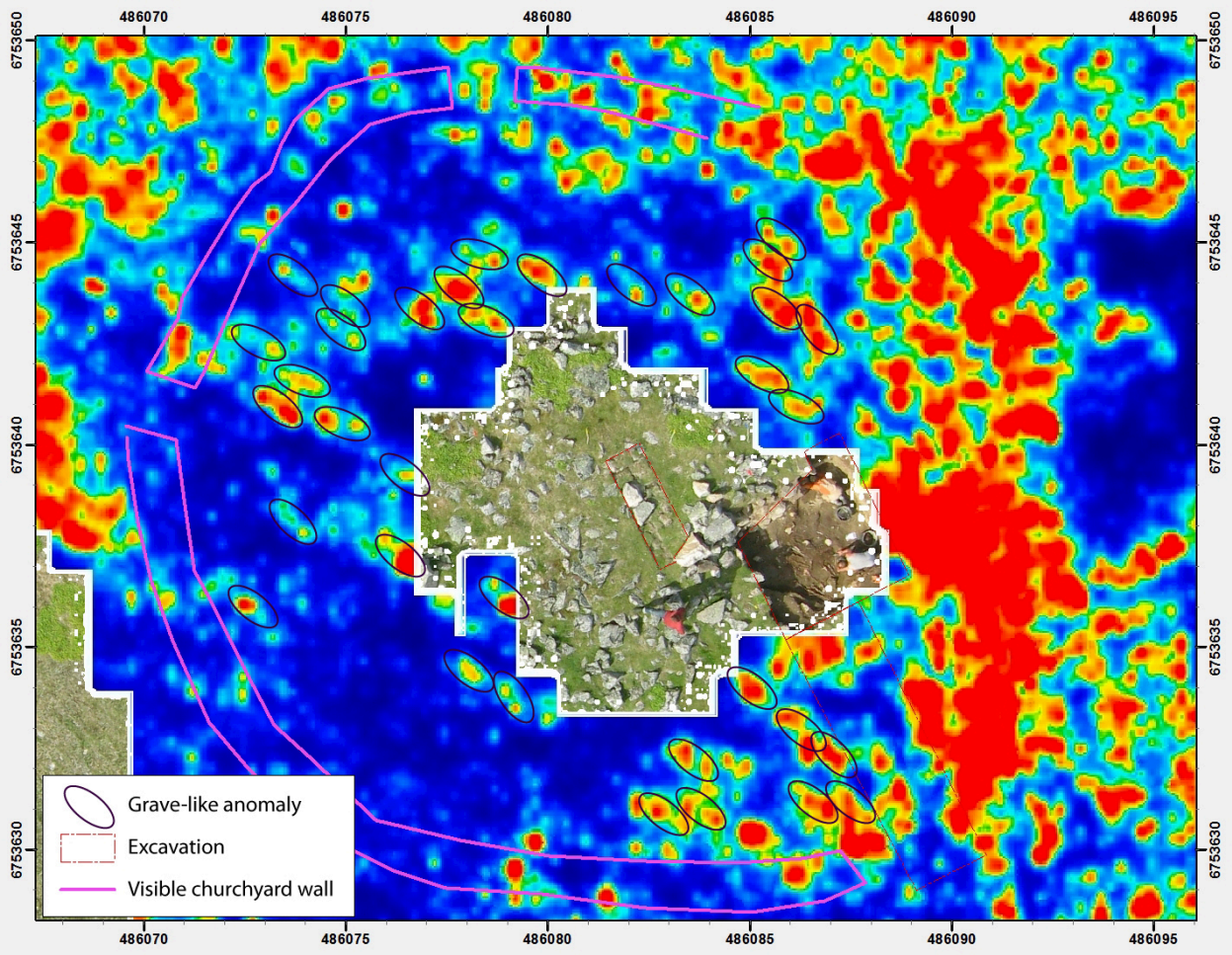

Figure 14. Results of GPR survey with 500 MHz antenna at Ø64 Churchyard, overlay of time slices 11-14 representing 35-53 cm BGS showing areas of possible graves.

The orientation of the reflections from individual features is important for identifying graves. Most obvious in Christian cemeteries is a consistent east-west orientation (Fiedler, et al. 2009). At the ØE64 the graves appear to be oriented roughly 45° northwest-to-southeast–45° relative to the UTM grid north that defined our survey transects (Figure 13). Therefore, the GPR survey transects spaced at 0.20 and 0.25 meters should intersect the long axes of the graves multiple times and each burial should be identifiable across several radargrams (Figure 14). In particular, we look for anomalies that appear on multiple transects that would create a 1.2-2.2 m long and 0.4 m wide deep strong reflector that would result from the remains of the box or grave shaft (Hammon, et al. 2000).

The surface rocks and uneven surfaces associated with many Norse sites present a serious problem for GPR. Rocks that protrude above the ground produce an uneven surface in which the GPR antenna can be lifted off the ground, thus resulting in poor energy coupling as well as creating a substantial airwave that complicates interpretation of radargrams. Large surface rocks also are generally strong reflectors thus reducing the penetration of energy below these features (Figure 8, Figure 13 & Figure 15). Navigating around large surface rocks is possible but still prevents collecting data where specific rocks are present and it may be impossible to navigate around rocks when many are present. Dramatic changes in surface topography can have similar effects. These problems are most severe on farm mounds, many of which

have substantial stone and turf ruins still visible on the surface. For example, at Ø66 we did not attempt to collect GPR data over the extensive farm mound, as it is very unlikely that we would have discovered anything that was not already apparent on the surface. However, it should be possible to collect small areas of high quality GPR data on farm mounds in areas between, or even inside, ruined architecture, at mound peripheries (such as the western edge of the farm mound at Ø64), or on smoother or turf dominated farm mounds such as Ø172. High quality mapping of topography and surface rocks will play an important role in interpreting GPR data of these areas.

Ground penetrating radar is an excellent method for mapping reflective geological features such as buried moraine surfaces, gravels layers, and bedrock surfaces. At Ø64 a curious interruption of a reflective buried surface is apparent in the 500 MHz GPR survey of the churchyard (Figure 16). Beginning at approximately 10 centimeters BGS a highly reflective surface appears to the west of the churchyard. Coring indicates a rocky layer. Over the next 10-20 centimeters the rocky layer extends to the north and east of the churchyard. The layer ends at the immediate boundary of the churchyard and does not appear to continue inside. There are three possible scenarios to explain the absence of this layer from the interior of the churchyard. One, the churchyard was intentionally situated in an area where this reflective layer was absent. This is possible but the degree of correspondence between the end of the layer and the curved churchyard wall makes this scenario improbable. Two, a build up of material in the churchyard has elevated the interior of the churchyard above the reflective layer found outside the cemetery wall. This is somewhat unlikely as the topographic survey indicates that the area inside the wall is roughly at the same elevation as the surrounding landscape and the fact that this reflective layer is not evident at a greater depth inside the churchyard. Alternatively, the reflective layer has been removed from the area inside the churchyard. This could be a result of intentional site preparation or a secondary effect of disturbances such as grave digging, although the later would more likely result in perforations in the layer. Additional excavation is required to determine which of these, or another, scenario is correct.

Figure 15. GPR antenna elevated off ground surface by rocks.

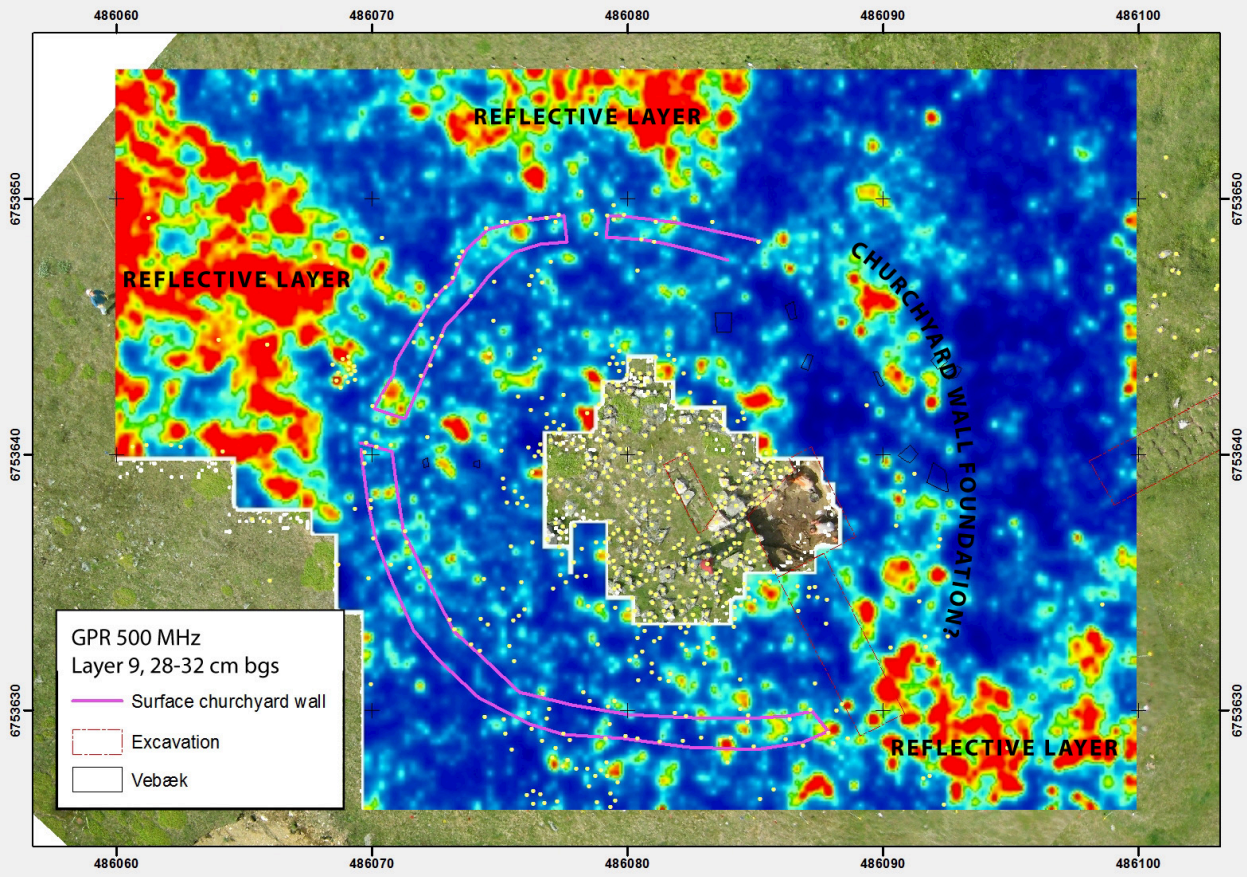

Figure 16. Results of GPR survey with 500 MHz antenna at Ø64, time slice 9 at ca. 28-32 cm BGS showing the interruption of a highly reflective geological layer corresponding to the boundary of the churchyard.

Appendix 1: GPS Base Points and Resectioned Total Station Setup Points

Table 1. Ø64 GPS Base Points and Total Station Reoccupied Set Up Points

Ø64, rock 1	East	North	Elevation
dGPS Base point	486159.725	6753678.83	26.814
Reoccupied set up point	486159.758	6753678.81	27.005
Ø64, rock 2			
dGPS Base point	486020.02	6753731.24	23.89
Reoccupied set up point	486019.958	6753731.25	23.738
Ø64, elevation datum			
Measured total station point	486089.144	6753715.649	25.171


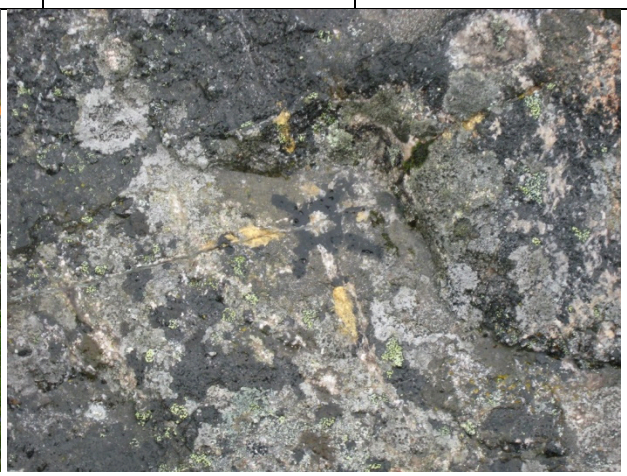

Ø64 Rock, 1 overview and close up.


Ø64 Rock 2, overview and close up.

Table 2. Ø172 GPS base points and total station reoccupied set up points

Ø172, FX	East	North	Elevation
dGPS Base point	471342.54	6741388.74	25.01
Reoccupied set up point	471342.51	6741388.74	25.214
Ø172, west rock			
dGPS Base point	471058.03	6741296.29	11.54
Reoccupied set up point	471058.07	6741296.29	11.153
Ø172, red circle			
Additional set up point	471162.399	6741358.19	12.75
Ø172, x-rock			
Additional set up point	471237.992	6741360.88	17.789s

Table 3. Ø66 GPS base points and total station reoccupied set up points

Ø66, boundary rock	East	North	Elevation
dGPS Base point	485131.727	6750722.48	32.15
Reoccupied set up point	485131.68	6750722.57	32.11
Ø66, high rock			
dGPS Base point	485071.5	6750759.97	37.01
Reoccupied set up point	485071.708	6750759.96	37.329
Ø66, church rock			
dGPS Base point	485039.532	6750821.42	32.112
Reoccupied set up point	485039.603	6750821.35	32.191

Appendix 2: Summary of Geophysical Datasets

Table 4. Greenland 2010, GPR index

Site	Date	Area	Oper.	Ant.	Transc. Space (m)	Point Int. (m)	Files (# Profiles)	Start Coord.	Dir	Mode	Fieldbook (raw/proc.)
E64	8/6/10	Church	BD	500	0.25	0.02	6494-6702 (209)	NE: 486100E 6753655N	N-S (uni)	fid (1m)	I: 1-11 I: 12-13
E64	8/9/10	Mound	BD	500	0.25	0.02	6703-6743	NW: 486100E 6753660N	N-S (bi)	fid (1m)	I: 39-42
E64	8/10/10	Church	BD	800	0.20-0.25	0.02	6748-6843 (96)	NW: 486070E 6753655N	N-S (uni)	fid (1m)	I: 55-60 I: 61-62
E172	8/13/10	Mound/Strip	BD	500	0.25	0.02	6844-6860 (17)	SW: 471193E 6741360N	S-N (uni)	fid (1m)	I: 74-75 I: 73
E66	8/15/10	Field	BD	800	0.33	0.02	6861-6891 (31)	SW: 485100E67 50765N	E-W (bi)	fid (1m)	I: 79-82
E66	8/15/10	Field	BD	500	0.33	0.02	6892-6922 (31)	SW: 485140E67 50815N	E-W (bi)	fid (1m)	I: 80, 83-85

Table 5. Greenland 2010, resistivity index

Site	Date	Area	Loc	Dir.	Length (m)	Min. Spac. m (levels)	File (Raw/Proc)	Num. Meas.	1st Electrode	1st Plot Point	Fieldbook (raw)
E064	8/8/10	Church	90E	N-S	29.5	0.5 (7)	90E.bin 90E_Corr.dat	282	486090 E 6753655.75 N	6753655.0 N	I: 32-33, 38
E064	8/8/10	Church	94E	N-S	29.5	0.5 (7)	94E.bin 94E_Corr.dat	282	486094 E 6753655.75 N	6753655.0 N	I: 34, 38
E064	8/8/10	Church	40N	E-W	35.5	0.5 (7)	40N.bin 40N.dat	348	486101.75 E 6753640 N	486101.0 E	I: 35-37
E064	8/8/10	Church	86E	N-S	17.5	0.5 (7)	86E.bin 86E.dat	150	486086 E 6753657.75 N	6753657.0 N	I: 37
E172	8/12/2010	Mound/Strip	195E	S-N	29.5	0.5 (7)	195E.bin 195E.dat	282	471195 E 6741359.25 N	6741360.0 N	I: 64-65
E172	8/13/2010	Mound/Strip	194E	S-N	29.5	0.5 (7)	194E.bin 194E.dat	282	471194 E 6741359.25 N	6741360.0 N	I: 76-77

Table 6. Greenland 2010, magnetometry index

Site	Date	Area	Type	Trans. Spac (m)	Sample Rate (Hz)	File (Raw/Proc) (# Transects)	Grid Size (m)	Start Coord.	Dir	Mode	Condition	Fieldbook (Raw)
E64	8/7/10	Church	Grad	0.25	10	Dataset1.bin (161) ChurchMag_Corr_B-T	40 x 29 irreg.	SW: 486060 E 6753640 N	S-N (uni)	fid (5m)	short grass	I: 15-30
E64	8/10/10	Mound	Grad	0.25	10	Dataset2.bin (121) Dataset2.dat	30 x 25	SW: 486100 E 6753635 N	S-N (uni)	fid (5m)	short grass, rocks	I: 43-54
E64	8/11/10	Long House	Grad	0.25	10	GA_set3. Bin Dataset3_Corr.dat	18 x 13 irreg.	SW: 486155 E 6753932 N	S-N (uni)	fid (3,5m)	dirt, rocks	I: 63
E172	8/13/10	Mound/ Strip	Grad	0.25	10	GA_set4.bin Strip.dat	4 x 30	SW: 471193 E 6741360 N	S-N (uni)	fid (5m)	short grass	I: 67-68
E172	8/13/10	Mound	Grad	0.5	10	GA_set5.bin Mound.dat	30 x 60 irreg.	NE: 471220 E 6741390 N	E-W (bi)	fid (5m)	short grass	I: 69-72

Table 7. Greenland 2010, electromagnetic conductivity index

Site	Date	Area	Oper.	Type	Trans. Spac (m)	Station Spacing (m)	File (Raw/Proc) (# Transects)	Grid Size (m)	Start Coord	Dir	Fieldbook
E64	8/7/10	Church	JMS	EM31	0.50	0.08		40 x 30		S-N (bi)	
E64	8/9/10	Church	JMS	EM38ip	0.25	0.025		10 x 30		S-N (bi)	
E64	8/11/10	Mound	JMS	EM31	0.50	0.05		15 x 35		S-N (uni)	
E172	8/12/10	Mound	JMS	EM31	0.50	0.08		60 x 30 (irreg.)		E-W (uni)	
E172	8/13/10	Mound/ Strip	JMS	EM38ip	0.25	0.05		4 x 30		S-N (uni)	
E172	8/13/10	Mound/ Strip	JMS	EM38q	0.25	0.05		4 x 30		S-N (uni)	
E172	8/13/10	Mound/ Strip	JMS	EM31	0.25	0.05		4 x 30		S-N (uni)	
E66	8/14/10	Field	JMS	EM31	1.00	0.10		60 x 150 (irreg.)		N-S (bi)	
E66	8/15/10	Field	JMS	EM38ip	0.50	0.05		30 x 10		E-W (bi)	
E66	8/15/10	Field	JMS	EM38q	0.50	0.05		30 x 10		E-W (bi)	

Appendix 3: Ø64 Survey and Datasets

The survey at Ø64 included a medieval churchyard, farm mound, and the ruins of a possible Viking Age longhouse across the river to the north of the site. Data collection focused on the churchyard and farm mound. The churchyard is visible on the surface with a roughly circular wall preserved on the northern, western, and southern sides and a concentration of stones in the center. The circular boundary wall is clearly visible in the electromagnetic, resistivity, magnetic, and GPR surveys. All geophysical methods indicate a continuation of the wall in the east below the contemporary surface. The GPR survey did not include the central stone structure as the surface was too rocky and uneven but the structure shows up in the other geophysical surveys. Concentrations of magnetic and electromagnetic anomalies suggest a rectilinear structure aligned southeast of grid east. This orientation would conform to the long axis of the churchyard enclosure but in both cases the scatter of surface rocks makes interpretation of the underlying foundations uncertain.

Electromagnetic and magnetic surveys over the farm mound generally confirm anomalies corresponding to visible clusters of rocks on the surface. The strongest concentration of anomalies indicates three architectural clusters in the surveyed area of the mound.

Two GPR surveys were conducted in the churchyard, one with the 500 MHz antenna covering the entire area of the churchyard and a smaller sample with the 800 MHz antenna covering the western and northern sections . GPR results effectively show the outlines of the church wall, including what appears to be the buried section to the east. The eastern wall corresponds to the location and depth of the wall in other datasets such as magnetometry and resistivity. Anomalies corresponding to expected criteria of graves can be seen in the churchyard area that fit the depth and geometry of graves. Without further tests and ground truthing it is impossible to tell if these anomalies are, in fact, graves, and whether or not the GPR is over or underestimating the number of graves.

A magnetic survey was conducted at a highly eroded structure comprised of large oblong outline of stones located on a small terrace overlooking the river north of the site.

Topographic Data

1. General coverage of church, farm mound, and surrounding areas …
2. High resolution (ca. 1 meter collection spacing) coverage of church and sections of farm mound.

Geophysical Surveys

1. Magnetometer (G858)
    a. Magnetometer, Church (E64_MAG_A)
    b. Magnetometer, Farm mound (E64_MAG_B)
    c. Magnetometer, “Longhouse” on ridge (E64_MAG_C)
2. Ground Penetrating Radar
    a. Mala 500 MHz, Church (E64_GPR500_A)
    b. Mala 800 MHz, Church (E64_GPR800_A)
3. Resistivity (Syscal Kid)
    a. Church, 86 east (E64_RES_86E)
    b. Church, 90 east (E64_RES_90E)
    c. Church, 94 east (E64_RES_94E)
    d. Church, 40 north (E64_RES_40N)
4. Electromagnetic conductivity
    a. EM-31, Church (E64_EM31_A)
    b. EM-31, Farm mound (E64_EM31_B)
    c. EM-38 (in-phase), Church (E64_EM38_ip_A)

Aerial Photograph Coverage

1. 07 August 2010, Farm mound and church (92 images)
2. 10 August 2010, Farm mound and church (132 images)

Site Specific Results:

1. Churchyard mound: EM, GPR, magnetometry, and resistivity
    a. Good delineation of structure, outer wall, and graves
2. Mound: EM, Mag
    a. Sorting surface stones from subsurface stones

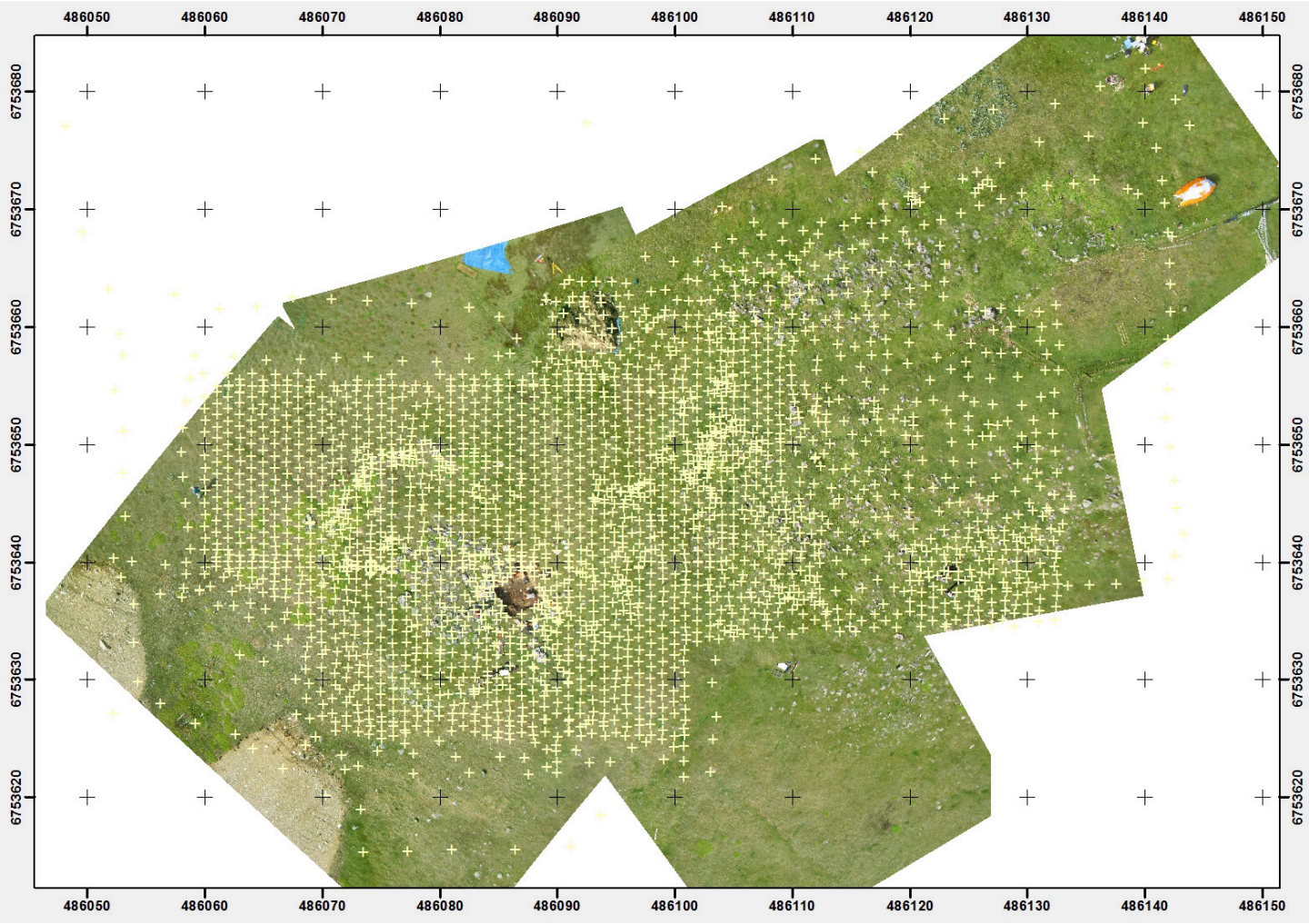

Figure 17. Ø64 Topographic sampling density over churchyard and farm mound.

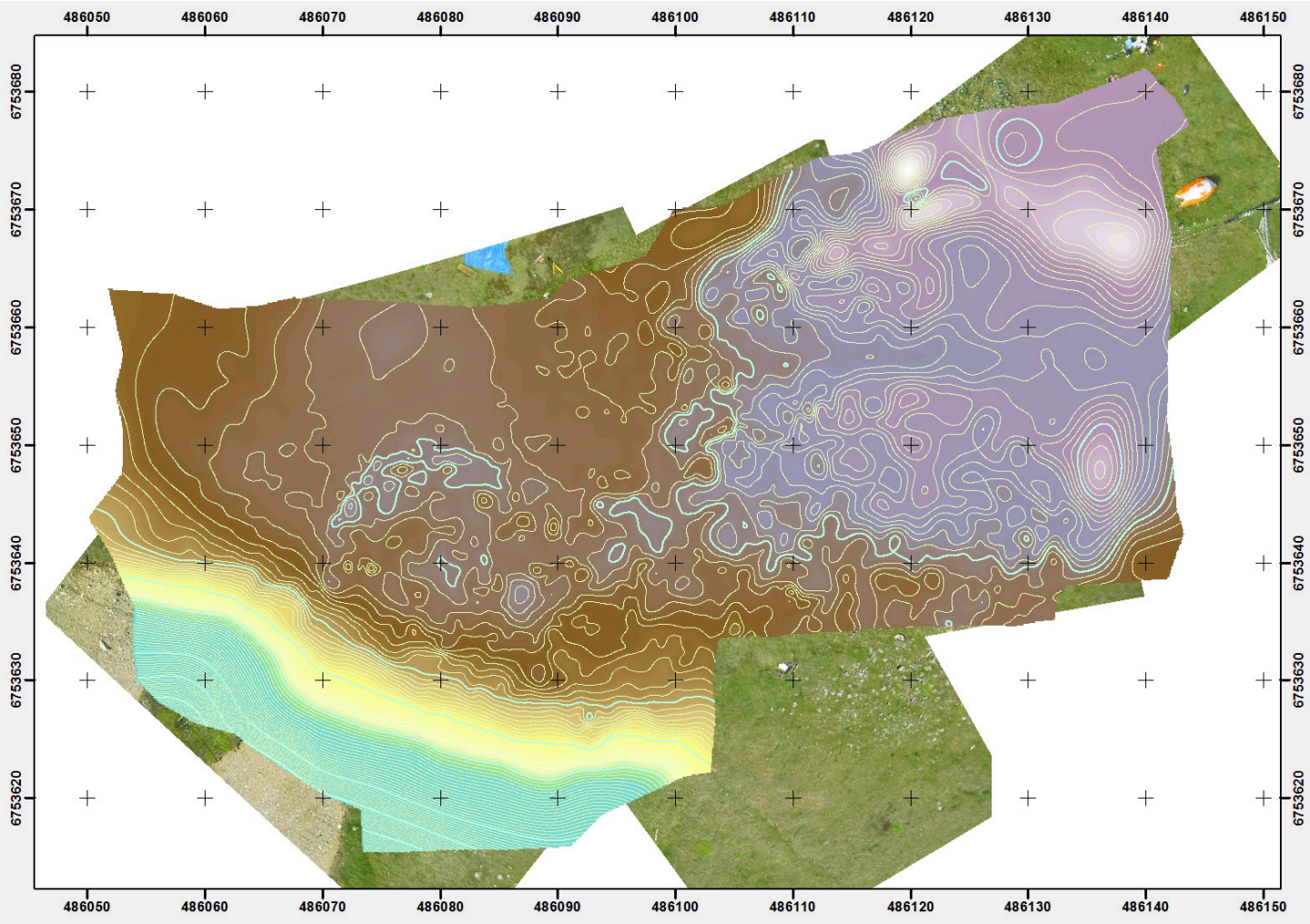

Figure 18. Ø64 Elevation map of churchyard and farm mound with contours at 0.10 meters.

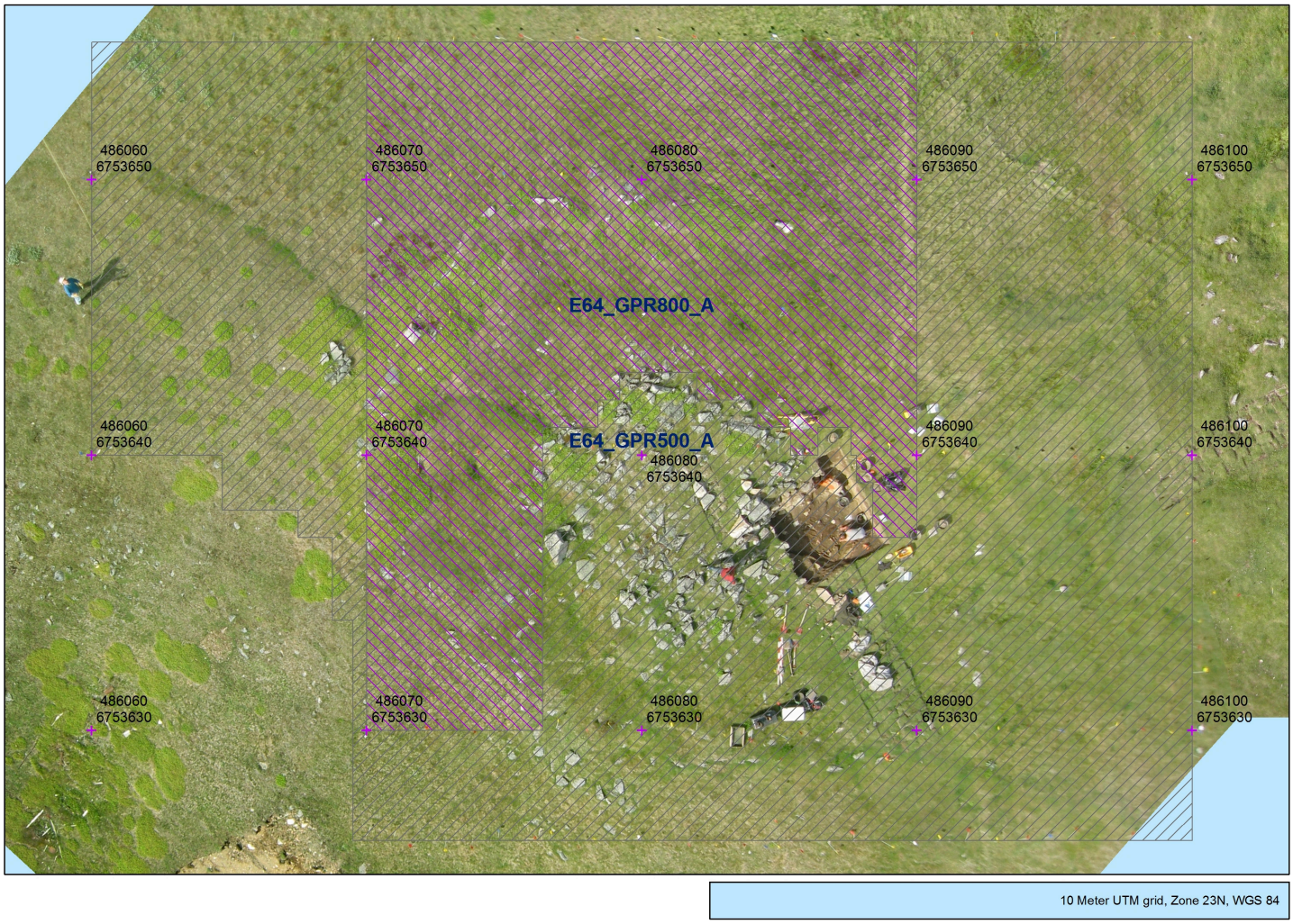

Figure 19. Ø64 Location of GPR survey (hatched area). GPR radargrams and time slices are incorporated into the text

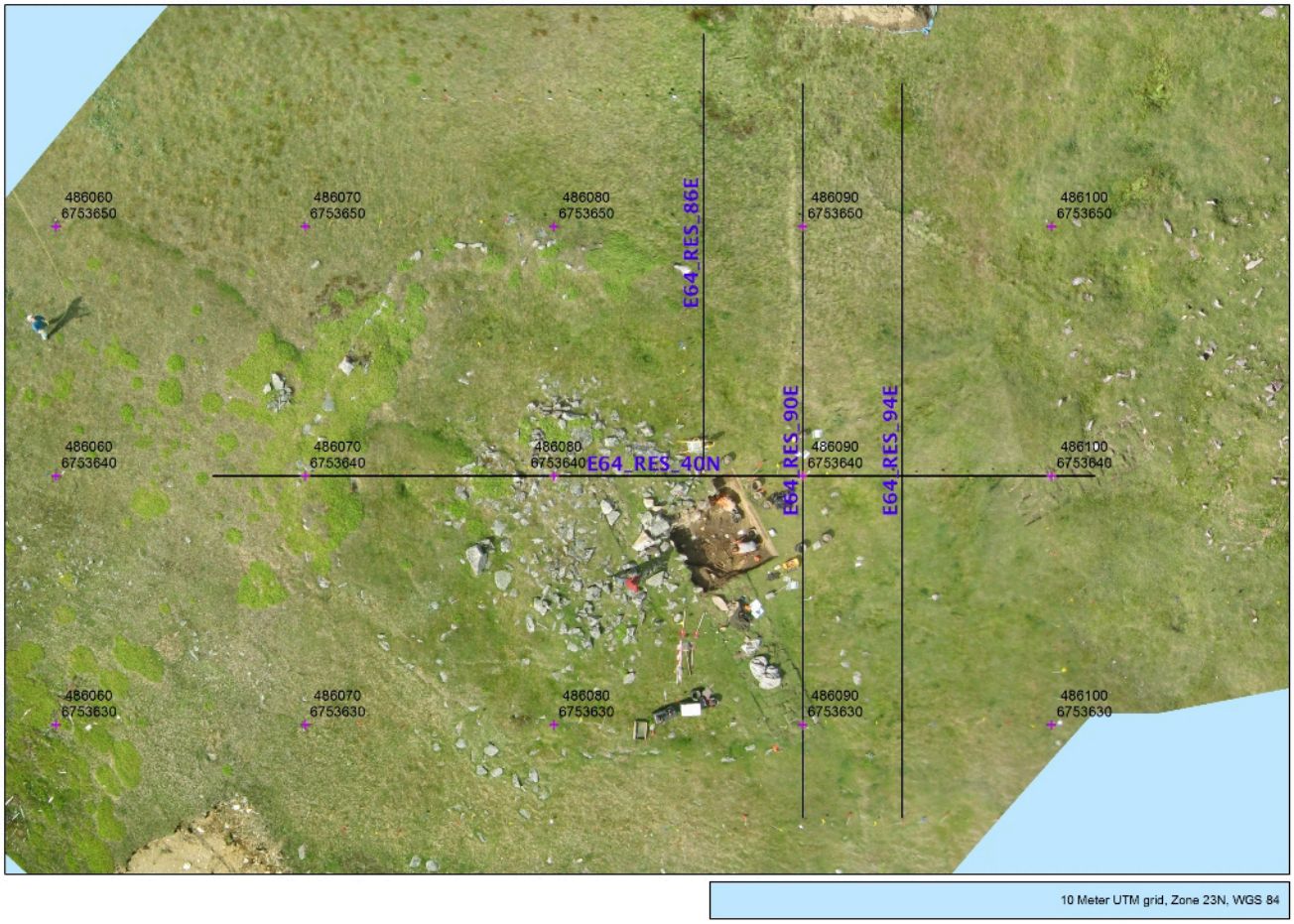

Figure 20. Ø64 Location of resistivity transects at churchyard.

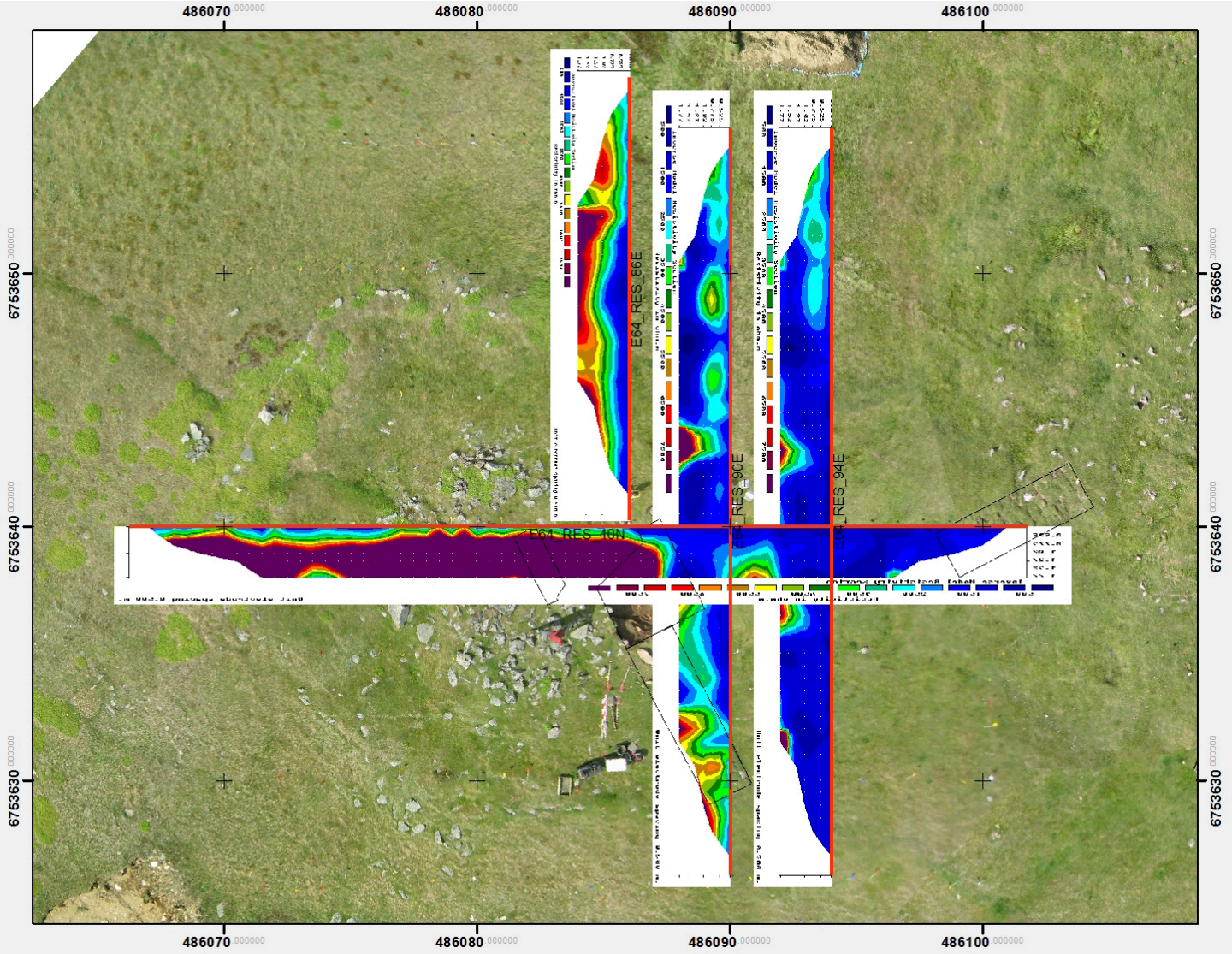

Figure 21. Ø64 Location of modeled resistivity profiles at churchyard. The vertical axis on the profiles represents depth below ground surface.

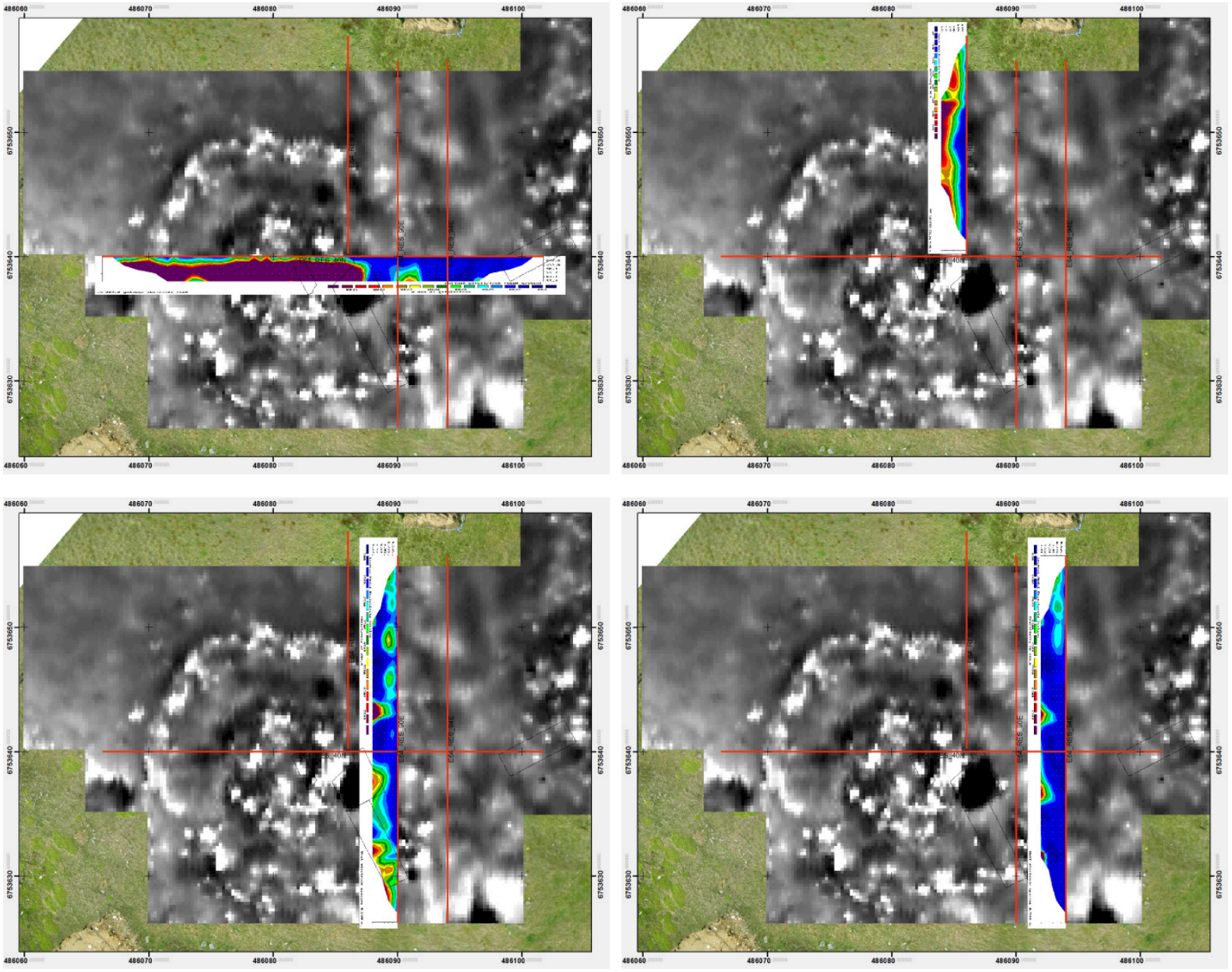

Figure 22. Ø64 Location of modeled resistivity profiles at churchyard. The vertical axis on the profiles represents depth below ground surface .

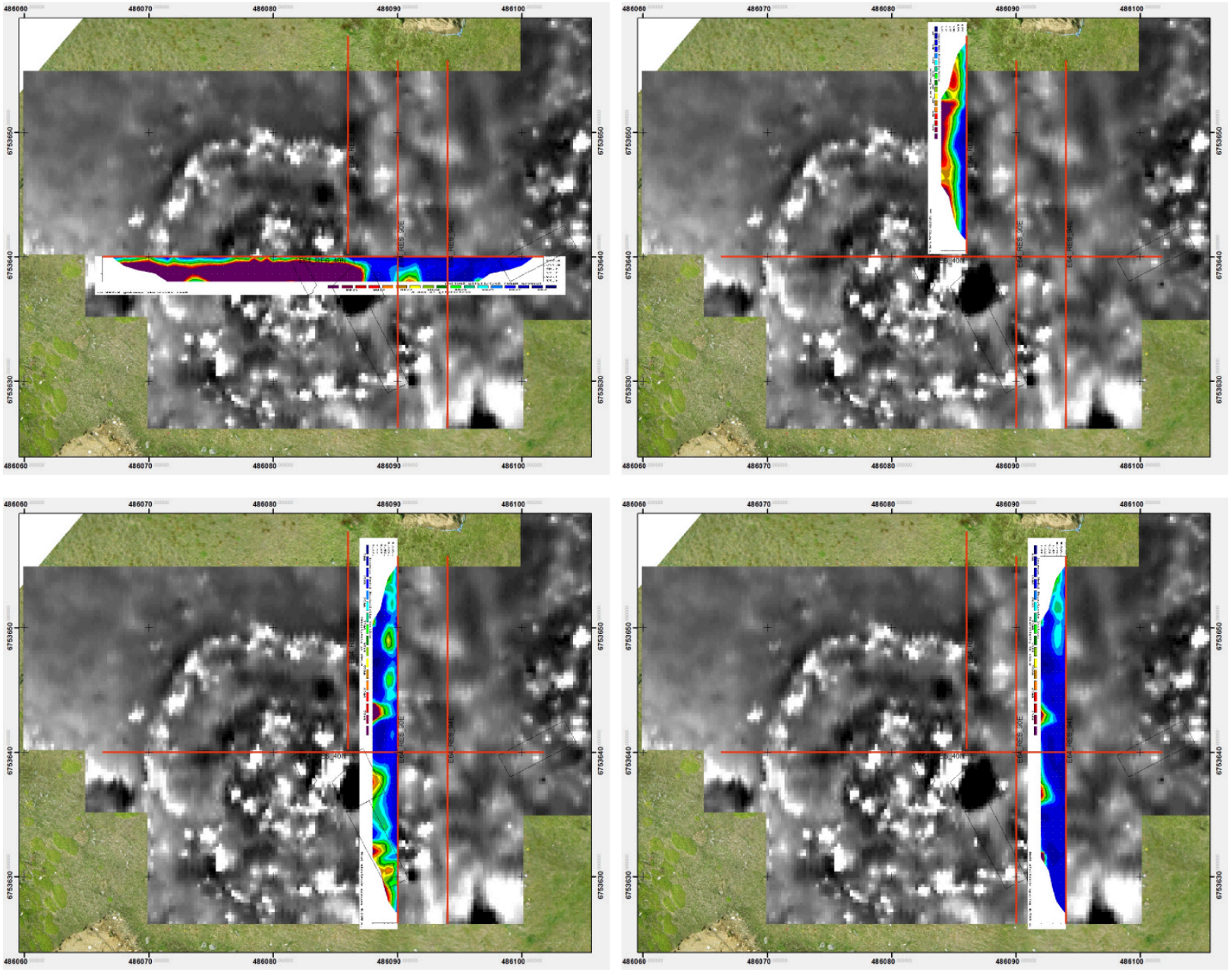

Figure 23. Ø64 Resistivity profiles superimposed over magnetic results for the churchyard. The vertical axis on the profiles represents depth below ground surface.

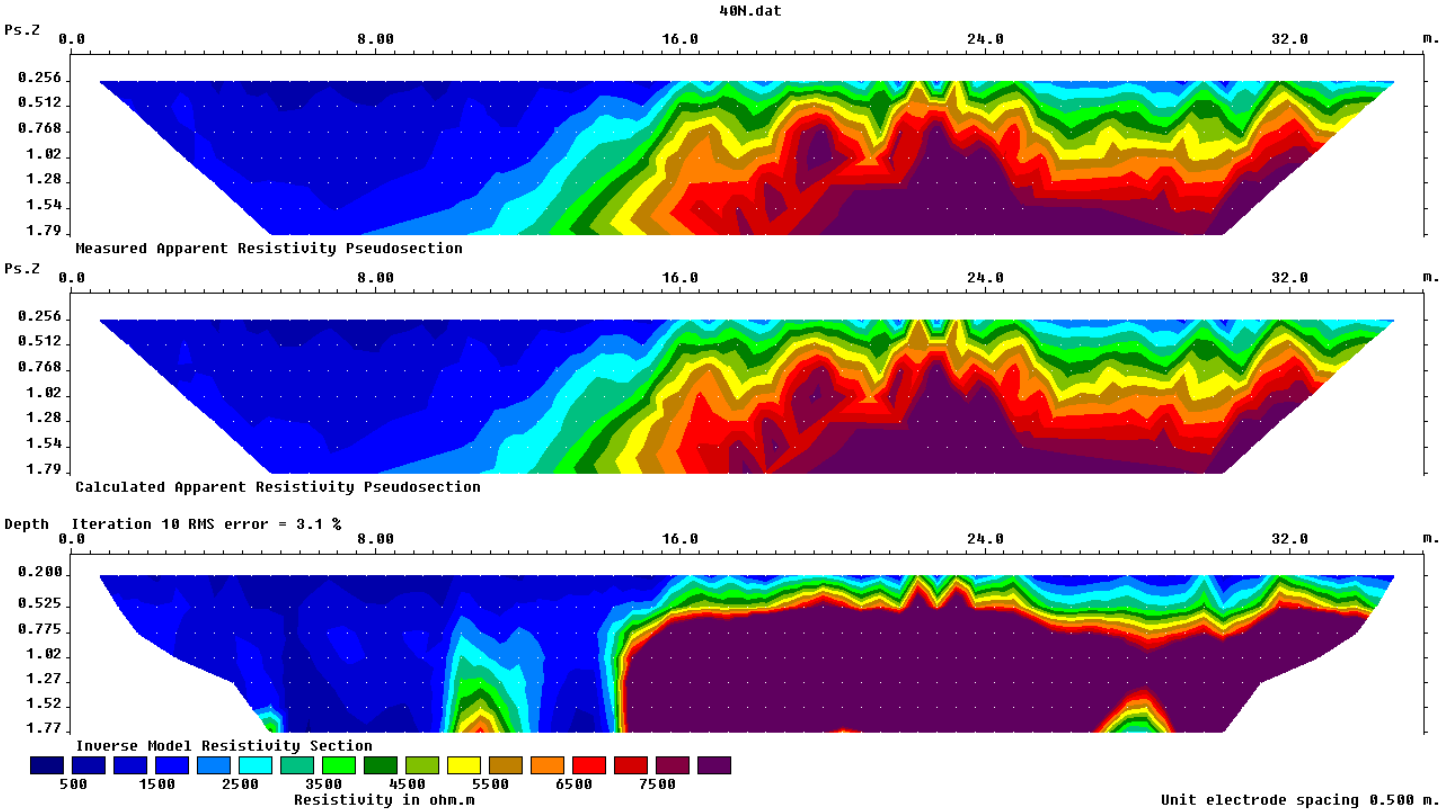

Figure 24. Ø64 Resistivity profile UTM N 6753640. The top image is a pseudosection of recorded data. The middle profile is the calculated pseudosection for the inverse modeled resistivity structure generated by RES2DINV shown in the lower figure. For a well-defined model, the upper and middle images should appear similar.

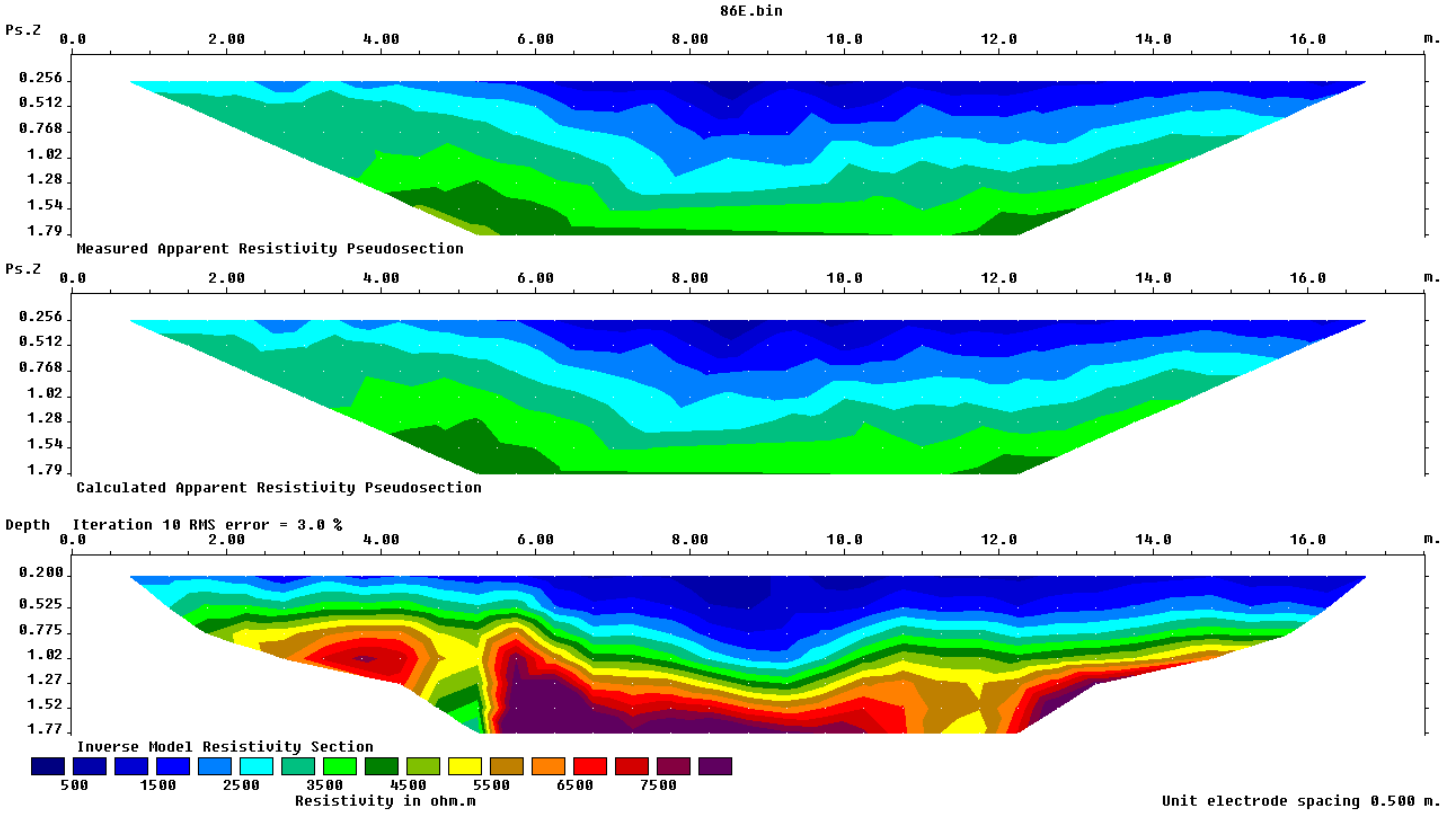

Figure 25. Ø64 Resistivity profile UTM E486086 The top image is a pseudosection of recorded data. The middle profile is the calculated pseudosection for the inverse modeled resistivity structure generated by RES2DINV shown in the lower figure. For a well-defined model, the upper and middle images should appear similar

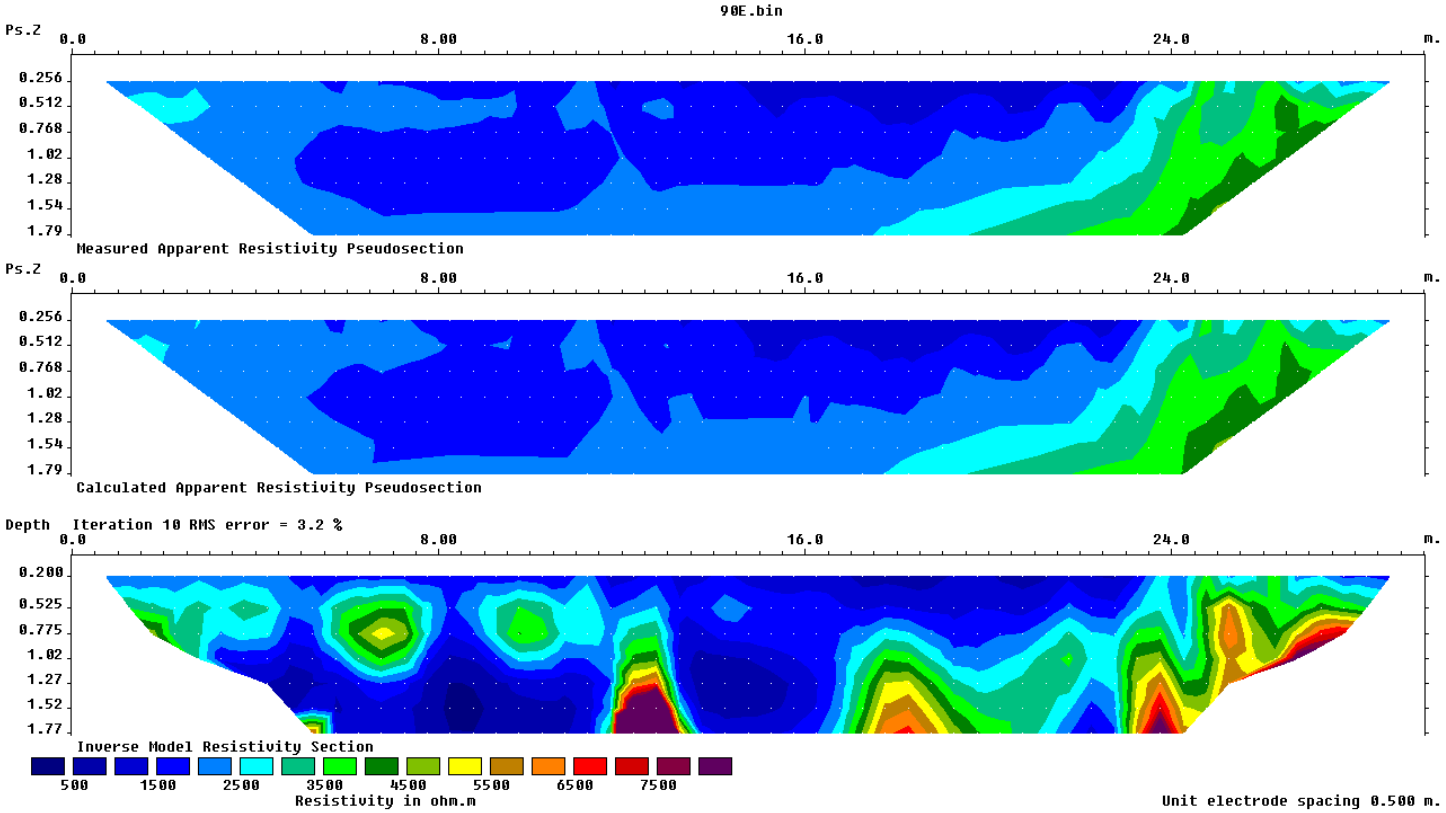

Figure 26. Ø64 Resistivity profile UTM 486090. The top image is a pseudosection of recorded data. The middle profile is the calculated pseudosection for the inverse modeled resistivity structure generated by RES2DINV shown in the lower figure. For a well-defined model, the upper and middle images should appear similar

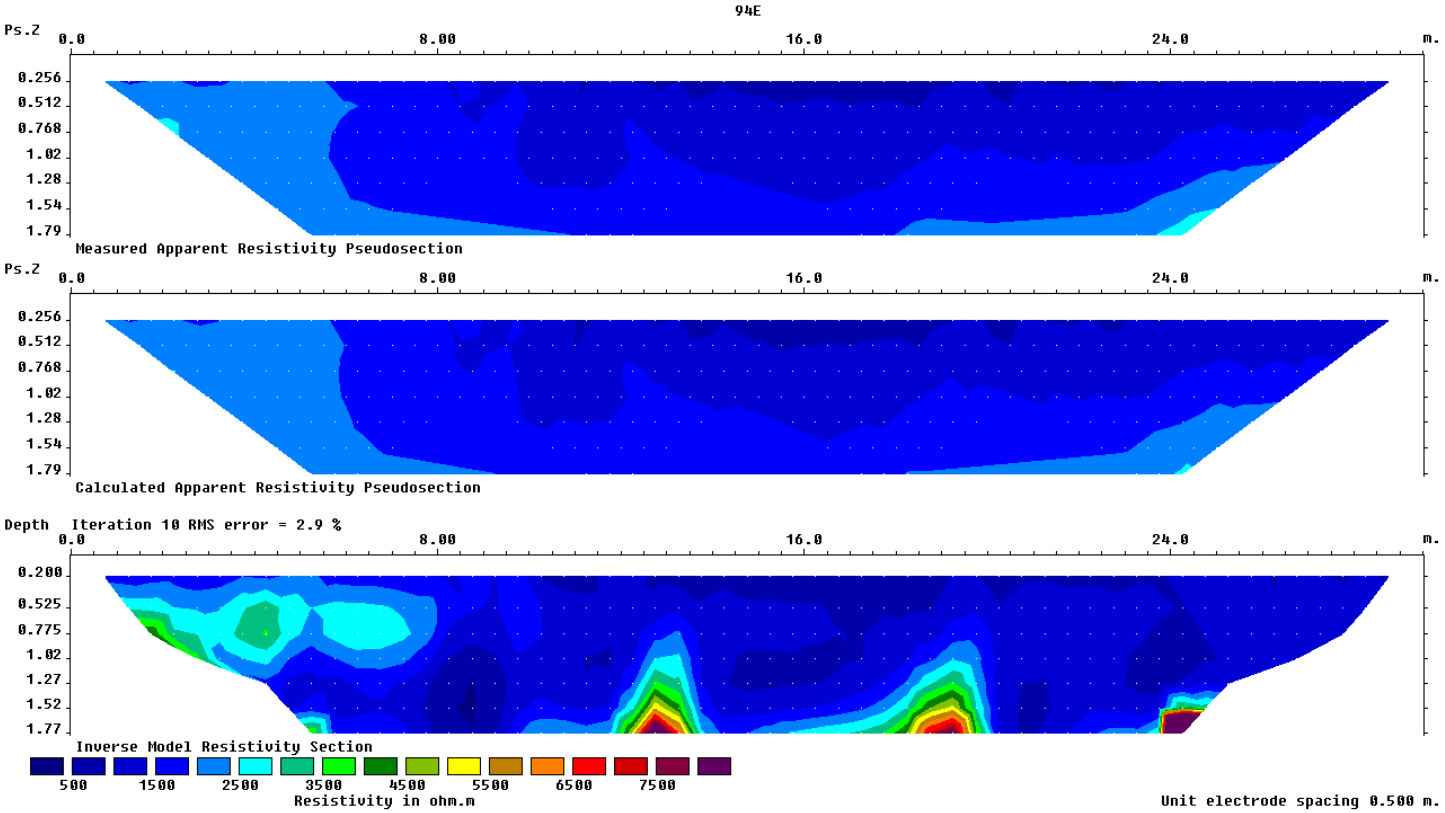

Figure 27. Ø64 Resistivity profile 486094. The top image is a pseudosection of recorded data. The middle profile is the calculated pseudosection for the inverse modeled resistivity structure generated by RES2DINV shown in the lower figure. For a well-defined model, the upper and middle images should appear similar

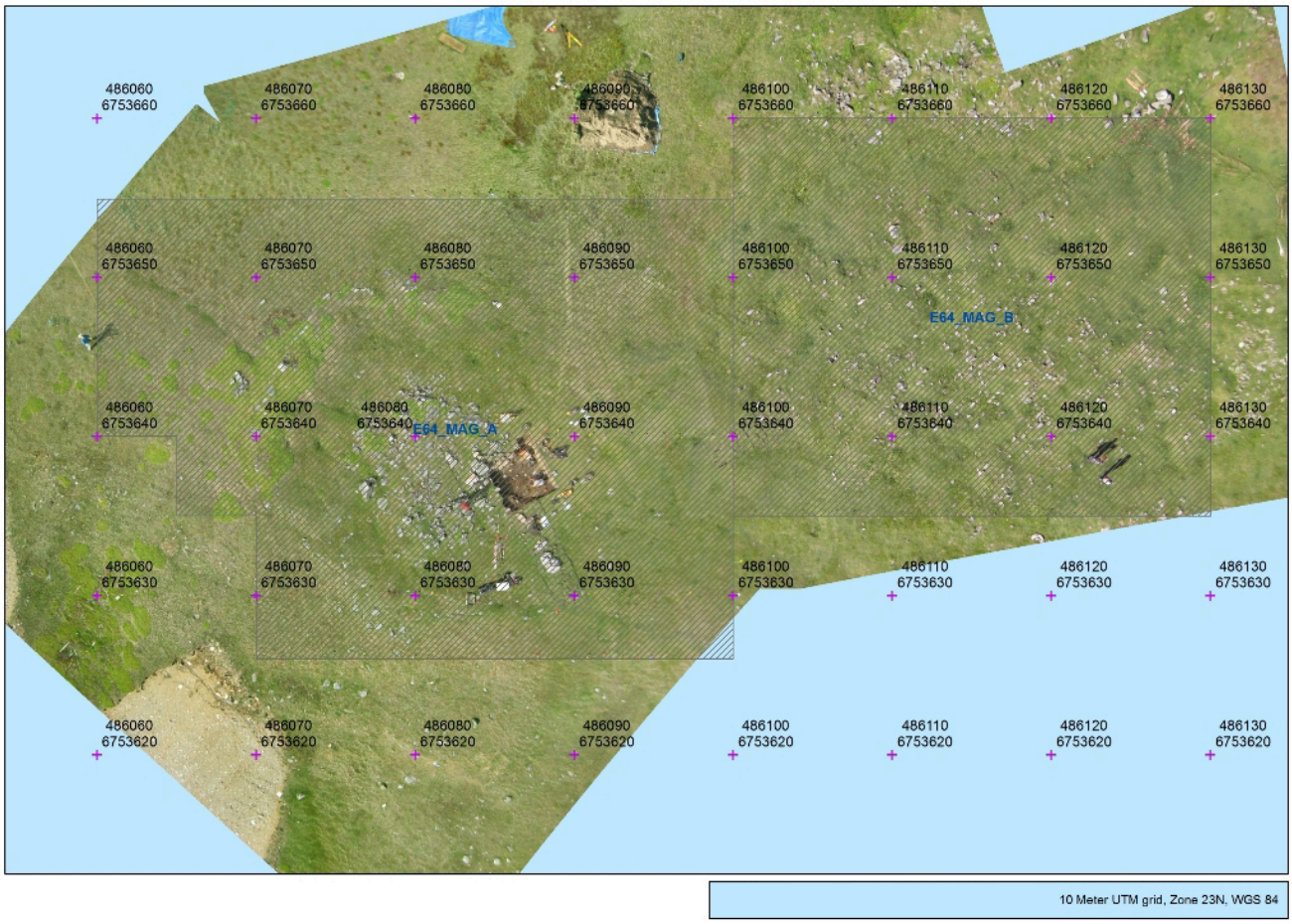

Figure 28. Ø64 Location of magnetic surveys (hatched areas). Magnetometer surveys were conducted in two conjoined areas, one centered over the churchyard, the other centered over the medieval farm ruins.

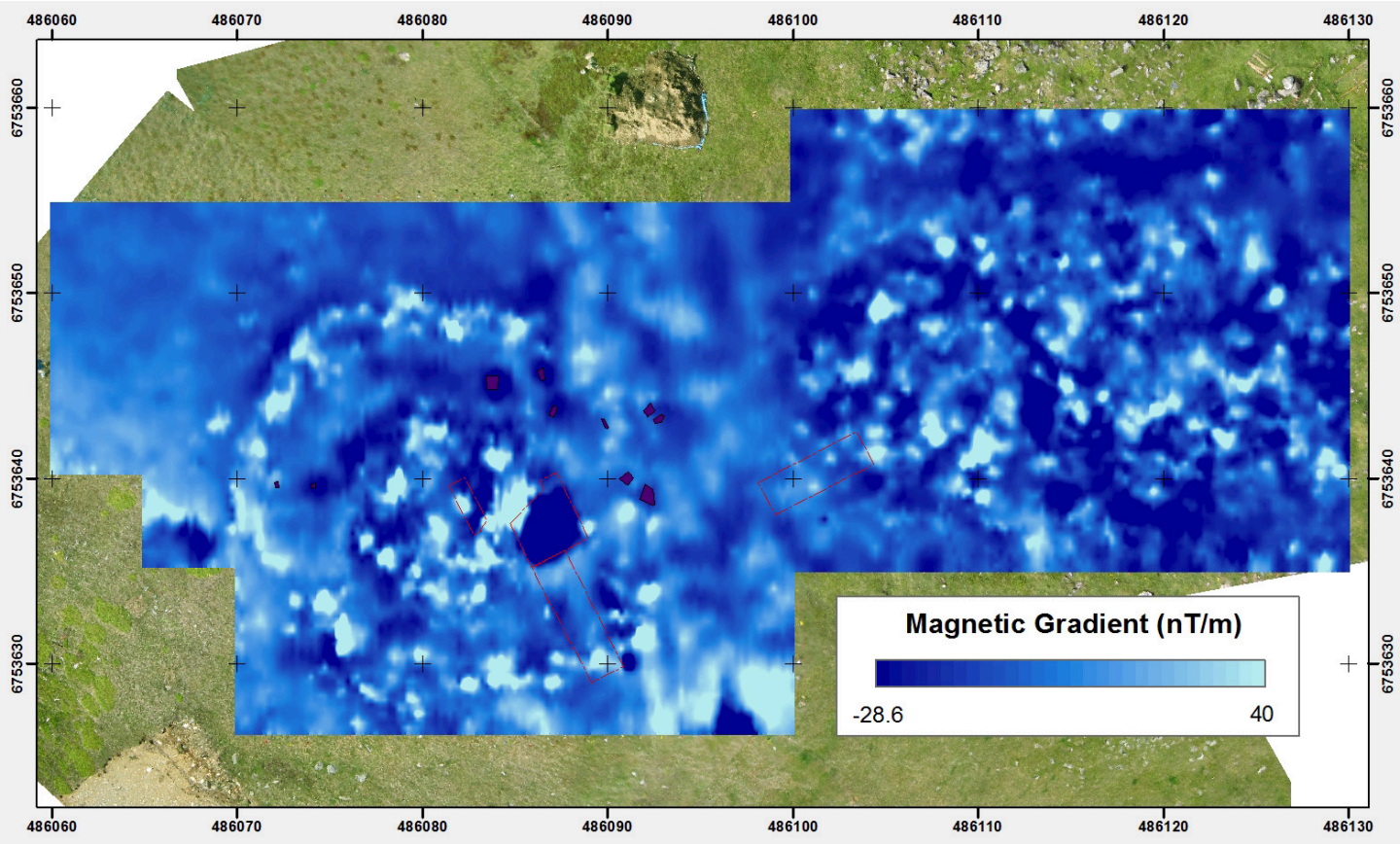

Figure 29. Ø64 Results of magnetic surveys. Excavations and depressions are also indicated.

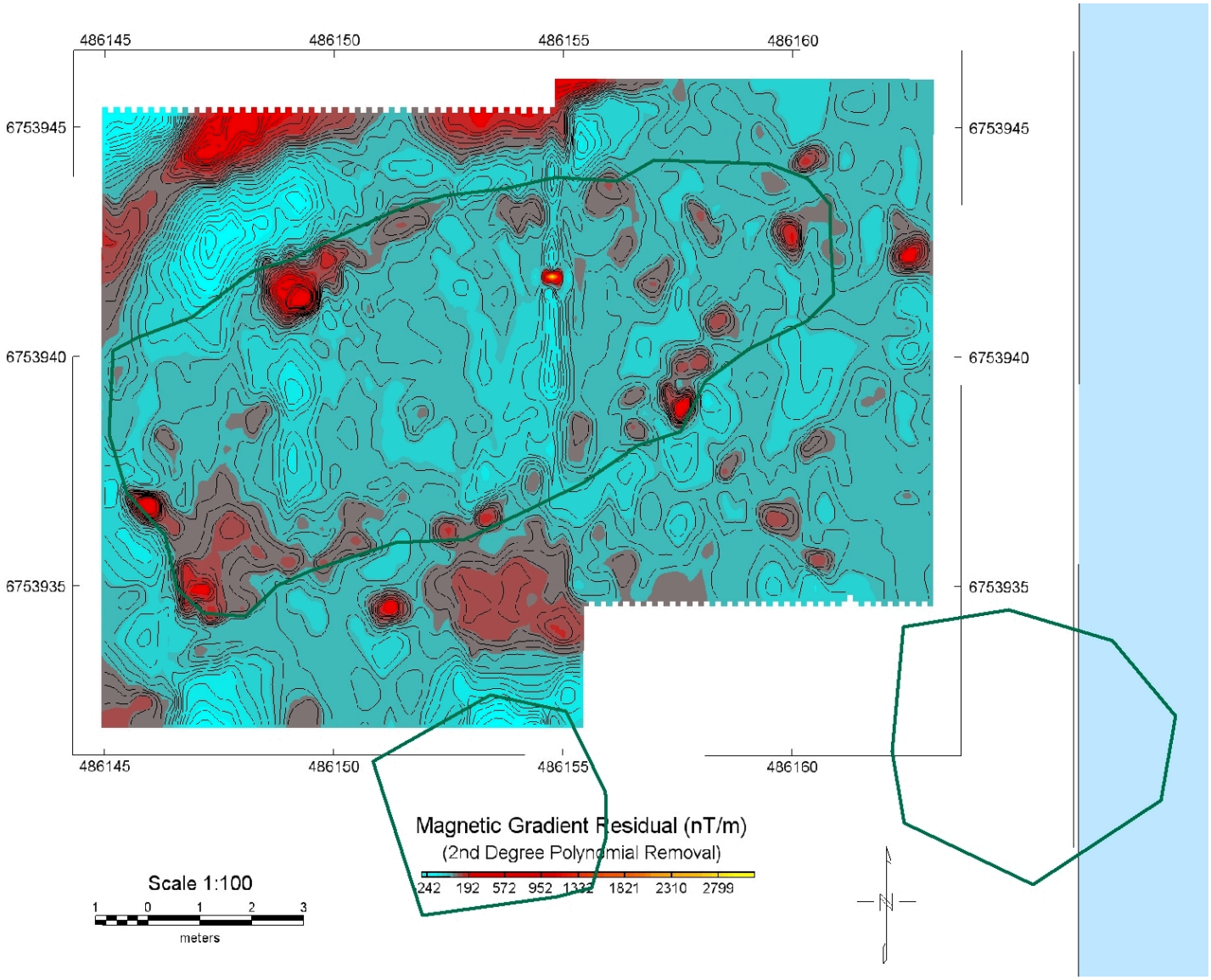

Figure 30. Magnetic survey at Ø64 Canyon House.

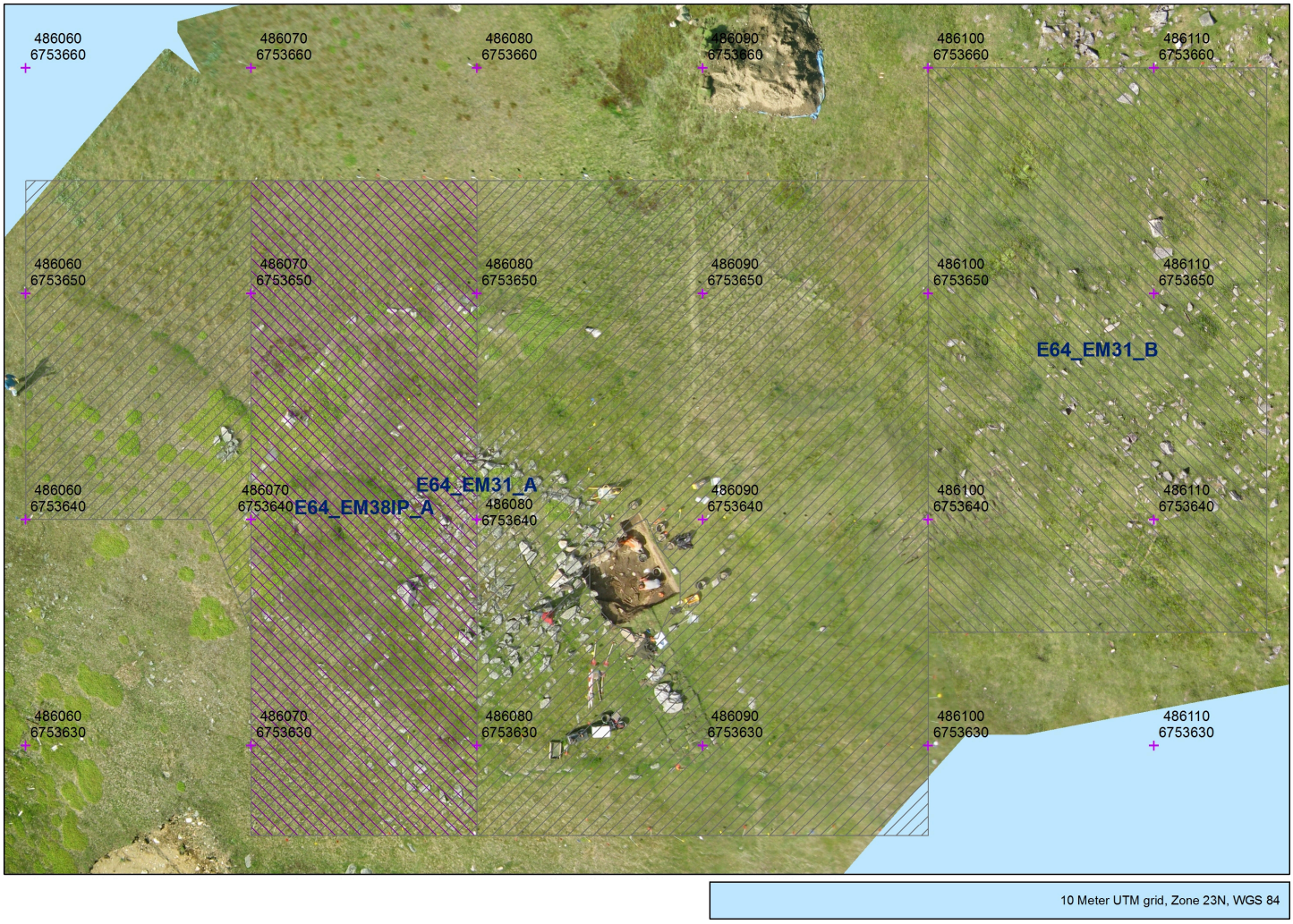

Figure 31. Ø64 Location of Electromagnetic surveys (hatched areas).

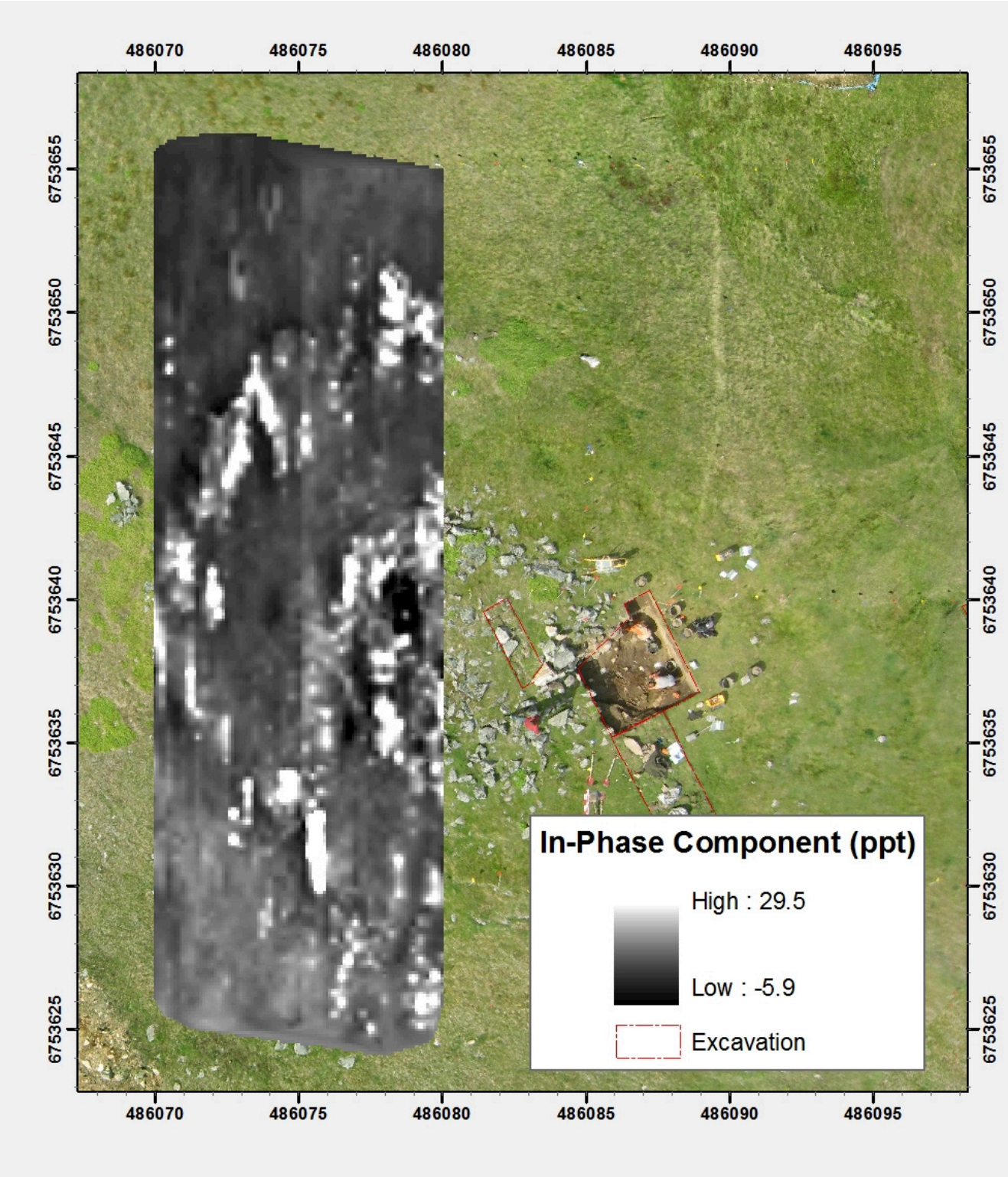

Figure 32. Ø64 Results of in-phase survey over churchyard using the EM-38.

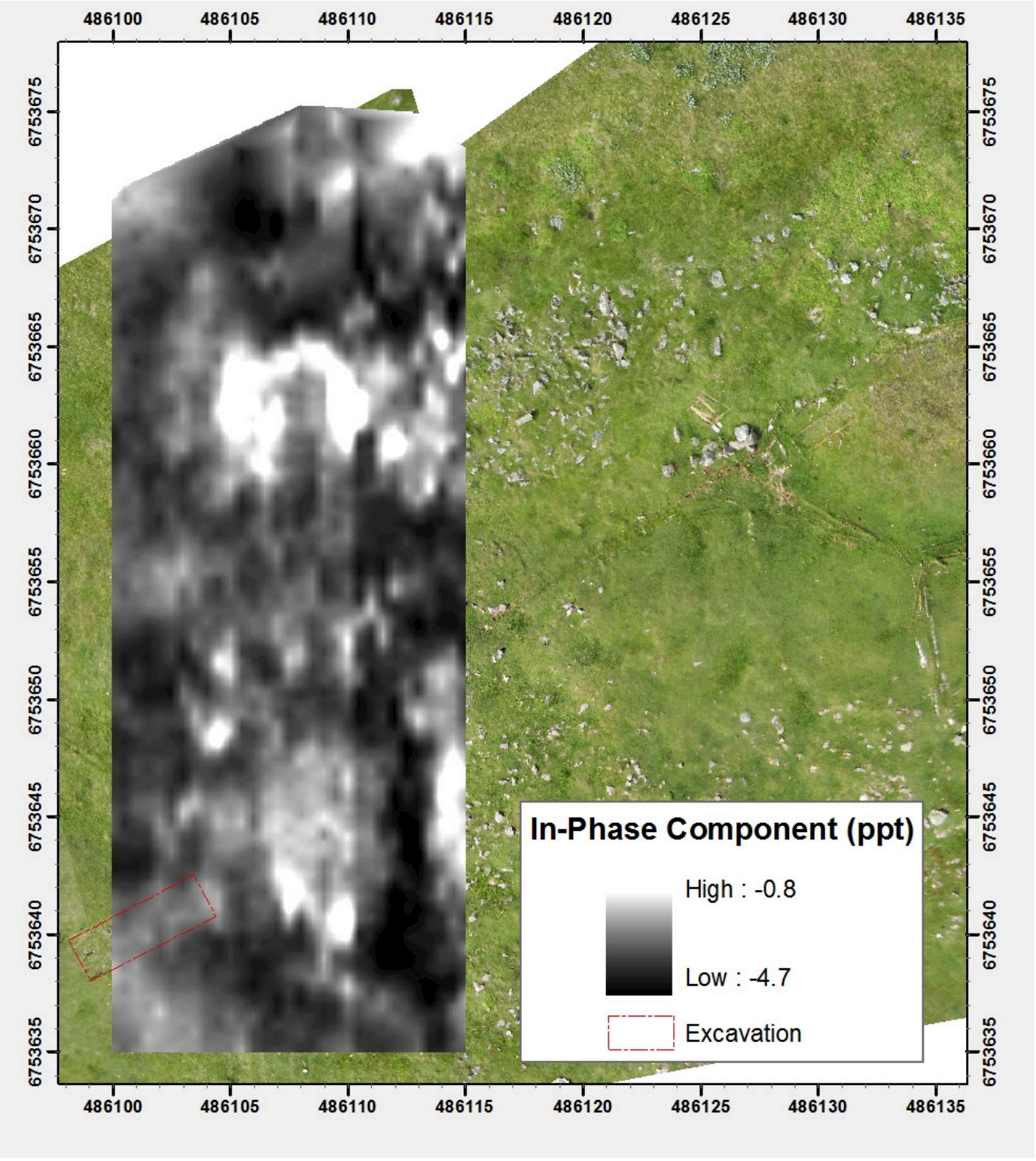

Figure 33. Ø64 Results of in-phase survey over farm mound using the EM31.

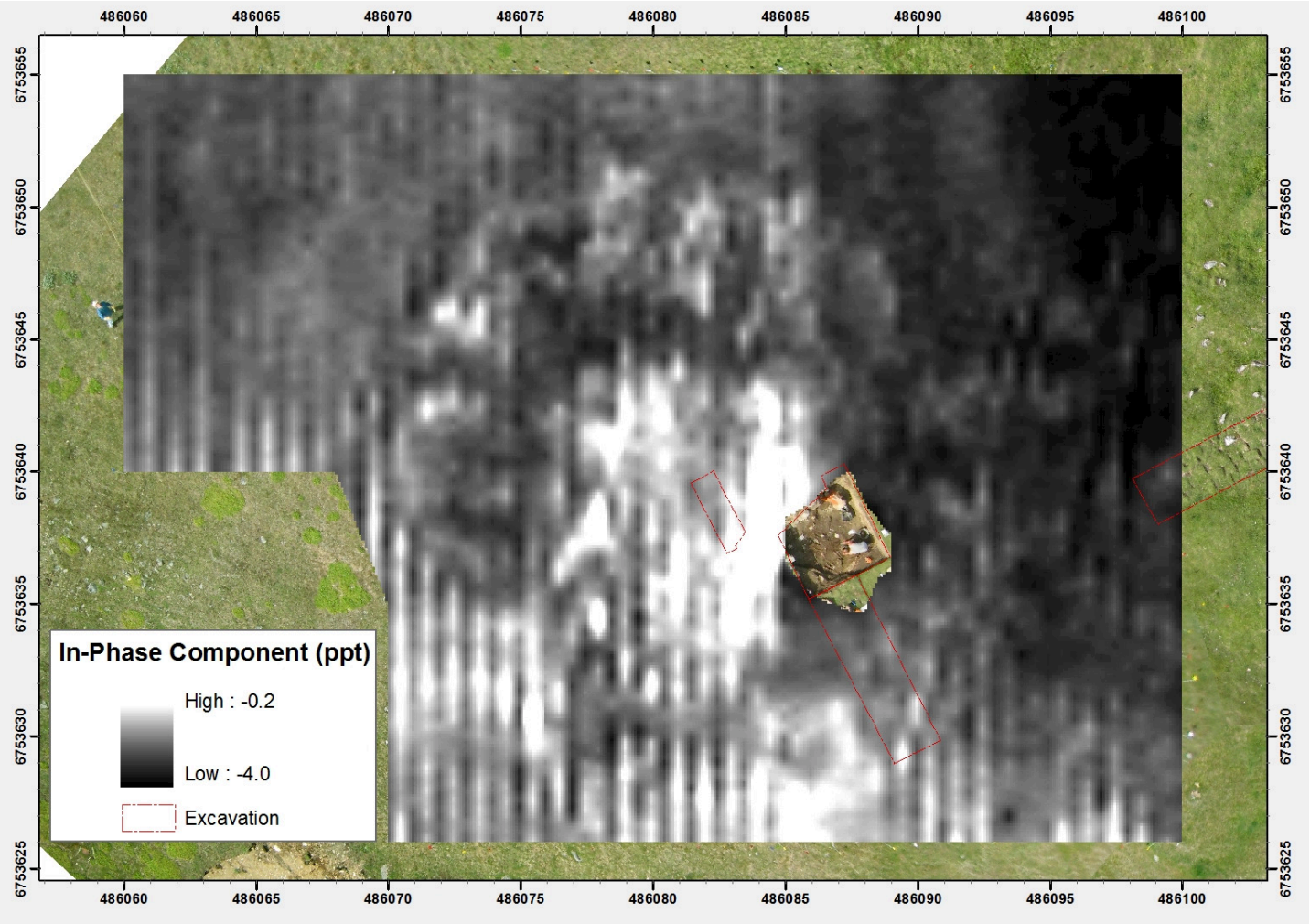

Figure 34. Ø64 Results of in-phase survey over churchyard using the EM31. Striping is due to walking profiles in alternating directions over a sloping surface.

Appendix 4: Ø172 Survey and Datasets

Conditions during the two-day survey at Ø172 were less than ideal with near continuous rain and fully saturated ground. The Norse farm mound ruins at Ø172 were surveyed with both electromagnetics (EM-31) and magnetometry. Moisture penetrated the control panel for the magnetometer approximately halfway through the survey causing it to malfunction. Geometrics was later able to recover most of the data from the controller but the magnetometer was rendered inoperable for the remainder of the field season. The wet, turfy conditions of the farm mound were better suited to electromagnetic surveying than the other test sites. Both the electromagnetic and magnetic surveys show concentrated anomalies in the area of the farm mound and appear to be suitable methods for delineating site boundaries and identifying concentrations of subsurface architecture.

A small north-south oriented strip, 4 x 30 meters, across the farm mound was surveyed using all geophysical methods employed in the study: two resistivity profiles collected along the UTM E471194 and 491195 grid lines, magnetometry, electromagnetics (both apparent ground conductivity and in-phase surveys using the EM31 and EM38), and GPR with the 500 MHz antenna. The strip is too thin to identify clear architectural features but all datasets show structured anomalies. Given the right conditions archaeogeophysical surveying should be able to identify subsurface architecture. In Iceland, we have had trouble translating geophysical anomalies into coherent architecture in farm mounds due in large part to the complexity of these multiphase sites. The shorter span of occupation at most Greenlandic farm mounds present opportunities.

The near complete lack of wind during our stay at Ø172 prevented the collection of kite-based aerial photographs.

Topographic Data

1. General coverage of farm mound and surrounding areas:
    a. 5-meter interval over the farm mound
    b. 1-meter and individual resistivity electrodes over north-south strip in center of farm mound
    c. General coverage of surrounding area
2. No kite-based aerial photography due to low wind conditions
    a.

Geophysical Surveys

5. Magnetometer (G858)
    a. Magnetometer, Farm mound (E64_MAG_B) (partial dataset, equipment failure due to rain)
    b. Magnetometer, Farm mound, central strip (E64_MAG_B)
6. Ground Penetrating Radar
    a. Mala 500 MHz, Central strip
    b. Mala 800 MHz, Central strip
7. Resistivity (Syscal Kid)
    a. Farm mound, Central strip, 195 east
    b. Farm mound, Central strip, 194 east
8. Electromagnetics
    a. EM-31 Farm mound
    b. EM-38 (in-phase), Central strip

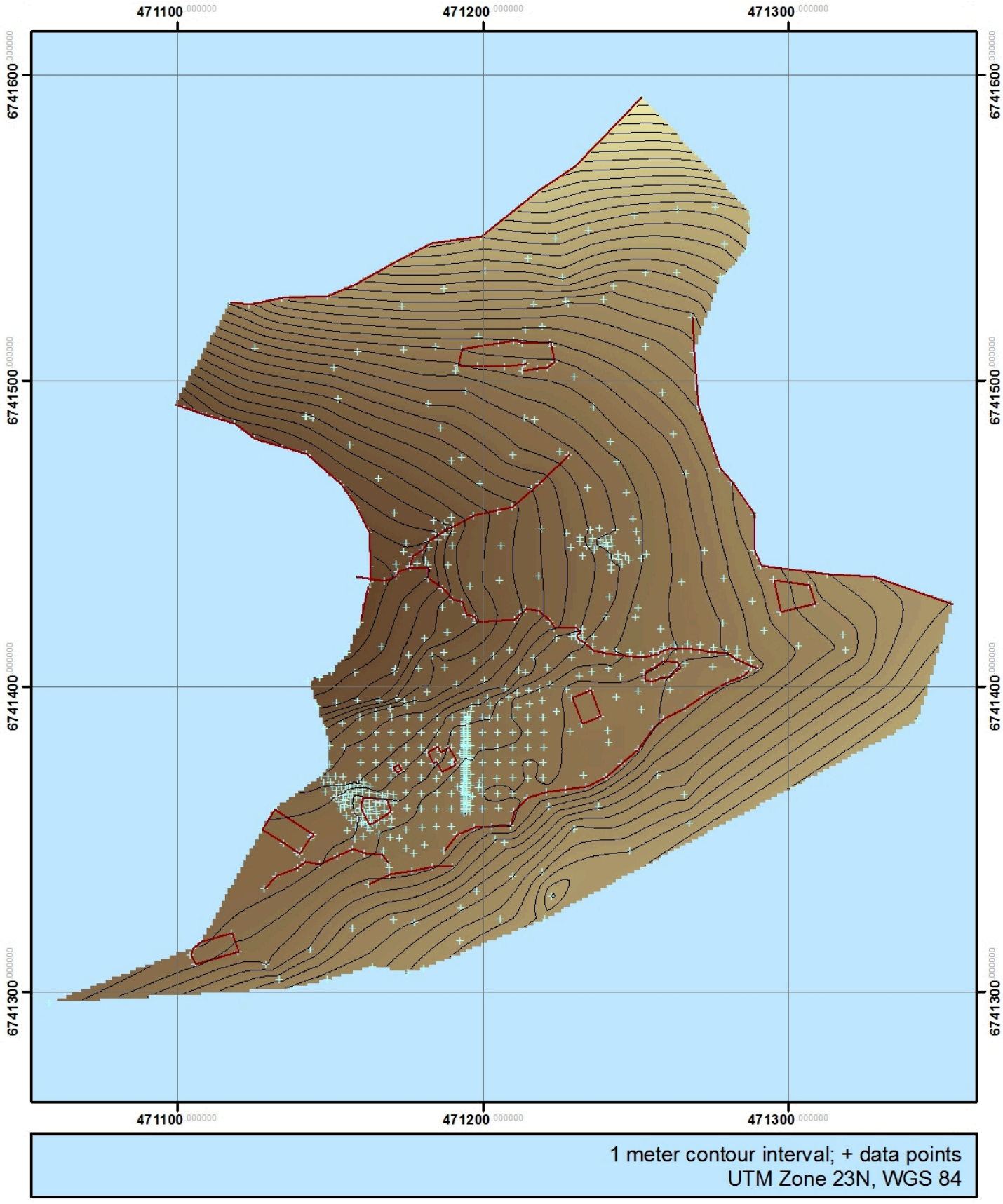

Figure 35.Ø172 topographic coverage.

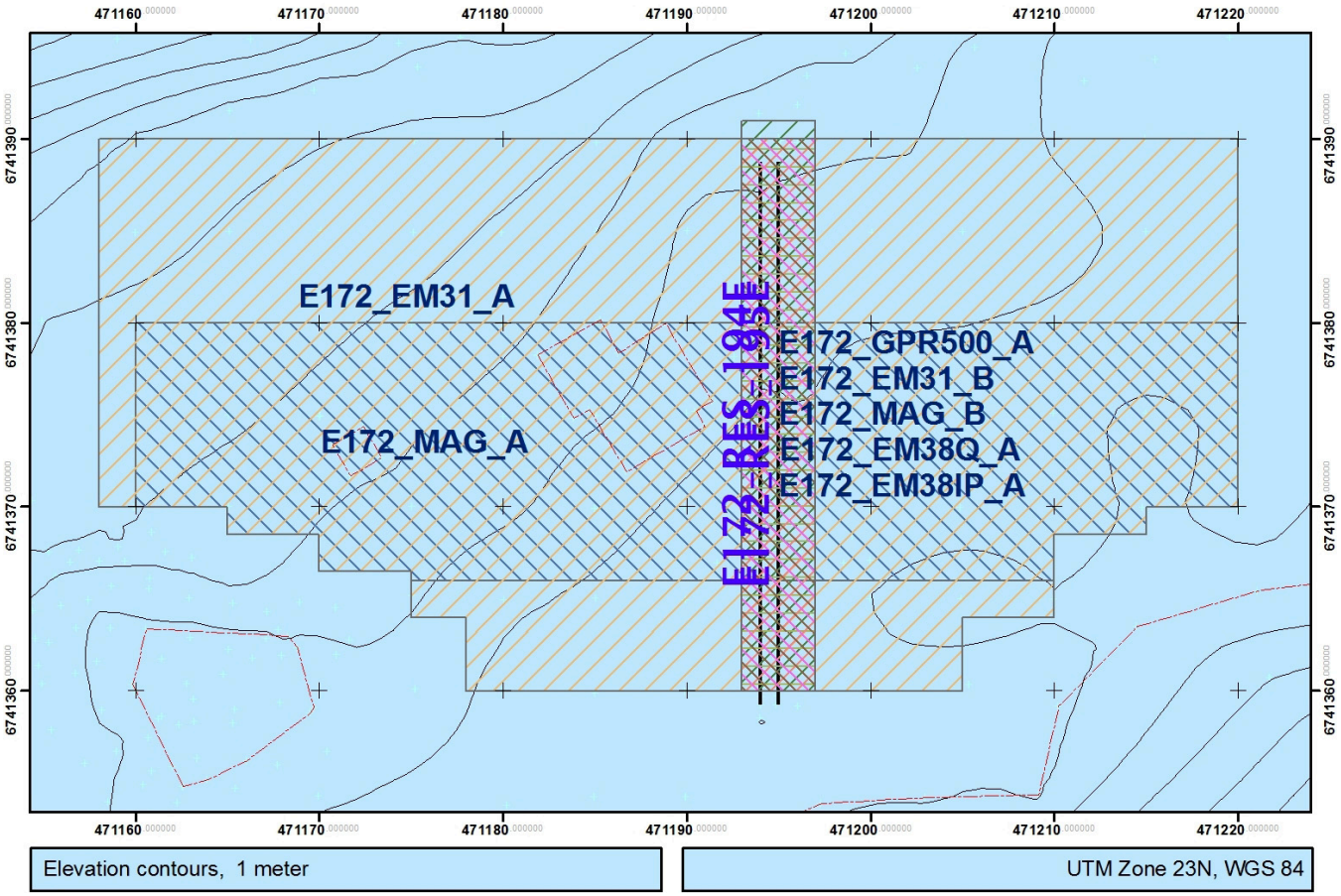

Figure 36. Ø172 Geophysical coverage.

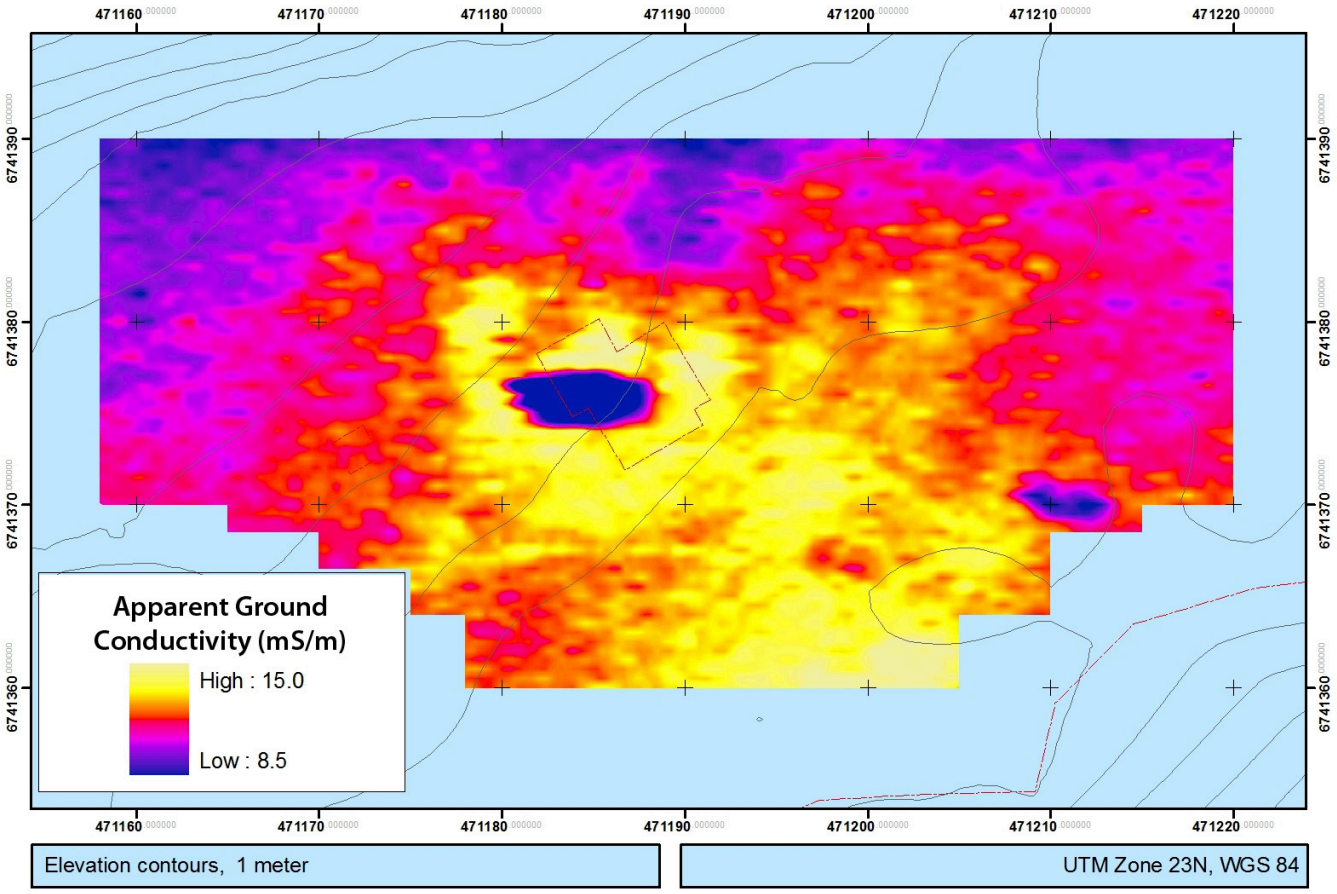

Figure 37. Ø172 Results of apparent ground conductivity survey using the EM-31.

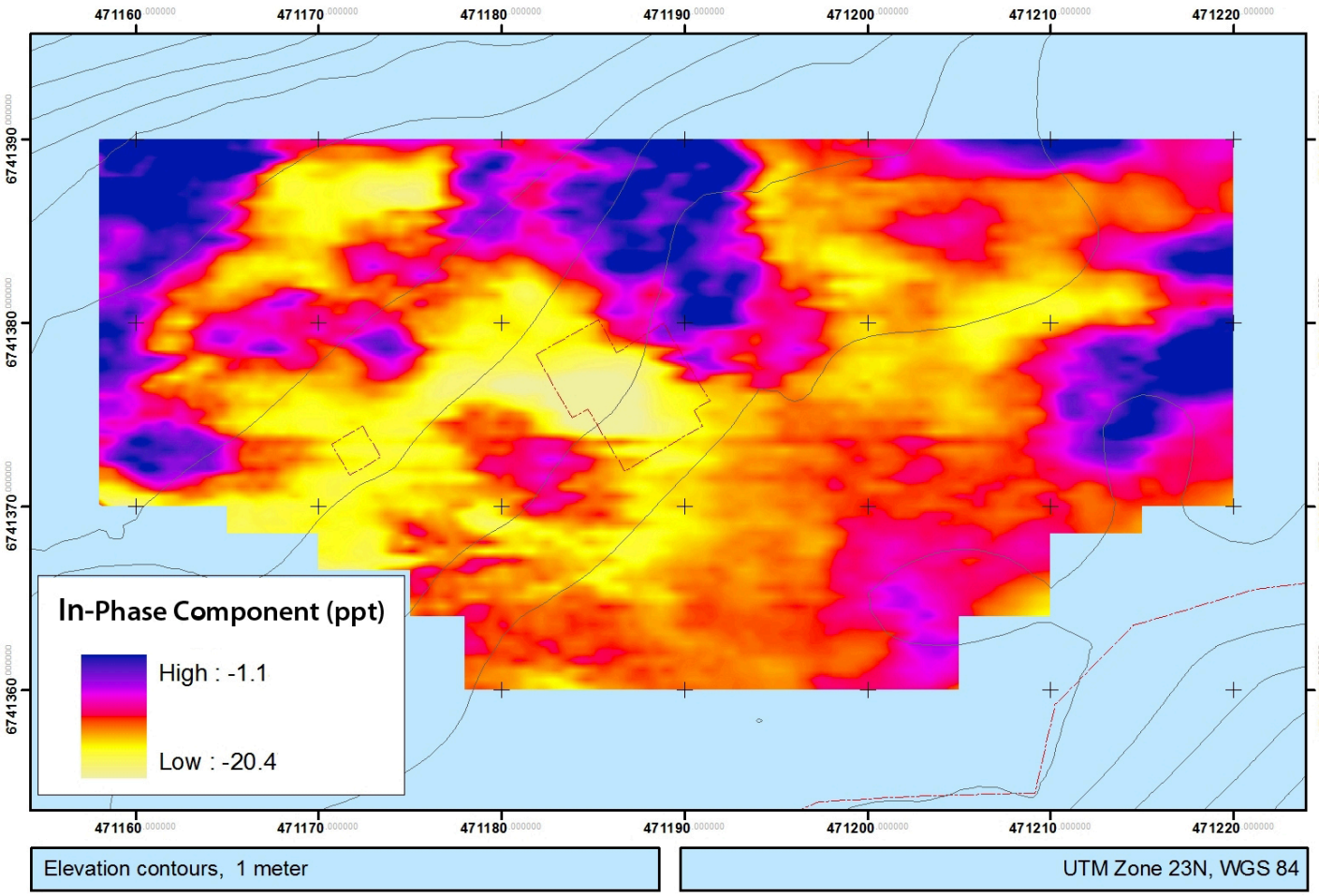

Figure 38. Ø172 Results of the in-phase survey using the EM-31.

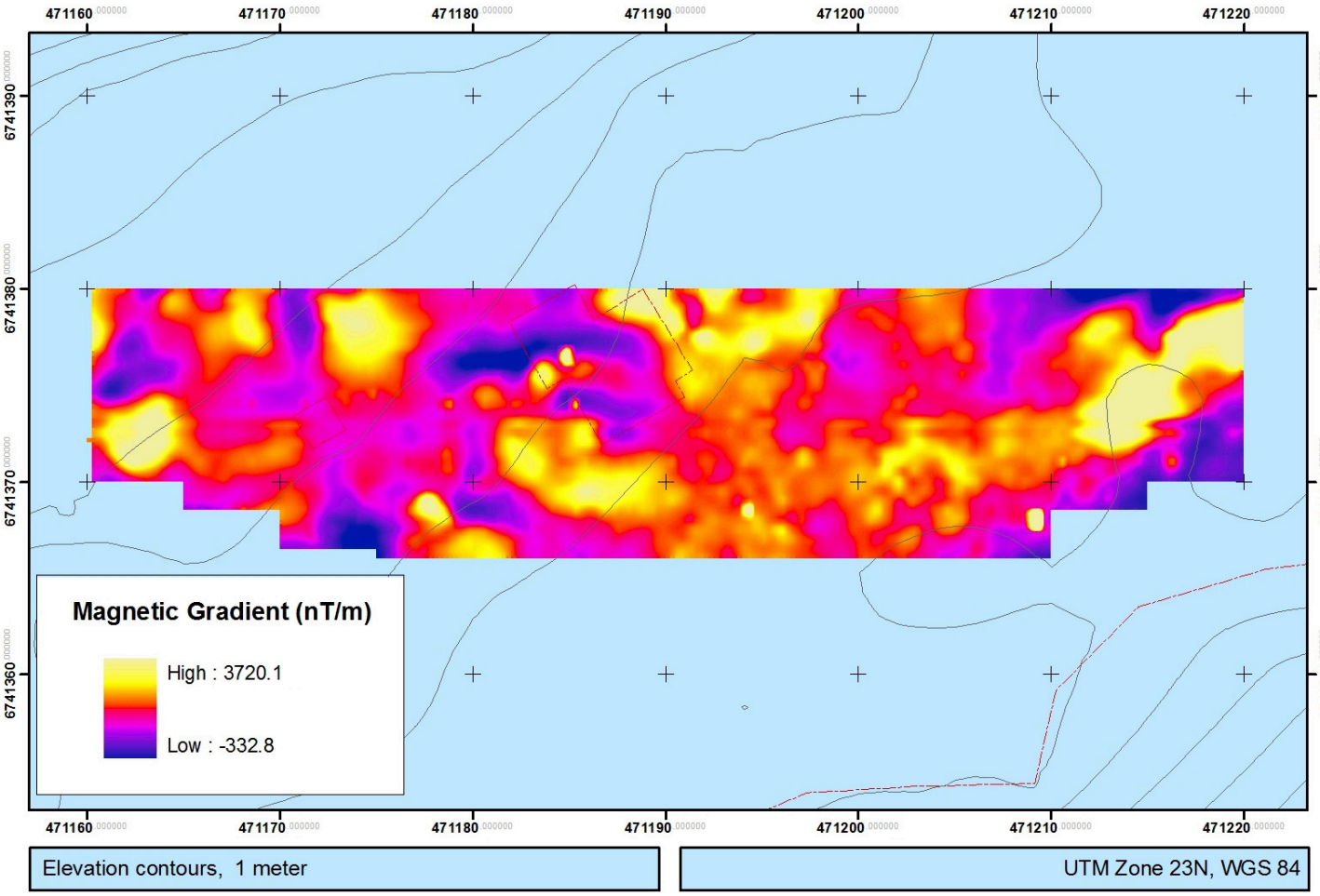

Figure 39. Ø172 Results of magnetic gradient survey.

Figure 40. Ø172 GPR surveying with the Mala unit equipped with 500 MHz antenna.

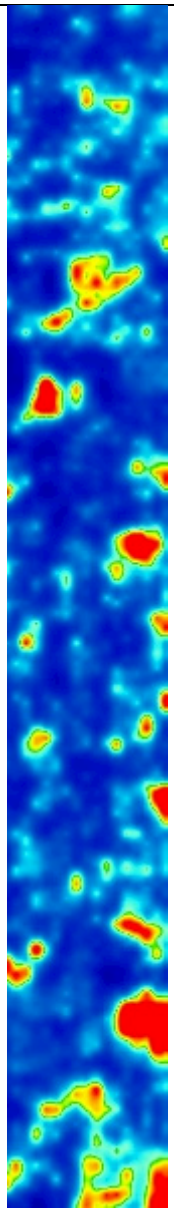	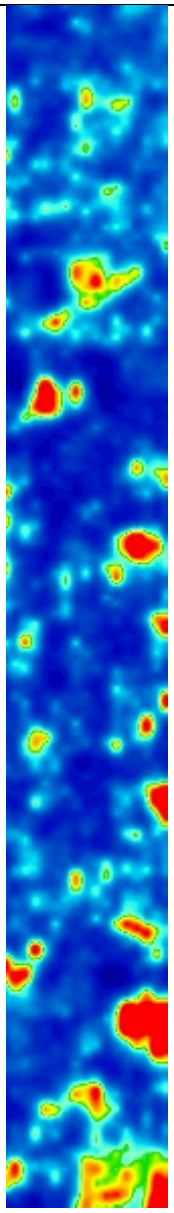	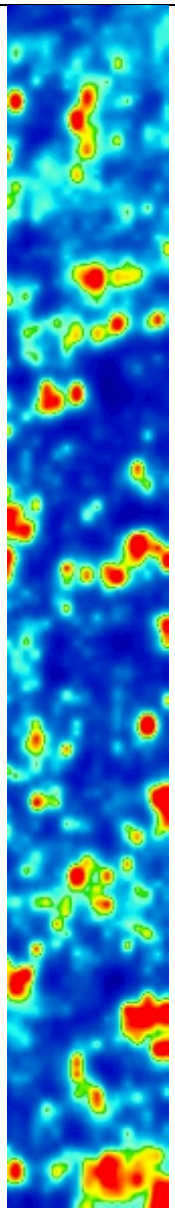	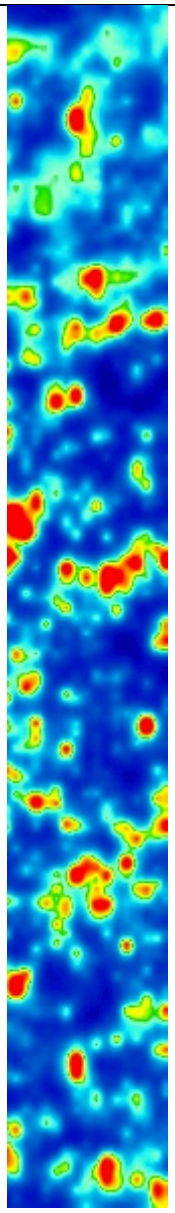	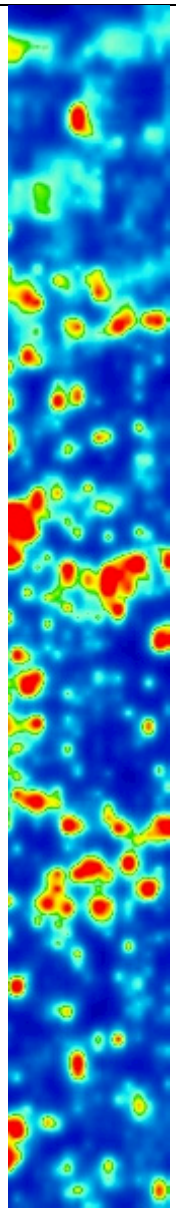
B01: 0-7 cm bgs	B02: 4-10 cm bgs	B03: 7-14 cm bgs	B04: 14-18 cm bgs	B05: 10-21 cm bgs

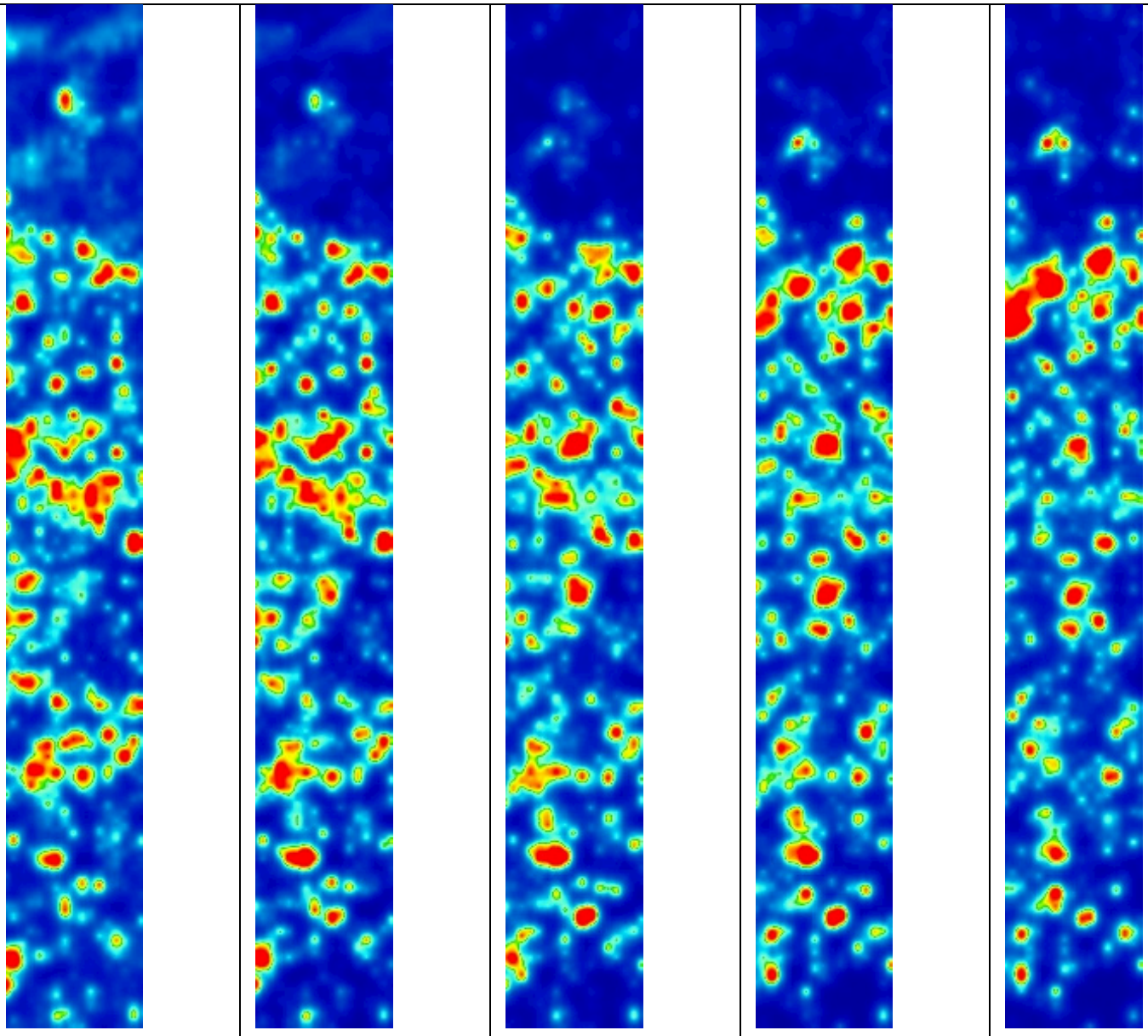

B06: 18-25 cm bgs	B07: 21-28 cm bgs	B08: 25-32 cm bgs	B09: 28-35 cm bgs	B10: 32-39 cm bgs

Figure 41. Ø172 GPR slices.

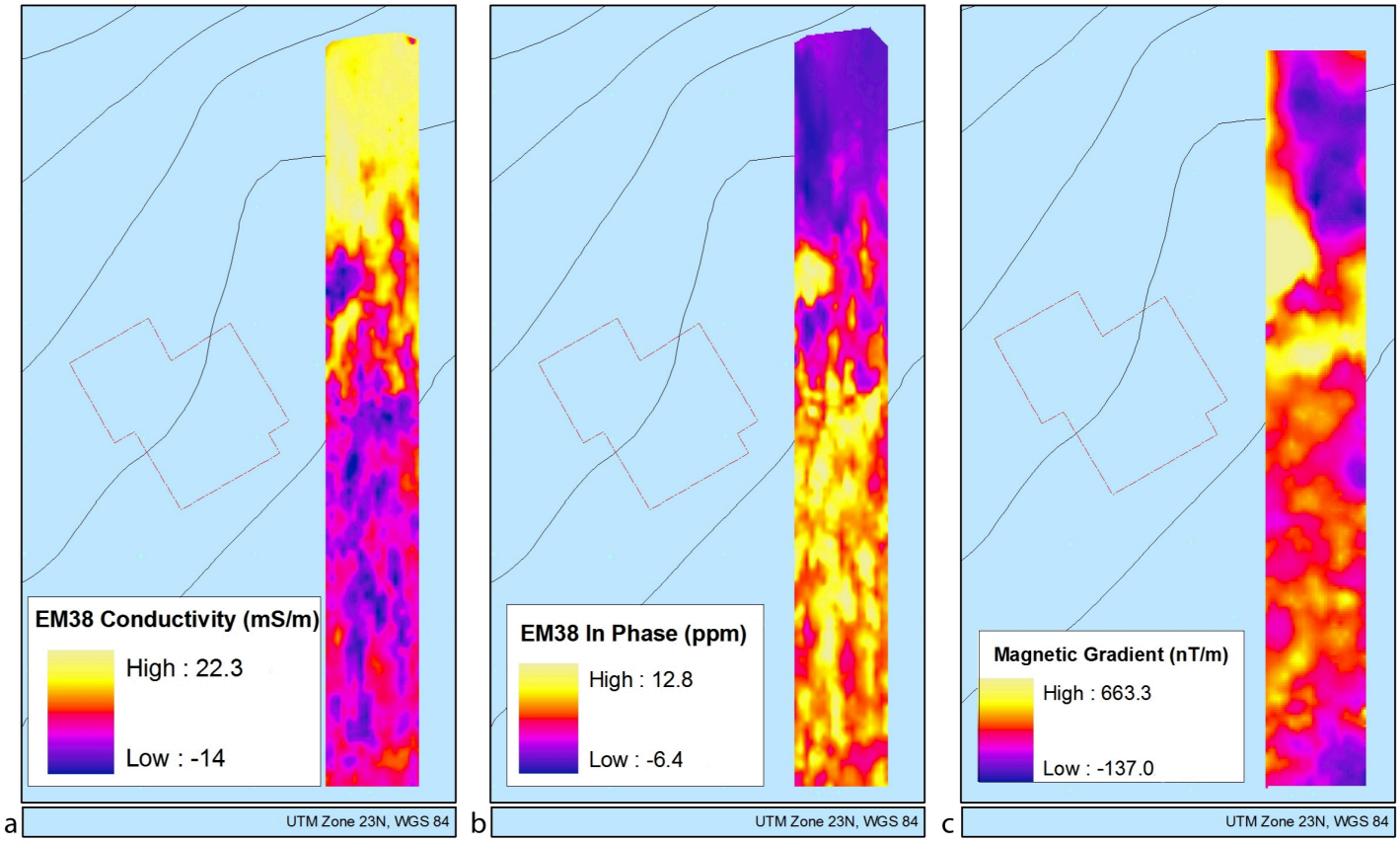

Figure 42. Ø172 Results of apparent ground conductivity in-phase surveys using the EM-38 (a,b) and magnetic gradient survey (c) over north-south strip.

Appendix 5: Ø66 Survey and Datasets

Surveying at Ø66 was conducted over a short, two-day period at the end of the fieldwork. Coring conducted at Ø66 in 2008 in attempts to identify the location of the medieval midden showed that much of the site is covered by a ca. 50 cm deposit of natural silt, presumably from the nearby Jespersens Glacier (Śmiarowski 2008a). Additional coring confirmed the earlier survey results and showed a layer of cultural material, mostly charcoal flakes, underneath approximately 50-100 cm of sandy soil. For the most part, cultural material was low density, typical of blown scatter around farm mounds, but a few cores indicated possible activity areas, middens, or buildings.

The primary purpose was to conduct a large-scale survey of a field to determine whether buried structures could be identified. With the magnetometer out of commission the prospection survey relied on the EM-31. The large field south and east below the main medieval mound was walked in both directions at a 1 meter transect spacing covering 7000 m^2. A quick, in-field analysis of the EM-31 survey produced few obvious targets for follow up survey. GPR and EM38 datasets were collected over two areas showing possible structural anomalies based on the EM-31 survey.

Topographic Data

1. Low density coverage of farm mound and surrounding fields.

Geophysical Surveys

1. Magnetometer (G858)
    a. No magnetometer data collected.
2. Ground Penetrating Radar
    a. Mala 500 MHz, Field, east of farm mound
    b. Mala 800 MHz, Field, south of farm mound
3. Resistivity (Syscal Kid)
    a. No resistivity data collected
4. Electromagnetic conductivity
    a. EM-31, area east and south of the farm mound
    b. EM-38 (in-phase), target area, field south of farm mound

Aerial Photograph Coverage

5. Flight 15 August 2010 (331 images); farm mound and surrounding areas; limited control points for georeferencing.

Coring Data

6. Soil cores from field east of the farm mound.

Figure 43. Topographic coverage at Ø172

Figure 44. Geophysical survey overview.

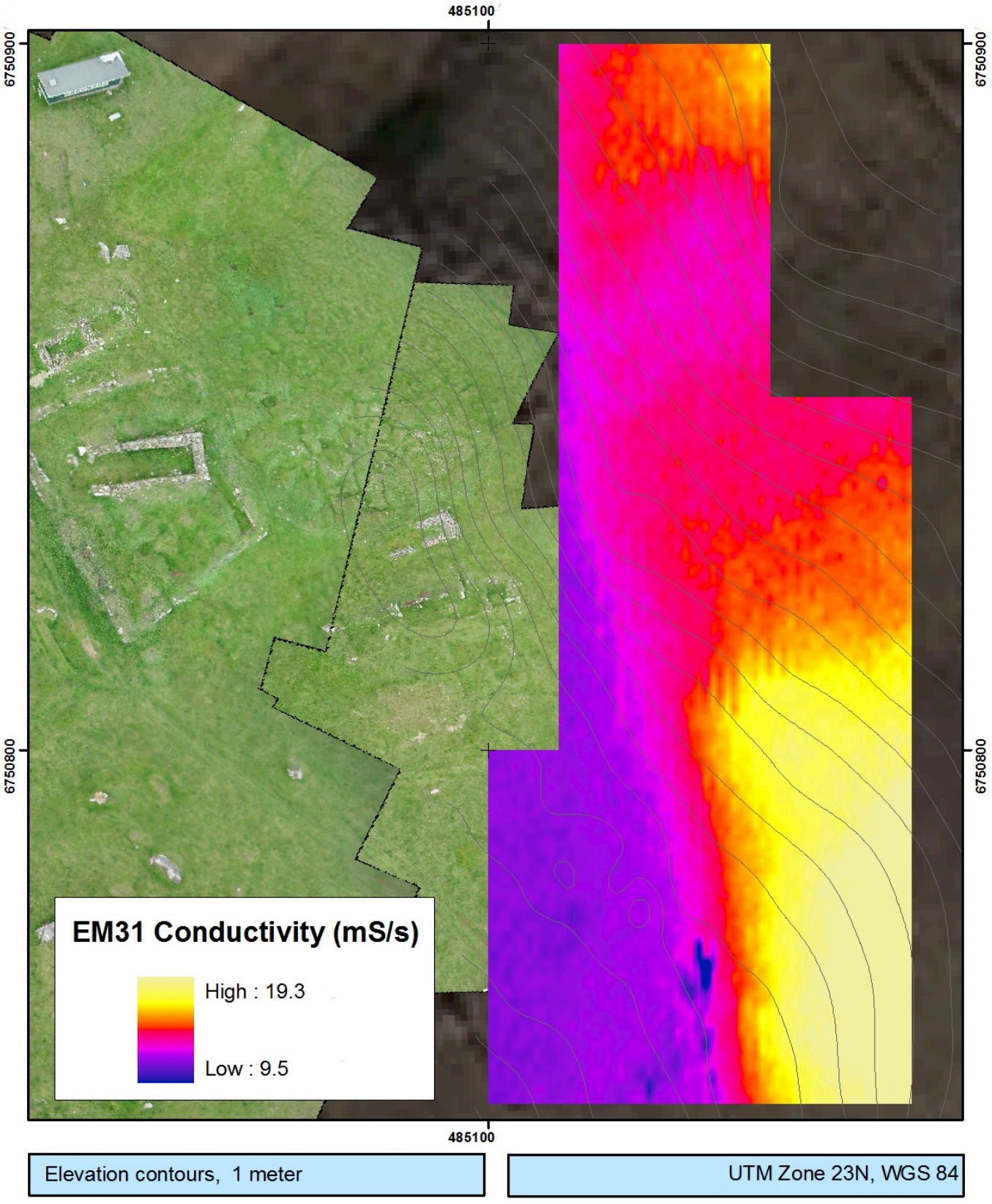

Figure 45. Ø66 Results of apparent ground conductivity survey using the EM-31.

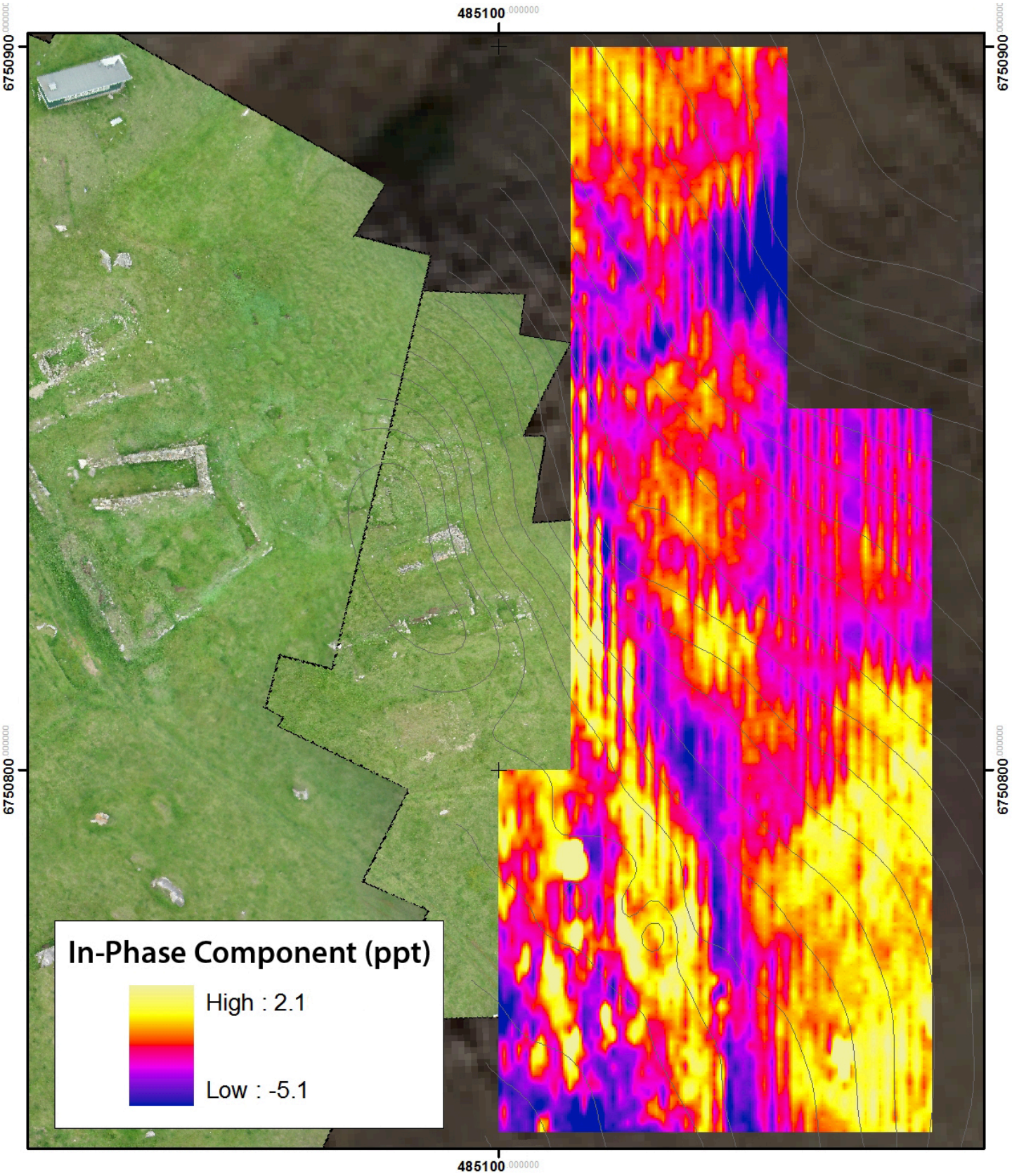

Elevation contours, 1 meter

UTM Zone 23N, WGS 84

Figure 46. Ø66 Results of in-phase survey using the EM-31.

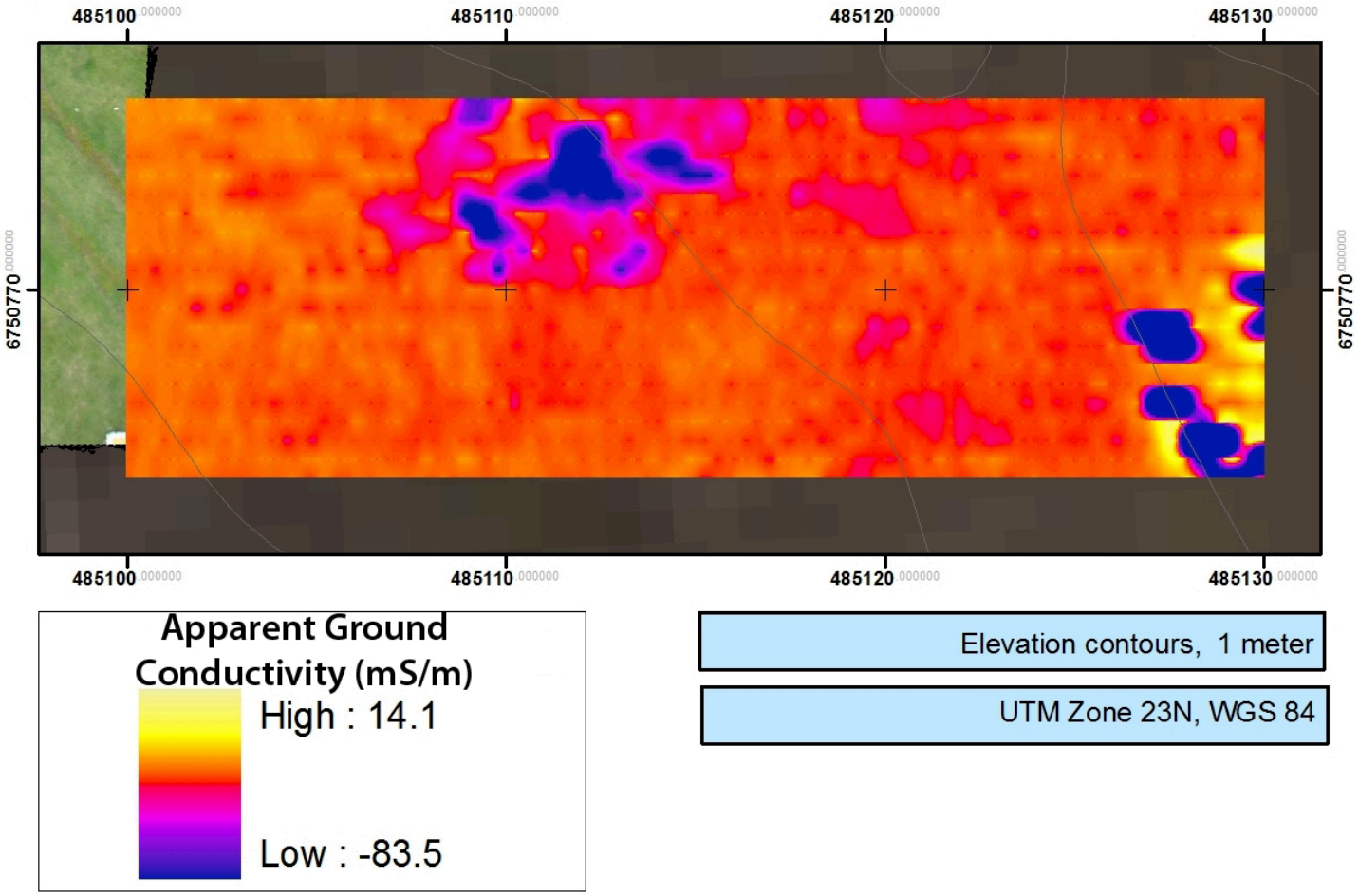

Figure 47. Ø66 Results of apparent ground conductivity survey using the EM-38.

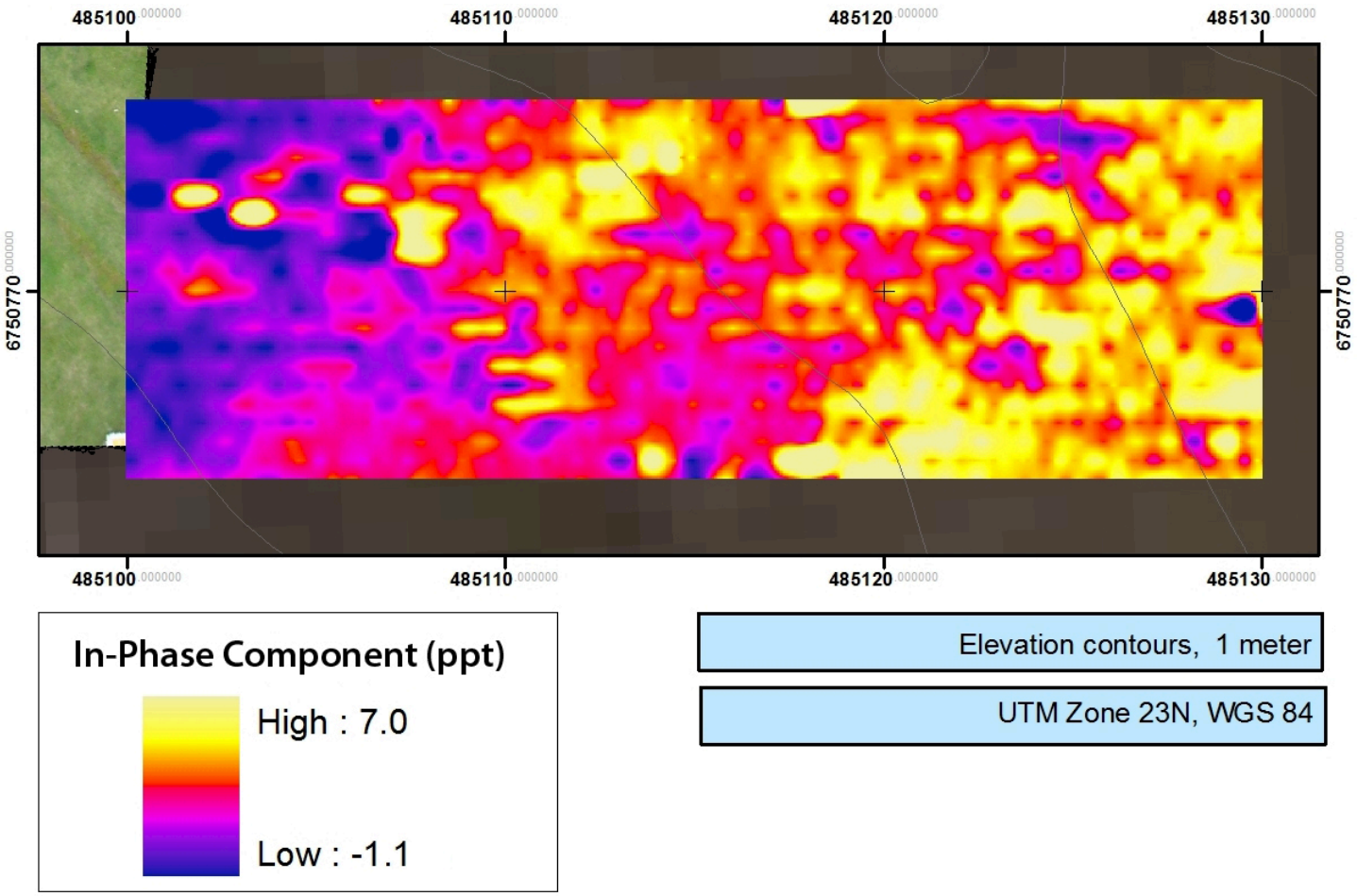

Figure 48. Ø66 Results of in-phase survey using the EM-38.

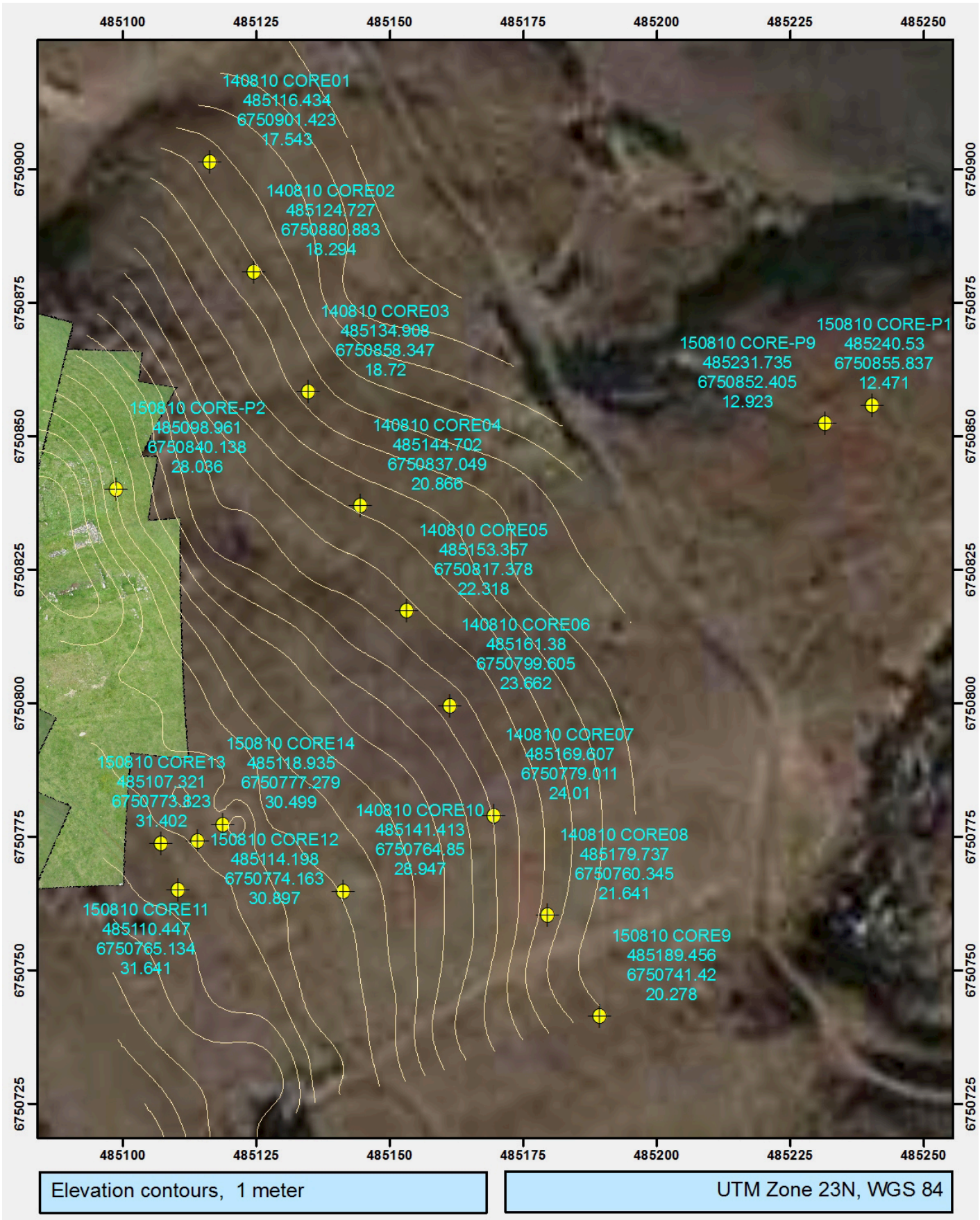

Figure 49. Ø172 coring locations.

Table 8. soil cores from at Ø66

Core	Layer	East	North	Elev	Top	Bottom	Description
1	1	485116.434	6750901.423	17.543	0	8	sandy topsoil
	2	485116.434	6750901.423	17.543	8	47	sand
	3	485116.434	6750901.423	17.543	47	53	sand, darker organic layer
	4	485116.434	6750901.423	17.543	53	63	sand with mid-brown banding, wetter/more compact than above; charcoal flakes
2	1	485124.727	6750880.883	18.294	0	10	sandy topsoil
	2	485124.727	6750880.883	18.294	10	45	sand
	3	485124.727	6750880.883	18.294	45	50	sand, darker organic layer
	4	485124.727	6750880.883	18.294	50	70	sand with mid-brown banding; charcoal flakes
3	1	485134.908	6750858.347	18.72	0	13	coarse sand
	2	485134.908	6750858.347	18.72	13	16	brown/organic layer
	3	485134.908	6750858.347	18.72	16	40	sand with mid-brown banding; charcoal flakes
	4	485134.908	6750858.347	18.72	40	55	sand
	5	485134.908	6750858.347	18.72	55	70	sand with mid-brown banding; charcoal flakes
4	1	485144.702	6750837.049	20.866	0	35	coarse sand
	2	485144.702	6750837.049	20.866	35	75	sand with mid-brown banding
	3	485144.702	6750837.049	20.866	75	76	blackish organic layer
	4	485144.702	6750837.049	20.866	76	82	compact striated brown/light sand and charcoal; cultural layer
	5	485144.702	6750837.049	20.866	82	84	light sand
5	1	485153.357	6750817.378	22.318	0	22	coarse sand
	2	485153.357	6750817.378	22.318	22	24	dark organic layer, compact
	3	485153.357	6750817.378	22.318	24	60	sand with mid-brown banding
	4	485153.357	6750817.378	22.318	60	90	striated brown/light sand and charcoal; charcoal flecks
	5	485153.357	6750817.378	22.318	90	100	striated brown/light sand and charcoal; cultural layer
	6	485153.357	6750817.378	22.318	100	103	light sand

Core	Layer	East	North	Elev	Top	Bottom	Description
	7	485153.357	6750817.378	22.318	103	108	mid-orange brown fine sand with silt, small clay component, subangular gravel ca. 4-8mm
6	1	485161.38	6750799.605	23.662	0	10	coarse sand
	2	485161.38	6750799.605	23.662	10	18	mid-gray sand
	3	485161.38	6750799.605	23.662	18	38	sand with mid-brown mottling
	4	485161.38	6750799.605	23.662	38	39	mid-black organic/charcoal lens
	5	485161.38	6750799.605	23.662	39	55	sand with mid-brown banding
	6	485161.38	6750799.605	23.662	55	65	sand with mid-brown banding; charcoal flakes
	7	485161.38	6750799.605	23.662	65	68	compact sandy mid-black cultural layer; charcoal flecks
	8	485161.38	6750799.605	23.662	68	71	light sand
	9	485161.38	6750799.605	23.662	71	75	coarse sand
7	1	485169.607	6750779.011	24.01	0	10	sandy topsoil
	2	485169.607	6750779.011	24.01	10	32	sand
	3	485169.607	6750779.011	24.01	32	34	mid-black sand, organic layer
	4	485169.607	6750779.011	24.01	34	42	sand with mid-brown banding
	5	485169.607	6750779.011	24.01	42	60	sand with mid-brown and coarse sand striations; v. small flecks of charcoal at bottom
	6	485169.607	6750779.011	24.01	60	64	light sand
	7	485169.607	6750779.011	24.01	64	68	mid-orange brown silty sand, subangular gravel ca. <5mm
8	1	485179.737	6750760.345	21.641	0	10	sandy topsoil
	2	485179.737	6750760.345	21.641	10	30	sand
	3	485179.737	6750760.345	21.641	30	55	sand with mid-gray/brown mottling and banding
	4	485179.737	6750760.345	21.641	55	57	mid-gray, organic sand (LNL?)
	5	485179.737	6750760.345	21.641	57	61	light sand
	6	485179.737	6750760.345	21.641	61	100	fine clayey sand and gravel ca. <5mm
9	1	485189.456	6750741.42	20.278	0	10	sandy topsoil

Core	Layer	East	North	Elev	Top	Bottom	Description
	2	485189.456	6750741.42	20.278	10	40	sand, some mid-brown mottling at 25-30 cm
	3	485189.456	6750741.42	20.278	40	50	banded coarse sand and fine mid-gray sand; possible charcoal flecks
10	1	485141.413	6750764.85	28.947	0	7	dark organic sandy topsoil
	2	485141.413	6750764.85	28.947	7	19	sand; thin wood fragment at 18 cm
	3	485141.413	6750764.85	28.947	19	22	mid-gray organic sand
	4	485141.413	6750764.85	28.947	22	42	sand with mid-brown banding
	5	485141.413	6750764.85	28.947	42	43	black charcoal; cultural layer; possible floor
	6	485141.413	6750764.85	28.947	43	70	sand with mid-gray/brown striations; charcoal concentrated at 60-70 cm, dense compact cultural layer; possible floor
	7	485141.413	6750764.85	28.947	70	72	light sand
	8	485141.413	6750764.85	28.947	72	74	dark orange-brown coarse sand; boundary with layer above sharp and angular
	9	485141.413	6750764.85	28.947	74	85	mid-orange-brown clayey sand with gravel
11	1	485110.447	6750765.134	31.641	0	10	sandy topsoil
	2	485110.447	6750765.134	31.641	10	38	sand
	3	485110.447	6750765.134	31.641	38	39	black lens
	4	485110.447	6750765.134	31.641	39	45	light sand mixed with brown sand and charcoal
	5	485110.447	6750765.134	31.641	45	80	coarse light sand
12	1	485114.198	6750774.163	30.897	0	10	topsoil
	2	485114.198	6750774.163	30.897	10	35	sand with come mottling from 12-18
	3	485114.198	6750774.163	30.897	35	41	sand with mid-brown banding; strange fiberous/rooty structure to sandy matrix (turf?)
	4	485114.198	6750774.163	30.897	41	45	light sand
	5	485114.198	6750774.163	30.897	45	80	coarse light orange sand
13	1	485107.321	6750773.823	31.402	0	13	turfy topsoil
	2	485107.321	6750773.823	31.402	13	18	sand with rots and possible turf; degraded wood fragments
	3	485107.321	6750773.823	31.402	18	39	light brown sand with rots and possible turf;

Core	Layer	East	North	Elev	Top	Bottom	Description
							degraded wood fragments
	4	485107.321	6750773.823	31.402	39	45	dark sandy charcoal layer
	5	485107.321	6750773.823	31.402	45	55	mid-brown sand with roots and some banding; charcoal at 50 cm
	6	485107.321	6750773.823	31.402	55	56	coarse sand
	7	485107.321	6750773.823	31.402	56	59	mid-brown with roots; turf?
	8	485107.321	6750773.823	31.402	59	63	fine gray sand
	9	485107.321	6750773.823	31.402	63	68	coarse gray sand
	10	485107.321	6750773.823	31.402	68	70	fine orange sand
14	1	485118.935	6750777.279	30.499	0	38	coarse sand
	2	485118.935	6750777.279	30.499	38	95	light sand with roots, small mid-brown mottles; sharp diagonal interface with above
15	1	485114	6750867	20.83	0	10	sandy topsoil
	2	485114	6750867	20.83	10	55	sand with mid-brown/light gray mottling; turfy/rooty
	3	485114	6750867	20.83	55	70	turfy sand with mid-orange/borwn mottles; turfy bits; charcoal
	4	485114	6750867	20.83	70	75	sand banded with mid-brown mottling; charcoal
16	1	485120	6750870	19.755	0	10	sandy topsoil
	2	485120	6750870	19.755	10	39	fine mid-brown sand with roots
	3	485120	6750870	19.755	39	71	striated midden; light/dark brown sand; charcoal
	4	485120	6750870	19.755	71	75	light sand
	5	485120	6750870	19.755	75	80	coarse sand
17	1	485129	6750835	22.422	0	20	coarse sand
	2	485129	6750835	22.422	20	23	mid-gray sandy turf layer
	3	485129	6750835	22.422	23	53	sand
	4	485129	6750835	22.422	53	55	sand with two thin black lenses, charcoal?
	5	485129	6750835	22.422	55	75	sand with mid-brown striations
	6	485129	6750835	22.422	75	80	light sand

Core	Layer	East	North	Elev	Top	Bottom	Description
10	1	485141.413	6750764.85	28.947	0	7	dark organic sandy topsoil
	2	485141.413	6750764.85	28.947	7	19	sand; thin wood fragment at 18 cm
	3	485141.413	6750764.85	28.947	19	22	mid-gray organic sand
	4	485141.413	6750764.85	28.947	22	42	sand with mid-brown banding
	5	485141.413	6750764.85	28.947	42	43	black charcoal; cultural layer; possible floor
	6	485141.413	6750764.85	28.947	43	70	sand with mid-gray/brown striations; charcoal concentrated at 60-70 cm, dense compact cultural layer; possible floor
	7	485141.413	6750764.85	28.947	70	72	light sand
	8	485141.413	6750764.85	28.947	72	74	dark orange-brown coarse sand; boundary with layer above sharp and angular
	9	485141.413	6750764.85	28.947	74	85	mid-orange-brown clayey sand with gravel
11	1	485110.447	6750765.134	31.641	0	10	sandy topsoil
	2	485110.447	6750765.134	31.641	10	38	sand
	3	485110.447	6750765.134	31.641	38	39	black lens
	4	485110.447	6750765.134	31.641	39	45	light sand mixed with brown sand and charcoal
	5	485110.447	6750765.134	31.641	45	80	coarse light sand
12	1	485114.198	6750774.163	30.897	0	10	topsoil
	2	485114.198	6750774.163	30.897	10	35	sand with come mottling from 12-18
	3	485114.198	6750774.163	30.897	35	41	sand with mid-brown banding; strange fiberous/rooty structure to sandy matrix (turf?)
	4	485114.198	6750774.163	30.897	41	45	light sand
	5	485114.198	6750774.163	30.897	45	80	coarse light orange sand
13	1	485107.321	6750773.823	31.402	0	13	turfy topsoil
	2	485107.321	6750773.823	31.402	13	18	sand with rots and possible turf; degraded wood fragments
	3	485107.321	6750773.823	31.402	18	39	light brown sand with rots and possible turf; degraded wood fragments
	4	485107.321	6750773.823	31.402	39	45	dark sandy charcoal layer
	5	485107.321	6750773.823	31.402	45	55	mid-brown sand with roots and some

Core	Layer	East	North	Elev	Top	Bottom	Description
							banding; charcoal at 50 cm
	6	485107.321	6750773.823	31.402	55	56	coarse sand
	7	485107.321	6750773.823	31.402	56	59	mid-brown with roots; turf?
	8	485107.321	6750773.823	31.402	59	63	fine gray sand
	9	485107.321	6750773.823	31.402	63	68	coarse gray sand
	10	485107.321	6750773.823	31.402	68	70	fine orange sand
14	1	485118.935	6750777.279	30.499	0	38	coarse sand
	2	485118.935	6750777.279	30.499	38	95	light sand with roots, small mid-brown mottles; sharp diagonal interface with above
15	1	485114	6750867	20.83	0	10	sandy topsoil
	2	485114	6750867	20.83	10	55	sand with mid-brown/light gray mottling; turfy/rooty
	3	485114	6750867	20.83	55	70	turfy sand with mid-orange/borwn mottles; turfy bits; charcoal
	4	485114	6750867	20.83	70	75	sand banded with mid-brown mottling; charcoal
16	1	485120	6750870	19.755	0	10	sandy topsoil
	2	485120	6750870	19.755	10	39	fine mid-brown sand with roots
	3	485120	6750870	19.755	39	71	striated midden; light/dark brown sand; charcoal
	4	485120	6750870	19.755	71	75	light sand
	5	485120	6750870	19.755	75	80	coarse sand
17	1	485129	6750835	22.422	0	20	coarse sand
	2	485129	6750835	22.422	20	23	mid-gray sandy turf layer
	3	485129	6750835	22.422	23	53	sand
	4	485129	6750835	22.422	53	55	sand with two thin black lenses, charcoal?
	5	485129	6750835	22.422	55	75	sand with mid-brown striations
	6	485129	6750835	22.422	75	80	light sand

Bibliography

Appel, E., J. Wilhelm and M. Waldhör
1997 Archaeological prospection of wall remains using geoelectrical methods and GPR. *Archaeological Prospection* 4(4):219-229.

Arneborg, J.
2000 Greenland and Europe. In *Vikings: the North Atlantic Saga*, edited by W. W. Fitzhugh and E. I. Ward, pp. 304-317. Smithsonian Institute Press, Washington.

2001 The Norse Settlement in Greenland: The Initial Period in Written Sources and Archaeology. In *Approaches to Vinland*, edited by A. Wawn and T. Sigurðardóttir, pp. 122-133. Nordalh Institute, Reykjavík.

Arneborg, J., J. Heinemeier, N. Lynnerup, H. L. Nielsen, N. Rud and Á. Sveinbjörnsdóttir
1999 Change of Diet on the Greenland Vikings Determined from Stable Carbon Isotope Analysis and 14C Dating of Their Bodies. *Radiocarbon* 41(2):157-168.

Barlow, L. K., J. P. Sadler, A. E. J. Ogilvie, P. C. Buckland, T. Amorosi, J. H. Ingimundarson, P. Skidmore, A. J. Dugmore and T. H. McGovern
1997 Interdisciplinary investigations of the end of the Norse Western Settlement in Greenland. *The Holocene* 7(4):489-499.

Becker, H.
2009 Caesium-magnetometry for landscape archaeology. In *Seeing the unseen : geophysics and landscape archaeology*, edited by S. Campana and S. Piro, pp. 129-166. CRC Press, Boca Raton.

Buckland, P. C., T. Amorosi, L. K. Barlow, A. J. Dugmore, P. A. Mayewski, T. H. McGovern, A. E. J. Ogilvie, J. P. Sadler and P. Skidmore
1995 Bioarchaeological and Climatological Evidence for the Fate of Norse Farmers in Medieval Greenland. *Antiquity* 70:88-96.

Conyers, L. B.
2005 *Ground-Penetrating Radar for Archaeology*. Altamira Press, Lanham, MD.

2006a Ground-Penetrating Radar. In *Remote Sensing in Archaeology: An Explicitly North American Perspective*, edited by J. K. Johnson, pp. 131-159. University Alabama Press, Tuscaloosa.

2006b Ground-Penetrating Radar Techniques to Discover and Map Historic Graves. *Historical archaeology* 40(3):64-73.

Diamond, J.
2005 *Collapse: How Societies Choose to Fail or Succeed*. Viking Press, New York.

Dionne, C. A., D. K. Wardlaw and J. J. Schultz
2010 Delineation and Resolution of Cemetery Graves Using a Conductivity Meter and Ground-Penetrating Radar. *Technical Briefs in Historical Archaeology* 5:20-30.

Doolittle, J. A. and N. F. Bellantoni
2010 The search for graves with ground-penetrating radar in Connecticut. *Journal of Archaeological Science* 37(5):941-949.

Dugmore, A. J., M. J. Church, P. C. Buckland, K. J. Edwards, I. Lawson, T. H. McGovern, E. Panagiotakopulu, I. A. Simpson, P. Skidmore and G. Sveinbjarnardóttir
2005 The Norse landnám on the North Atlantic islands: an environmental impact assessment. *Polar Record* 41(216):21-37.

Dugmore, A. J., C. Keller and T. H. McGovern
2007 Norse Greenland Settlement: Reflections on Climate Change, Trade, and the Contrasting Fates of Human Settlements in the North Atlantic Islands. *Arctic Anthropology* 44(1):12-36.

Fiedler, S., B. Illich, J. Berger and M. Graw
2009 The effectiveness of ground-penetrating radar surveys in the location of unmarked burial sites in modern cemeteries. *Journal of Applied Geophysics* 68(3):380-385.

Gaffney, C. and J. Gater
2003 *Revealing the buried past : geophysics for archaeologists*. Tempus, Stroud.

Goodman, D. and L. B. Conyers
1997 *Ground Penetrating Radar: An Introduction for Archaeologists*. AltaMira Press, Walnut Creek, MD.

Goodman, D., S. Piro, Y. Nishimura, K. Schneider, H. Hongo, N. Higashi, J. Steinberg and B. Damiata
2008 GPR Archaeometry. In *Ground Penetrating Radar Theory and Applications*, edited by H. Jol, pp. 479-508. Elsvier, New York.

Goodman, D., J. Steinberg, B. Damiata, Y. Nishimura, S. Piro and K. Schneider
2007 GPR Imaging of Archaeological Sites. In *Reconstructing Human-Landscape Interactions, Dig 2005 Conference, Developing International Geoarchaeology*, edited by L. Wilson, P. Dickinson and J. Jeandron, pp. 202-217. Cambridge Scholars Publishing, Cambridge.

Griffin, D. R.
1987 Foreword to papers on magnetic sensitivity in birds. *Learning & Behavior* 15(2):108-109.

Guldager, O., S. S. Hansen and S. Gleie
2002 *Medieval Farmsteads in Greenland — The Brattahlid region 1999-2000*. Danish Polar Center, Copenhagen.

Hammon, W. S., G. A. McMechan and X. X. Zeng
2000 Forensic GPR: finite-difference simulations of responses from buried human remains. *Journal of Applied Geophysics* 45(3):171-186.

Hargrave, M. L., L. E. Somers, T. K. Larson, R. Shields and J. Dendy
2002 The role of resistivity survey in historic site assessment and management : an example from Fort Riley, Kansas. *Historical archaeology* 36(4):89-110.

Horsley, T. J. and S. J. Dockrill
2002 A preliminary assessment of the use of routine geophysical techniques for the location, characterization and interpretation of buried archaeology in Iceland. *Archaeological Islandica* 2:10-33.

Horsley, T. J., A. Schmidt and S. J. Dockrill
2003 The potential of archaeological prospection techniques in Iceland. *Archaeologia Polona*.

Hunter, J. and M. Cox
2005 *Forensic archaeology : advances in theory and practice*. Routledge, London ; New York.

Jacobsen, N. K.
1987 Studies on the soils and potential for soil erosion in the sheep farming area of south Greenland. *Arctic and Alpine Research* 19:498-507.

Jacobsen, N. K. and H. B. Jakobsen
1986 C14 datering af en fossil overfladehorisont ved Igaliku Kujalleq, Sydrønland, set i relation to nordboernes landnam. *Geografisk Tidsskrift* 86:74-77.

Jones, G.
2008 Geophysical Mapping of Historic Cemeteries. *Technical Briefs in Historical Archaeology* 3:25-38.

Keller, C.
1989 The Eastern Settlement Reconsidered. Some analyses of Norse Medieval Greenland. PhD, University of Oslo, Oslo.

1990 Vikings in the west Atlantic: a model of Norse Greenlandic medieval society. *Acta Archaeologica* 61:126-141.

King, J. A., R. J. Hurry and B. W. Bevan
1993 Reliability of geophysical surveys at historic-period cemeteries: an example from the Plains cemetery, Mechanicsville, Maryland. *Historical archaeology* 27:4-16.

Kvamme, K. L.
2006 Magnetometry: Nature's Gift to Archaeology. In *Remote Sensing in Archaeology: An Explicitly North American Perspective*, edited by J. K. Johnson, pp. 205-233. University Alabama Press, Tuscaloosa.

Lamb, H. H.
1982 *Climate, history, and the modern world*. Methuen, London ; New York.

Leckenbusch, J.
2002 Ground-penetrating radar: a modern three-dimensional prospection method. *Archaeological Prospection* 10:213-240.

Linford, N., P. Linford, L. Martin and A. Payne
2007 Recent results from the English Heritage caesium magnetometer system in comparison with recent fluxgate gradiometers. *Archaeological Prospection* 14:151-166.

Mann, M. E., Z. Zhang, S. Rutherford, R. S. Bradley, M. K. Hughes, D. Shindell, C. Ammann, G. Faluvegi and F. Ni
2009 Global Signatures and Dynamical Origins of the Little Ice Age and Medieval Climate Anomaly. *Science* 326(5957):1256-1260.

McGovern, T. H.
1980 Cows, harp seals, and churchbells: adaptation and extinction in Norse Greenland. *Human ecology* 8(3):245-275.

1981 The economics of extinction in Norse Greenland. In *Climate and History*, edited by T. M. L. Wigley, pp. 404-434. Cambridge University Press, Cambridge.

1991 Climate, correlation, and causation in Norse Greenland. *Arctic Anthropology* 28(2):77-100.

1992 Bones, buildings, and boundaries: patterns in Greenlandic paleoeconomy. In *Norse and Later Settlement and Subsistence in the North Atlantic*, edited by C. D. Morris and J. Rackham, pp. 193-230. University of Glasgow Press, Glasgow.

1994 Management for Extinction. In *Historical Ecology*, edited by C. L. Crumley, pp. 127-154. School of American Research Press, Santa Fe, NM.

2000 The Demise of Norse Greenland. In *Vikings: the North Atlantic Saga*, edited by W. W. Fitzhugh and E. I. Ward, pp. 327-339. Smithsonian Institute Press, Washington.

McGovern, T. H., O. Vesteinsson, A. Fridriksson, M. Church, I. A. N. Lawson, I. A. Simpson, A. Einarsson, A. Dugmore, G. Cook, S. Perdikaris, K. J. Edwards, A. M. Thomson, W. P. Adderley, A. Newton, G. Lucas, R. Edvardsson, O. Aldred and E. Dunbar

2007 Landscapes of Settlement in Northern Iceland: Historical Ecology of Human Impact and Climate Fluctuation on the Millennial Scale. *American Anthropologist* 109(1):27-51.

McNeill, J. D.

1980 *Electromagnetic terrain conductivity measurement at low induction numbers*. Technical Note TN-6. Geonics Limited, Mississaunga.

Ogilvie, A. E. J., L. K. Barlow and A. E. Jennings

2000 North Atlantic climate c. 1000: millennial reflections on the Viking discoveries of Iceland, Greenland and North America. *Weather* 55:34-45.

Olhoeft, G. R.

2000 Maximizing the information return from ground penetrating radar. *Journal of Applied Geophysics* 43(2-4):175-187.

Rodrigues, S. I., J. L. Porsani, V. R. N. Santos, P. A. D. DeBlasis and P. C. F. Giannini

2009 GPR and inductive electromagnetic surveys applied in three coastal sambaqui (shell mounds) archaeological sites in Santa Catarina state, South Brazil. *Journal of Archaeological Science* 36(10):2081-2088.

Schmidt, A.

2007 Archaeology, magnetic methods. In *Encyclopedia of Geomagnetism and Paleomagnetism of dsfa* edited by D. Gubbins and E. Herrero-Bervera, pp. 23-31. Springer, New York.

Scollar, I., A. Tabbagh, A. Hesse and I. Herzog

1990 *Archaeological prospecting and remote sensing*. Cambridge University Press, Cambridge.

Śmiarowski, K.

2008a *Archaeological Investigations in Vatnahverfi, Greenland 2008 Field Season Preliminary Report*. Northern Science and Education Center at City University of New York.

2008b *Greenland 2007 Field Season Preliminary Report*. Northern Science and Education Center at City University of New York.

2009 *Archaeological Investigations in Vatnahverfi, Greenland 2008 Field Season Preliminary Report*. Northern Science and Education Center at City University of New York.

Smith, K. P.

1995 Landnám: the settlement of Iceland in archaeological and historical perspective. *World Archaeology* 26(3):319-346.

Steinberg, J. M. and J. L. Byock

2000 *High risk exploratory research: Political economy of Free State Iceland - regional archaeology in the Mosfell Valley. Report of the 1999 season*. National Museum of Iceland.

Tabbagh, A.
1984 On the Comparison between Magnetic and Electromagnetic Prospection Methods for Magnetic Features Detection. *Archaeometry* 26(Aug):171-182.

Tabbagh, A., G. Bossuet and H. Becker
1988 A Comparison between Magnetic and Electromagnetic Prospection of a Neolithic Ring Ditch in Bavaria. *Archaeometry* 30:132-144.

Trouet, V., J. Esper, N. E. Graham, A. Baker, J. D. Scourse and D. C. Frank
2009 Persistent Positive North Atlantic Oscillation Mode Dominated the Medieval Climate Anomaly. *Science* 324(5923):78-80.

Vésteinsson, O., T. McGovern and C. Keller
2002 Enduring impacts: social and environmental aspects of Viking Age settlement in Iceland and Greenland. *Archaeological Islandica* 2:98-136.

Þorgilsson, A.
1930 *The Book of the Icelanders [Íslendingabók]*. Translated by H. Hermannsson. Islandica 20. Cornell University Library, Ithaca.